University Library

A gateway to Melbourne's research publications

Minerva Access is the Institutional Repository of The University of Melbourne

Author/s:
Yang, Lie

Title:
The control of melanoma by the Hippo pathway

Date:
2018

Persistent Link:
https://hdl.handle.net/11343/220752

Terms and Conditions:
Terms and Conditions: Copyright in works deposited in Minerva Access is retained by the copyright owner. The work may not be altered without permission from the copyright owner. Readers may only download, print and save electronic copies of whole works for their own personal non-commercial use. Any use that exceeds these limits requires permission from the copyright owner. Attribution is essential when quoting or paraphrasing from these works.

The control of melanoma by the Hippo pathway

by Lie Yang

Under the supervision of Professor Kieran Harvey,

Professor Mark Shackleton and Dr. Xiaomeng Zhang

Thesis submitted for the Master of Research (MR-RESMED)

The Sir Peter MacCallum Department of Oncology

The University of Melbourne

Table of Contents

Table of Contents **2**
Abstract **5**
Abbreviations **8**
Chapter 1 Background **10**
1.1 Introduction of the Hippo pathway 10
1.1.1 The discovery of the Hippo pathway 10
1.1.2 The mammalian Hippo pathway 11
1.1.3 Regulation of the Hippo pathway 13
1.1.4 Downstream transcription factors 15
1.1.5 Crosstalk pathways 16
1.1.6 Outputs of the Hippo pathway 18
1.1.7 The Hippo pathway and human diseases 19
1.2 Introduction to melanoma 20
1.2.1 Disease conditions 21
1.2.2 The classification of melanoma 22
1.2.3 Melanoma phenotype switch 23
1.2.4 Current treatments 24
1.3 The Hippo pathway in melanoma 26
1.3.1 The Hippo pathway and uveal melanoma 26
1.3.2 Hippo pathway components in melanoma 27
1.3.3 The Hippo pathway in melanoma tumorigenesis and metastasis 27
1.3.4 The Hippo pathway in drug resistance 28
1.4 Summary and project rationale 29
Chapter 2 Materials and Methods **29**
2.1 Cell Culture 29
2.2 SiRNAs transfection 30
2.3 Establishment of MeWo-RhoA/RhoA-F stable cell lines 30
2.4 Western Blotting 30
2.5 RNA Extraction, Reverse Transcription, and Quantitative Real-Time PCR 32
2.5.1 RNA isolation 32
2.5.2 Reverse transcription 32
2.5.3 Quantitative real-time polymerase chain reaction (qPCR) analysis 33
2.6 Cell Viability Assay 33
2.7 Soft agar Assay 33
2.8 Invasion Assay 34
2.9 Fluorescent Activated Cell Sorting (FACS) 34
2.10 Animal Experiments 35
2.10.1 Establishment of melanoma xenograft model 35
2.10.2 Dissociation of melanoma cells form solid tumours 35
2.10.3 Staining and FACS of dissociated tumour cells 36
2.11 Histopathology and Immunochemistry Analysis 37

2.11.1 Histological and Immunochemical Staining 37
2.11.2 Histological and Immunochemical Quantification 38
2.12 Statistical Analysis 39
Chapter 3 Results 40
3.1 YAP influences melanoma cell colony formation *in vitro* 40
3.1.1 Growth of ten melanoma cell lines in soft agar 40
3.1.2 Knockdown of YAP reduces colony formation of melanoma cells 41
3.1.3 YAP increases colony formation of melanoma cells 42
3.2 YAP promotes spontaneous melanoma metastasis 44
3.2.1 YAP promotes invasion of melanoma cells in culture 44
3.2.2 Establishment of a spontaneous murine metastasis xenograft model 45
3.2.3 YAP promotes melanoma metastases *in vivo* 46
3.2.4 YAP-5SA causes primary tumours to grow slower 48
3.2.5 YAP-5SA promotes necrosis of primary tumours 49
3.2.6 YAP-5SA increases vascular components of primary tumours 49
3.2.7 Investigation of YAP in depigmentation of melanoma cells 50
3.3 Identification of YAP target genes 52
3.3.1 Validation of RNA-sequencing 52
3.3.2 Identification of four candidate target genes of YAP 52
3.3.3 *AXL, THBS1, CYR61*, and *CRIM1* mediate YAP-induced invasion of melanoma cells 53
3.3.4 YAP promotes melanoma invasion in a TEAD-dependent manner 54
3.4 Investigation of statin-induced YAP inactivation in melanoma cells 55
3.4.1 Introduction 55
3.4.2 Results 56
3.4.2.1 Simvastatin inhibits melanoma cell viability 56
3.4.2.2 Simvastatin inhibits activity of YAP 57
3.4.2.3 Simvastatin inhibits melanoma cell viability through suppression of GGPP 57
3.4.2.4 GGPP is the key to simvastatin-induced inactivation of YAP 58
3.4.2.5 Investigation of RhoA in statin-induced YAP inactivation 59
Chapter 4 Discussion 61
4.1 The potential role of YAP in melanoma tumorigenesis 61
4.2 The potent capacity of YAP in promoting melanoma progression 61
4.2.1 Invasion and metastasis 61
4.2.2 Necrosis and angiogenesis 62
4.2.3 Tumour growth 64
4.2.4 Depigmentation 65
4.2.5 YAP as a prognostic marker in melanoma 66
4.3 The mechanism of YAP-promoted melanoma invasion 67
4.4 YAP as a therapeutic target in melanoma 68
4.5 Conclusions, limitations and future directions 70
Acknowledgements 73
References 75
Table 1. Optimised cell densities for melanoma cell lines in soft agar assay 114

Table 2. Relative mRNA levels measured by RNAseq and qPCR 115
Appendix 1. Melanoma cell lines used in this project 116
Appendix 2. Reagents, buffers and media 117
Appendix 3. Antibodies 120
Appendix 4. Sequences of siRNAs 122
Appendix 5. Sequences of primers 123

Abstract

Melanoma is an aggressive cancer with extremely unfavourable prognosis. Two main types of melanoma include cutaneous melanoma (CM) accounting for around 95% and uveal melanoma (UM) around 5%. In Australia, melanoma is in the top five most commonly diagnosed cancers, estimated to contribute to over 10% of all new cancer diagnoses in 2017 (Cancer Australia, 2018.). While the overall death rate caused by all cancer is decreasing, the mortality of melanoma has increased in recent years (Howlader *et al.*, 2012; AIHW, 2017). Patients diagnosed only with primary melanoma have relatively high survival rates, whereas when patients are diagnosed with metastatic melanoma, the survival rate is very low (Gershenwald *et al.*, 2017). Currently, the mechanisms that drive melanoma progression and metastasis remain poorly understood; but better therapies are definitely required. *BRAF* mutations are most common in melanoma, occurring in around 50% of this disease (Akbani *et al.*, 2015), which provides a possibility for targeted therapy. Indeed, the United States Food and Drug Administration (USFDA) has approved BRAF inhibitors (BRAFi) and MEK inhibitors (MEKi) as the standard treatment for metastatic melanoma patients harbouring *BRAF* mutations. However, drug resistance occurs in the majority of these patients within two years of treatment (Long *et al.*, 2016). Therefore there is an urgent need to understand the mechanism of BRAFi and MEKi resistance, and find new therapeutic strategies for melanoma. One gene that has been linked to BRAFi resistance is the *YAP*, which is the key downstream effector of a pathway called the Hippo pathway. The Hippo pathway is an important regulator of organ growth in development. Deregulation of the Hippo pathway stimulates the activity of the YAP oncoprotein, which can cause several human cancers (Zanconato, Cordenonsi and Piccolo, 2016). However, the impacts of YAP deregulation in melanoma are not thoroughly understood.

In this project, the roles of YAP in melanoma were examined. Firstly, the impacts of knockdown, overexpression, and activation of YAP on anchorage-independent growth of melanoma cells were assessed using soft agar assays. The results showed that either YAP

activation or overexpression promotes colony formation, whilst YAP knockdown reduces this, suggesting potential influences of YAP on melanoma tumorigenesis. Secondly, the effects of YAP in melanoma invasion and metastasis were investigated. Melanoma cells stably expressing an active YAP mutant (YAP-5SA) have a greater invasive ability, as determined with transwell invasion assays. A spontaneous murine metastasis model was used to investigate the impact of YAP on metastasis. The results demonstrated that YAP-5SA promotes metastasis to multiple organs such as the lung and the liver; YAP-5SA enhances vascularity and necrosis of primary melanoma. Thirdly, mechanisms responsible for YAP-induced invasion were explored. Four potential target genes of YAP, derived from RNA-sequencing data, were found crucial, as well as the key YAP transcription factor partners, TEAD1-4. Finally, a lipid-lowering drug called simvastatin was found to kill melanoma cells and inhibits YAP activity *in vitro*. A post-translational modification, geranylgeranylation, was found to be essential in the statin-induced melanoma cell death and YAP inactivation; RhoA and other geranylgeranylated proteins might be important in these phenotypes.

To conclude, this study explored the role of YAP in melanoma metastatic progression, and identified crucial transcription factors and target genes that mediate YAP-induced impacts on melanoma invasion. Additionally, inhibition of YAP and its mechanism in melanoma cells was preliminarily assessed using simvastatin. Understanding the molecular mechanism of melanoma metastasis and inhibition may help us establish more effective therapies for this disease.

DECLARATION

I hereby declare that all work in this thesis is my own except for what stated within the text. The thesis has not been accepted for any degree and is not concurrently submitted for award of other degree. Until submission of the thesis, the work in this thesis has been publicly presented with a poster by Lie Yang in the 2018 Australasian Melanoma Conference.

Name: Lie Yang

Signature: 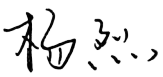

Abbreviations

BSA	Bovine serum albumin
BRAFi	BRAF inhibitor
CM	Cutaneous melanoma
CRIM1	Cysteine-rich motor neuron 1 protein
CTGF	Connective Tissue Growth Factor
CV	Crystal Violet
CYR61	Cysteine-rich angiogenic inducer 61
DAPI	4',6-diamidino-2-phenylindole
dH_2O	Distilled water
Dox	Doxycycline
EC50	Half maximal effective concentrations
ECM	Extracellular matrix
EGTA	Ethylene glycol bis(2-aminoethyl ether)-N,N,N'N'-tetraacetic acid
EMT	Epithelial-to-mesenchymal transition
FACS	Fluorescent activated cell sorting
FBS	Fetal bovine serum
FFPE	Formalin-fixed paraffin-embedded
FPP	Farnesyl pyrophosphate
FTI	Farnesyl transferase inhibitor
GAPDH	Glyceraldehyde-3-Phosphate Dehydrogenase
GFP	Green fluorescent protein
GGPP	Geranylgeranyl pyrophosphate
GGTase I	Geranylgeranyl transferase I
GGTI	Geranylgeranyl transferase I inhibitor
GPCR	G-protein coupled receptor
H&E	Haematoxylin and eosin
hr	Hour
i.p.	Intra-peritoneal
IHC	Immunohistochemistry
IL	Interleukin
IPP	Isopentenyl pyrophosphate
LATS	Large tumor suppressor
MEKi	MEK inhibitor
min	Minute
MITF	Microphthalmia-associated transcription factor
MMPs	Matrix metalloproteinases
MST	Mammalian Ste20-like serine/threonine protein kinase
NDR1/2	Nuclear Dbf2-related protein kinases 1 and 2
NF2	Neurofibromatosis type 2
NSG	NOD/SCID Il2rg-/-

OTP	Orthopedia Homeobox
P/S	Penicillin and streptomycin
PBS	Phosphate buffered saline
PMCC	Peter MacCallum Cancer Centre
p-YAP	Phosphorylated YAP
qPCR	Real-time quantitative polymerase chain reaction
RASSF	Ras association domain family
RIPA	Radioimmunoprecipitation Assay
RNAseq	RNA-sequencing
rpm	Round per minute
RT	Room temperature
SAV1	Salvador homologue 1
sec	Second
TAZ	Transcriptional co-activator with PDZ-binding motif
TBS	Tris-Buffered Saline
TBST	Tris-Buffered Saline supplemented with Tween 20
TEAD	TEA domain transcription factors
TEG	Trypsin-EGTA
TFs	Transcription factors
THBS1/TSP-1	Thrombospondin 1
TYR	Tyrosinase
UM	Uveal melanoma
USFDA	United States Food and Drug Administration
VEGF	Vascular endothelial growth factor
WB	Western blot
wt	Wild type
YAP	Yes-associated protein

Chapter 1 Background

1.1 Introduction of the Hippo pathway

The Hippo signalling pathway is a highly conserved pathway whose main function is to control organ growth during development. The Hippo pathway, also called the Salvador-Warts-Hippo pathway, was first discovered in *Drosophila*. Subsequently, the Hippo pathway was identified in mammals and was found to be highly evolutionarily conserved. Now, the Hippo pathway is recognised as an important pathway that regulates cell behaviours (including cell proliferation, cell survival, cell cycle, cell polarity, and cell adhesion), organ growth, tissue regeneration, tumorigenesis and metastasis. Its activity is controlled by signals such as mechanical forces, attachment to extracellular matrix (ECM), cell junctions, G-protein coupled receptors (GPCRs), and several stress signals. While knowledge on this pathway has grown rapidly, many questions remain as to how it controls tissue growth in development and diseases like cancer.

1.1.1 The discovery of the Hippo pathway

The Hippo pathway was discovered and characterized within the last two decades. This section will introduce the history of the discovery of the Hippo pathway.

In 1995, by loss-of-function examination, the *Drosophila* nuclear Dbf2-related (NDR) family protein kinase Warts (Wts) was discovered as a tumour suppressor, functioning in controlling organ growth and shape as well as cell proliferation (Justice *et al.*, 1995; Xu *et al.*, 1995). *wts* was identified as *wts* mutant tissue gave rise to striking overgrowths. In 2002, the WW-domain-containing protein Salvador (Sav) was identified as a restrictor of cell proliferation, and a promoter of apoptosis (Kango-Singh, 2002; Tapon *et al.*, 2002). Sav was also shown to bind to Wts and work with it to control organ size (Tapon *et al.*, 2002). This was the first time that two proteins of what we now call the Hippo pathway were shown to work together and is often

considered the "discovery" of the Hippo pathway. In 2003 the homologue of a mammalian Ste20-like serine/threonine protein kinase (MST), Hippo (Hpo), was identified by several groups of researchers to be a partner of Sav and to work together with it and Wts to control organ size (Harvey, Pfleger and Hariharan, 2003; Jia, 2003; Pantalacci, Tapon and Léopold, 2003; Udan *et al.*, 2003; Wu *et al.*, 2003; Varelas *et al.*, 2008). Two years later, a new tumour suppressor Mats (Mob as tumour suppressor), a component of the Mob protein superfamily, was discovered as a regulator of organ size in the fly. It was also a physical associator of Wts and found to activate Wts' activity as a protein kinase (Lai *et al.*, 2005; Wei, Shimizu and Lai, 2007). In the same year, Yorkie was identified as a key link between the Hippo pathway kinase cascade and transcriptional regulation (Huang *et al.*, 2005). This was important because it provided the first link between the Hippo pathway core kinase cassette and transcription.

1.1.2 The mammalian Hippo pathway

Although some current known mammalian components of the Hippo pathway were identified earlier than in flies, such as MST1/2 (Creasy and Chernoff, 1995b, 1995a), YAP (Yagi *et al.*, 1999), and transcriptional co-activator with PDZ-binding motif (TAZ) (Kanai, 2000), these proteins had not been investigated carefully until their *Drosophila* homologues were identified and characterised as components of the Hippo pathway. The mammalian Hippo pathway is highly conserved, composed of a core kinase cassette, upstream regulators and downstream transcriptional co-activators. The core kinase cassette includes MST1/2 (*Drosophila* homologue Hpo), Salvador homologue 1 (SAV1, *Drosophila* homologue Sav), MOB kinase activator 1A/B (MOB1A/B, *Drosophila* homologue Mats), and large tumor suppressor 1/2 (LATS1/2, *Drosophila* homologue Wts). MST1/2, the serine/threonine kinases, phosphorylate and activate LATS1/2 with the help of two scaffold adaptor proteins SAV1 and MOB1A/B. Activated LATS1/2 phosphorylate and inactivate two downstream transcriptional co-activators, YAP and TAZ (*Drosophila* homologue Yorkie), which are the key downstream effectors of the Hippo pathway. A recent paper reported that instead of statically residing in one compartment, Yorkie dynamically traffics between the nucleus and cytoplasm, which

indicates that Yorkie's mammalian orthologs YAP/TAZ could also constantly shuttle between the two compartments in a very rapid manner (Manning *et al.*, 2018). LATS1/2-mediated phosphorylation controls the nuclear import of YAP and TAZ and can also sequester them in the cytoplasm, thus restricting their transcriptional function. When YAP/TAZ translocate into the nucleus they bind transcription factors (TFs) such as TEADs to promote transcription of a wide range of target genes. TEAD1-4 are the main TFs that mediate YAP/TAZ-dependent gene transcription to promote tissue growth (Zhao *et al.*, 2008; Zhang *et al.*, 2009). There are also other TFs reported to interact with YAP such as SMADs (Ferrigno *et al.*, 2002), TBX5 (T-box transcription factor 5) (Murakami *et al.*, 2005), p73 (a p53 family member) (Strano *et al.*, 2001), whose transcriptional outputs with YAP have not been established yet.

Organisms must carefully control organ size and tissue homeostasis during development, and the Hippo pathway is believed to play an important role in these. Thus, the core kinases and the downstream effectors must be regulated accurately. Besides the canonical pathway, where YAP/TAZ are regulated by the core kinase cassette, other molecules regulate YAP/TAZ either independent of or partly through the core kinase cascade. For example, neurofibromatosis type 2, NF2 (*Drosophila* homologue Merlin), a tumour suppressor, was found to directly bind and activate LATS1/2 without initiating MST1/2 (Yin *et al.*, 2013). Two subgroups of MAP4Ks, MAP4K1/2/3/5 and MAP4K4/6/7, also act as alternative kinases to phosphorylate LATS1/2 in a similar manner to MST1/2 (Meng *et al.*, 2015; Zheng *et al.*, 2015).

In the canonical pathway, YAP is phosphorylated and inactivated by LATS1/2, a member of the NDR family of protein serine/threonine kinases. Since the yeast Dbf2 kinase recognises HXRXXS motifs, LATS1/2 were hypothesised to inhibit YAP by phosphorylation of the serine on HXRXXS motifs. Zhao et al. (2007) found that YAP2, one of the eight alternatively spliced forms of human YAP, has five HXRXXS motifs, among which the most important residue is the S127 because it showed most resistance to MST1/LATS2 when replaced with alanine. Phosphorylation on the other four LATS1/2 sites in YAP is also important for their regulation as a YAP mutant named YAP-5SA, which contains mutations of five serine residues in the

HXRXXS motifs, cannot be phosphorylated by LATS1/2 and highly active compared to wild-type YAP (wt-YAP) and YAP-S127A (Zhao *et al.*, 2007).

1.1.3 Regulation of the Hippo pathway

Unlike many other well-established pathways, the Hippo pathway is not a linear pathway that receives input signals from a diffusible ligand(s) to a transmembrane protein(s) that subsequently transfers the signals to downstream effectors. The Hippo pathway is regulated by a wide range of upstream signals including 1) Environmental signals mediated by GPCRs, 2) Mechanical cues, and 3) Intracellular molecules, such as TAO1, Ras association domain family (RASSF) and PP2A. Given that YAP/TAZ are the main effectors of the pathway, signals that regulate YAP/TAZ without affecting the core kinases are also summarised in this section.

Environmental signals that are mediated by GPCRs. GPCRs are seven-transmembrane domain receptors that are coupled with G proteins. GPCRs respond to extracellular signals and activate internal signalling pathways involved in a range of physiological processes, especially in metabolism and growth. Many signals such as hormones and growth factors have been proved to either promote or restrict the activity of YAP/TAZ via regulating GPCRs. Initially, YAP/TAZ were found to respond to serum-derived lysophosphatidic acid (LPA) and sphingosine-1-phosphate (S1P) through GPCR signalling. LPA and S1P, the GPCR inhibitors, dephosphorylate YAP/TAZ and stimulate YAP/TAZ activity through Rho GTPases. When LPA/S1P are deficient, such as in serum starvation conditions, YAP phosphorylation is dramatically increased (Miller *et al.*, 2012; Yu *et al.*, 2012). Further studies showed that GPCRs regulate YAP/TAZ depending on the type of coupled G protein. The GPCR inhibitors angiotensin II and oestrogen can activate YAP/TAZ in mammalian cells (Wennmann *et al.*, 2014; Zhou *et al.*, 2015), while the GPCR activators adrenaline and glucagon mediate inhibition of YAP/TAZ by phosphorylating and activating LATS1/2 (Yu *et al.*, 2012). In addition to these small molecules, GPCR-YAP signalling also responds to pH changes,

controlling cell proliferation and survival through the regulation of Rho signalling (Zhu *et al.*, 2015). Mutations in G proteins and GPCRs are frequent in many cancers, especially in melanoma (Kan *et al.*, 2010). The GRM3 (a member of GPCRs family) mutants have shown ability in promoting cell proliferation, survival, and migration of melanoma cells (Prickett *et al.*, 2011).

Mechanical cues: cell-cell adhesion and polarity. Multicellular organisms need intricate regulatory mechanisms to avoid overgrowth during development. Cell contact inhibition has been long considered to contribute to growth control. However, its molecular mechanisms still remain to be understood. The Hippo pathway plays an important role in cell adhesion and polarity. YAP activity is inhibited by LATS1/2 when cells are at high density (Zhao *et al.*, 2007), where TEADs work as major transcriptional mediators (Ota and Sasaki, 2008; Nishioka *et al.*, 2009). Further studies found that cell-cell junctions including basal-lateral junctions, adherens junctions, and tight junctions are all potentially involved in the YAP-mediated inhibition of proliferation induced by high cell density. For example, α-catenin and E-cadherin, two components of adherent junctions, help to maintain cytoplasmic YAP (Kim *et al.*, 2011; Schlegelmilch *et al.*, 2011; Silvis *et al.*, 2011). SCRIB, the mammalian homologue of scribble which was initially found to localise to the basolateral membrane in *Drosophila* (Bilder and Perrimon, 2000), is required to maintain cytoplasmic YAP/TAZ through the activation of the core Hippo kinases (Cordenonsi *et al.*, 2011; Mohseni *et al.*, 2014). Angiomotin family proteins, a component of tight junction complexes in endothelial cells (Bratt *et al.*, 2005), interact and sequester YAP/TAZ either in a Hippo-dependent (Adler *et al.*, 2013; Hirate *et al.*, 2013) or –independent (Chan *et al.*, 2011; Wang, Huang and Chen, 2011; Zhao *et al.*, 2011) manner. PTPN14 (also known as PTPD2, PTP36, and Pez), previously shown to affect cell adhesion (Ogata *et al.*, 1999), is also associated with and inhibits YAP at high cell density (Wang *et al.*, 2012). Thus, generally speaking, YAP/TAZ are mediators of high cell density-induced inhibition of cell proliferation and cell growth.

Mechanical cues: fluid shear stress. Fluid shear stress is an important physical signal for

endothelial cells in both blood vessels and lymphatic vessels, and is responsible for endothelial cells to proliferate, maintain, or process apoptosis. Recent studies have implied that YAP is responsive to flow shear stress in both blood vessels (Wang *et al.*, 2016) and lymphatic vessels (Sabine *et al.*, 2015), contributing to the maintenance of vessels (Nakajima *et al.*, 2017).

Mechanical cues: ECM stiffness. ECM is required for tissues and organs as a supporting scaffold, providing an insoluble environment for cells to attach, migrate, and maintain homeostasis. ECM also transmits environmental signals to cells, ultimately influencing cell growth, differentiation and apoptosis. YAP/TAZ were found to be responsive to ECM stiffness, which is conducted either by a Rho-GTPase-mediated Hippo-independent (Dupont *et al.*, 2011) or JNK-mediated Hippo-dependent manner (Codelia, Sun and Irvine, 2014).

Other intracellular regulators. Some upstream regulators of the Hippo pathway are regulated by more than one signalling input. For example, TAO1, a serine/threonine-protein kinase which is involved in a variety of processes such as the MAPK pathway, DNA damage response and the regulation of cytoskeleton stability, is also detected as a regulator of the Hippo pathway by phosphorylating and activating MST2 (Boggiano, Vanderzalm and Fehon, 2011; Poon *et al.*, 2011). RAF1 (also called c-RAF), a member of RAF family of serine/threonine kinases, is canonically a regulator of MAPK cassettes. RAF1 was found to physically bind MST2, preventing its dimerisation and phosphorylation, thus suppressing MST2-mediated apoptosis (O'Neill, 2004). The inhibitory RAF1-MST2 complex can be dissociated by Ras association domain family 1 isoform A (RASSF1A) which also promotes the interaction of MST2 and LATS, finally inducing YAP-p73-mediated apoptosis (Matallanas *et al.*, 2007).

1.1.4 Downstream transcription factors

YAP acts as a transcriptional co-activator since it does not bind DNA. Several TFs have been reported to interact with YAP including TEADs family, SMADs family, AP-1 (a heterodimer

of c-JUN and c-Fos), NF-E2 and p73 (a member of p53 family). Among these TFs, TEADs are the only one that bind to YAP on its proline-rich region while others bind the WW domains of YAP with their PPxY motifs (Zhao *et al.*, 2010; Hong and Guan, 2012). Mediating the main outputs of YAP, the TEAD family are also the only TFs that have the YAP-induced proliferation output (Zhao *et al.*, 2010). TEADs were the first TFs that were reported to have a strong interaction with YAP, mediating YAP-dependent gene transcription (Vassilev *et al.*, 2001), at the same time this interaction was also confirmed to be conserved in *Drosophila* where Scalloped (the TEAD homologue) binds to Yorkie (the YAP/TAZ homologue) (Wu *et al.*, 2008; Zhang *et al.*, 2008). Previously, the AP-1 transcription factor was defined as a "promoter" of skin cancers (Young *et al.*, 1999; Briso *et al.*, 2013). Later on, its tumour promotion ability was revealed to depend on the YAP/TEAD complex (Zanconato *et al.*, 2015). Accordingly, AP-1 binds to many of the same genes as YAP/TEAD, forms a complex and synergistically activates transcription of target genes (Zanconato *et al.*, 2015).

1.1.5 Crosstalk pathways

As a newly established pathway, the Hippo pathway, regarded to have an important role in organ growth and size control, has linkages with other classical developmental pathways, such as the Wnt/β-catenin, TGF-β, and MAPK pathways. The Wnt/β-catenin pathway plays a crucial role in controlling cell stemness, mediating cell fate during embryonic development and regulating adult tissue homeostasis. Both Wnt/β-catenin and Hippo pathways regulate cell proliferation, by activating and inhibiting it, respectively. Cytoplasmic TAZ can inhibit β-catenin by activating Dishevelled (DVL, one of the partners that bind with phosphorylated β-catenin to form a degradation complex of β-catenin) (Varelas, Miller, *et al.*, 2010), while cytoplasmic YAP can also inhibit β-catenin by sequestrating it in the cytoplasm (Imajo *et al.*, 2012). However, nuclear YAP/TAZ act as cooperators of Wnt signalling. Activated YAP can interact with β-catenin in the nucleus and cooperate in promoting cell proliferation (Heallen *et al.*, 2011). On the other hand, Wnt signalling can also inhibit the Hippo pathway by attracting YAP/TAZ into the nucleus (Azzolin *et al.*, 2014).

The TGF-β signalling pathway is another well-established and highly conserved pathway that largely contributes to cell states and development stages. Inputs of this pathway include TGF-β family cytokines, such as TGF-β, BMPs, activins, and Nodal, delivering signals to downstream TFs, crucially the SMADs family. The Hippo pathway mainly links with the TGF-β pathway by interaction of YAP/TAZ and SMADs. Phosphorylated YAP was reported to bind SMAD2/3 and sequester the complex in cytoplasm, thus inhibiting TGF-β signalling (Varelas, Samavarchi-Tehrani, *et al.*, 2010). On the other hand, activated YAP/TAZ can bind with SMADs and promote their nuclear accumulation and transcriptional activity (Varelas *et al.*, 2008; Nallet-Staub *et al.*, 2015). Besides, YAP/TAZ can form a larger transcription complex with the binding of SMADs, TEADs, and another factor, activating target genes (Fujii *et al.*, 2012; Beyer *et al.*, 2013). In addition to the direct binding of YAP/TAZ and SMADs, TGF-β signalling can also crosstalk with the Hippo pathway by modifying the activity of its core kinases such as LATS2 (Luo, 2017).

The MAPK pathway is another signal transduction pathway that is composed of a chain of protein kinases, transferring various signals from cell membrane receptors to the nucleus. Overall, the MAPK pathway interacts with the Hippo pathway by inhibiting Hippo signalling and promoting YAP activity, while YAP activation increases MAPK activity via transcriptional regulation, possibly in a feedback loop (O'Neill, 2017). For example, RASSF1 can activate MST1/2 by dimerisation and exerting autophosphorylation of MST1/2 (O'Neill, 2004; Hamilton *et al.*, 2009), whereas RAF can prevent the dimerisation and limit Hippo signalling (O'Neill, 2004; Yu *et al.*, 2015). Loss of NF2, the upstream activator of Hippo pathway as mentioned before, can induce RAS activity partly through inactivation of Hippo, in a YAP-TEAD dependent manner (Garcia-Rendueles *et al.*, 2015). The MAPK pathway is one of the most widespread oncogenic pathways across a wide range of tumours. In melanoma, more than half of patients harbour *BRAF* or *NRAS* mutations, highlighting the importance of investigating the role of the Hippo pathway in melanoma, which will be discussed in later sections.

1.1.6 Outputs of the Hippo pathway

Although discovered within the last two decades, the Hippo pathway has been reported to have a multitude of functions in cells, tissues, and organs. Generally, the main role of the Hippo pathway is to regulate organ development and to maintain organ size. At the cellular level, components of the Hippo pathway were shown to be required to limit Cyclin A and Cyclin B level, mediating mitotic exit (Pellock *et al.*, 2007; Shimizu, Ho and Lai, 2008; Jang *et al.*, 2017). Activated or overexpressed YAP causes cells proliferation in a YAP-TEAD-dependent manner (Zhao *et al.*, 2008). In addition to cell proliferation or division, mutants of the Hippo pathway have also shown ability to promote cell growth (Harvey, Pfleger and Hariharan, 2003; Jia, 2003; Wu *et al.*, 2003). Since the Hippo pathway regulates cell proliferation and growth, it also controls organ growth. Mutations or knockdown of core kinases of the Hippo pathway, or overexpression of YAP, results in significant organ overgrowth in both *Drosophila* and mice (Harvey, Pfleger and Hariharan, 2003; Jia, 2003; Wu *et al.*, 2003; Camargo *et al.*, 2007; Zhou *et al.*, 2009; Lee *et al.*, 2010; Lu *et al.*, 2010; Song *et al.*, 2010; Chen *et al.*, 2015). The Hippo pathway also controls apoptosis. Core kinases of the Hippo pathway can promote cell apoptosis in response to stressful conditions (Creasy and Chernoff, 1995b, 1995a; Taylor, Wang and Erikson, 1996; Kakeya, Onose and Osada, 1999; Tapon *et al.*, 2002). Phosphorylated YAP mediated by c-JUN can bind with p73 and promote cell apoptosis in response to DNA damage (Danovi *et al.*, 2008; Tomlinson *et al.*, 2010). In addition, the Hippo pathway regulates cell differentiation/stemness, although the direction may be cell type-dependent. For example, in the liver and neural systems, activated YAP can prevent cell differentiation and keep cell stemness (Cao, Pfaff and Gage, 2008; Yimlamai *et al.*, 2014), whereas hyperactive YAP promotes cell differentiation in the kidney and intestine (Barry *et al.*, 2012; Reginensi *et al.*, 2013). Consistent with these roles, efficient wound healing requires activated YAP and TAZ. In response to tissue injury, Hippo signalling is repressed, resulting in YAP/TAZ accumulation and nuclear translocation, thus promoting cell proliferation and migration and, thereby, tissue repair (Zhao *et al.*, 2008; Cai *et al.*, 2010; Lee *et al.*, 2014; Elbediwy *et al.*, 2016). Generally,

development and regeneration of various organs, including the brain, heart, liver, lung, intestine, breast, and muscle, are under regulation of the Hippo pathway (Fu, Plouffe and Guan, 2017). In addition to controlling cells and organs, YAP/TAZ are also crucial in sprouting angiogenesis and vascular barrier formation and maturation (Kim *et al.*, 2017), which could be a potential mechanism of angiogenesis during tumorigenesis. Predictably, the Hippo pathway is thus associated with various human diseases, especially a wide range of cancers, which will be discussed in the next section.

1.1.7 The Hippo pathway and human diseases

Given the Hippo pathway plays such important roles in cell biology, from embryonic development to adult tissue homeostasis, dysregulation of the Hippo pathway is predictably associated with a variety of human diseases, including cancer. In the nervous system, MST1 was found as a modulator of amyotrophic lateral sclerosis (Lee *et al.*, 2013). In eyes, mice with *NF2* knockout can develop cataracts (Giovannini *et al.*, 2000). TEAD-YAP interactions were found to be disrupted in patients with choroid and retinal degeneration, characterised as Sveinsson's chorioretinal atrophy, where TEAD1 has either mutation or deletion of specific residues that are important for YAP binding (Fossdal, 2004; Kitagawa, 2007). In the cardiovascular system, Hippo signalling restricts cardiomyocyte expansion, whereas activated YAP is important for cardiac function (Xin *et al.*, 2013; Lin and Pu, 2014). Of note, MST1/2, LATS1/2, as well as YAP are all phosphorylated in arrhythmogenic cardiomyopathy, and possibly contributing to this disease (Chen *et al.*, 2014).

Links between tumorigenesis and the Hippo pathway were first shown when mutants of core kinases developed overgrown organs in both *Drosophila* and mice (Tapon *et al.*, 2002; Udan *et al.*, 2003; Lu *et al.*, 2010). Subsequent studies revealed the important role of the Hippo pathway in various human cancers. Unlike many other genes that are mutated in cancers, the Hippo pathway is linked with cancers via accumulation of oncoproteins or downregulation of tumour suppressors rather than mutations of genes. For example, downregulation of MST1/2

and LATS1/2 are frequent in soft tissue sarcomas (Seidel *et al.*, 2007), and are also linked to an aggressive state of breast cancer (Takahashi, 2005). Aberrantly activated YAP is detected in many cancers, and has been shown to promote tumorigenesis, metastasis, and maintenance of cancer-associated cells, drug resistance, and cancer relapse. Amplification of YAP has been reported in a wide range of cancers including liver cancer (Zender *et al.*, 2006), lung cancer (Dai *et al.*, 2003), pancreas cancer (Bashyam *et al.*, 2005), and oesophagus cancer (Imoto *et al.*, 2001). Multiple tumour metastasis has also been proved to be partly promoted by inappropriately upregulated YAP/TAZ (Janse van Rensburg and Yang, 2016). For instance, YAP can promote cell proliferation as well as migration in pancreatic cancer (Kapoor *et al.*, 2014), and Lamar et al. showed that activation of YAP stimulates metastasis in both mammary carcinoma and melanoma (Lamar *et al.*, 2012). Cancer is difficult to cure because patients usually develop drug resistance during therapy. Interestingly, activation of YAP is emerging as a mechanism of drug resistance in many cancers, including hepatocellular carcinoma (Huo *et al.*, 2013; Mao *et al.*, 2014), cholangiocarcinoma (Marti *et al.*, 2015), ovarian cancer (Xia *et al.*, 2014), and oral squamous cell carcinoma (Yoshikawa *et al.*, 2015). Notably, RAF- and MEK-targeted therapies reportedly fail because of increased YAP (Lin *et al.*, 2015).

Although infrequent, mutations of the Hippo pathway are related to cancer. For example, mutation of *NF2* is the cause of a disease called Neurofibromatosis Type 2, an autosomal dominant condition associated with meningiomas and schwannomas (Xiao, Chernoff and Testa, 2003). *NF2* mutations were also observed in around 40–50% of patients with malignant mesothelioma (Bianchi *et al.*, 1995; Sekido *et al.*, 1995). Remarkably, loss of YAP can block *NF2* knockout-induced tumorigenesis of livers in mice, which implies that YAP may be the main effector in cancers caused by *NF2* mutations in human cancers (Zhang *et al.*, 2010).

1.2 Introduction to melanoma

Melanoma is caused by aberrant accumulation of transformed melanocytes. Melanoma includes CM and UM, amongst which CM is the predominant type, accounting for more than

95% of all cases (McGuire, 2016). Melanocytes are function-specific cells mostly located in the basal layer of the epidermis of skin, as well as the middle layer of the eyes (called uvea). They are also localized in the inner ear, the vaginal epithelium, the meninges, the bones, and the heart, producing melanin which is a dark colored pigment that contributes to the colour of these tissues and organs. Melanocytes are highly differentiated cells and are normally in a dormant state, although can proliferate when required such as after injury. Unlimited growth and proliferation of transformed melanocytes cause melanoma, which accounts for ~2% of all skin cancers (Kardynal and Olszewska, 2014). However, it is the most aggressive and lethal skin cancer, setting it apart from most other non-melanoma skin cancers. The incidence of melanoma has increased in the past few decades worldwide, especially among Caucasian populations (McGuire, 2016). Metastatic melanoma has poor prognosis and frequently becomes resistant to therapies.

1.2.1 Disease conditions

The incidence of melanoma is rapidly increasing (AIHW, 2017). The worldwide incidence of melanoma is not evenly distributed, varying 100-fold among countries and regions. Oceania has the highest incidence of melanoma in the world. It is estimated that melanoma in Australia occurs with an incidence of 50 cases per 100,000 people and has a mortality rate of 6.1 case per 100,000 (AIHW, 2017). According to the Australian government, it is among the top five common cancers in Australia, with an estimated over 10% of all new cancer diagnosis in 2017 (Cancer Australia, 2018). Across a lifetime, an Australian has a 5.91% risk (1 in 17) of being diagnosed with melanoma before 85 years old (AIHW, 2017). Patients diagnosed at an early stage with localized melanoma have a relatively high survival rate and good prognosis if the tumour is removed with adequate surgical excision. However, melanoma is aggressive and easily invades distant regions and organs. Metastatic melanoma has a relatively low survival rate as well as poor prognosis. Although invasive melanoma accounts for only approximately 1% of all skin cancers (including basal and squamous cell carcinoma, which are the most common skin cancers), it leads to the majority of deaths due to skin cancer (Facts, 2017).

A key risk factor for melanoma is excessive exposure to ultraviolet radiation from sunlight or artificial tanning devices (McGuire, 2016). Other risk factors include the number of nevi, personal or familiar history of melanoma, and individual susceptibility such as rare germline mutations and personal sun sensitivity (Rastrelli *et al.*, 2014; Facts, 2017). People with intermittent intense exposure to sunlight, especially during childhood and early adolescence, are also in high risk of melanoma. Thus children and adolescents are of vital importance as a target group for prevention of melanoma (Elwood and Jopson, 1997; Tsao and Sober, 1998). Prevention of melanoma should be based on avoiding excessive exposure to ultraviolet rays from both sunlight and other tanning sources, especially during childhood and adolescence. Applying sunblock regularly has been proven to prevent of melanoma and other skin cancers (Green *et al.*, 2011).

1.2.2 The classification of melanoma

Clinical classification

Melanoma, like other malignant tumours, is classified by the TNM staging system. Briefly, T refers to the size of the primary tumour (tumour in situ); N refers to the number of invaded nearby lymph nodes; M refers to distant metastasis. According to the *8th Edition of the American Joint Committee on Cancer (AJCC) Melanoma Staging System*, primary melanoma, defined as T1-T4, N0M0 and pathological stage I-II, can be removed by surgery and has a 5-year survival rate from 82% to 99% and a 10-year survival rate from 75% to 98% (Gershenwald *et al.*, 2017), which is high compared to metastatic disease. Once nearby lymph nodes are involved, the pathological stage goes to stage III, which dramatically reduces patients' survival rates. For example, stage IIID (T4bN3M0) melanoma patients have a ~32% 5-year survival rate (Gershenwald *et al.*, 2017). The outcome of stage IV patients is even poorer, with a median overall survival of only 5-22 months (depending on the exact stage) (Song *et al.*, 2015), and a 5-year survival rate of 15-20% according to the America Cancer Society (Facts, 2017). Compared to the poor prognosis of metastatic melanoma, patients with

primary melanoma have good chance to be cured. However, early diagnosis of melanoma can be challenging (Bishop *et al.*, 2007). Pre-clinical research has identified two phenotypic states of melanoma cells, proliferative and invasive, which will be discussed shortly.

Genetic classification

Cancer is now well known to be driven by aberrant gene function. The first driver mutation of melanoma was unveiled as activating *BRAF* (Davies *et al.*, 2002), in which the most common variant, V600E, occurs early in melanoma development (Pollock *et al.*, 2002). Unlike some other cancers, melanoma derives from more than one driver mutation. Based on multi-platform characterization of a large cohort of 333 CM samples, a genomic landscape study of melanoma revealed the main genomic subgroups: *BRAF* mutation (52%), *NRAS* mutation (28%), and *NF1* mutation (14%), with the rest defined as triple wild type (6%). In the BRAF mutant subgroup, the codon V600E mutation occurs most frequently (Akbani *et al.*, 2015). Interestingly, a study undertaken of the frequency of genetic alterations found that the majority of histologically benign lesions exclusively harboured BRAF V600E mutants, whereas in the remaining histological categories (intermediate lesions, melanomas in situ, and invasive melanoma), additional mutational subtypes were observed, including *NRAS* mutations and others (Shain *et al.*, 2015).

1.2.3 Melanoma phenotype switch

Metastasis a key and life-limiting property of many cancers, especially in melanoma where patients with metastasis have a dramatically worsened prognosis, compared to those with only early-stage tumours. Much effort has been put into understanding the molecular biology of metastatic potential of melanoma. Many genes promote invasiveness of melanoma, such as *TSPAN8* (Berthier-Vergnes *et al.*, 2011), *Thrombospondin 1* (*THBS1*) (Jayachandran *et al.*, 2014), and *NEDD9* (Kim *et al.*, 2006). Others, such as microphthalmia-associated transcription factor (MITF), are inversely linked to invasion and expressed at lower levels in invasive cells. Indeed, MITF was reported to be required for melanoma proliferation (Carreira *et al.*, 2006), but down-regulated during cell invasion (Jeffs *et al.*, 2009). In recent years, it was established

that melanoma cells display heterogeneity at the same lesion. *In vitro* studies have shown that many cultured melanoma cells can be classified into two states based on their gene expression panels, which cluster either with proliferative or invasive phenotypes. These two phenotypes can switch and determine the characteristics of melanoma *in vivo*. However, the gene expression profiles that relate to metastatic behaviour are not correlated with *BRAF* or *NRAS* activating mutations (Hoek *et al.*, 2006).

1.2.4 Current treatments

Current treatment of melanoma is multi-modal. Early-stage melanomas (primary melanomas) can be removed by wide excision of surgery of the skin and subcutaneous tissues, offering a relatively high 5-year relative survival rate. Despite decades of clinical research and trials, the prognosis for patients with metastatic melanoma remains poor. Treatments for malignant melanoma are complex, including surgery, chemotherapy, radiation therapy, and newly emerging targeted therapies and immunotherapy. Surgery is applied to the melanoma in situ, while drug therapies and radiation are used for unresectable metastasis. High-dose interleukin-2 (IL-2) and dacarbazine used to be the only two therapies for advanced melanoma approved by USFDA (Spagnolo and Queirolo, 2012), and are still widely used. However, the response rates are as low as 10-20% (Pectasides *et al.*, 1989; Atkins *et al.*, 1999).

Standard treatment for metastatic melanoma has changed in recent years. According to the National Comprehensive Cancer Network, the first-line therapy for metastatic stage IV melanoma is now immunotherapy (pembrolizumab/nivolumab, or nivolumab/ipilimumab). The two subtypes of immunotherapy drugs are anti-programmed cell death-1 (anti-PD-1) monoclonal antibodies such as pembrolizumab and nivolumab, and anti-cytotoxic T lymphocyte-associated antigen 4 (anti-CTLA-4) monoclonal antibodies such as ipilimumab. Immunotherapy has shown promising efficacy in recent clinical trials. However, the overall response to these monoclonal antibodies is relatively low. Hitherto data showed that immune checkpoint therapies are able to achieve long-term survival of more than 30% advanced

melanoma patients (Wolchok *et al.*, 2017). Immunotherapy drugs can be toxic to normal cells, such that ~10%-15% of patients develop serious side-effects after ipilimumab treatment, sometimes causing death (Hodi *et al.*, 2010). Although nivolumab has a relatively lower ratio of side effects, grade 3 to 5 adverse events occurred in around 10% of patients during the trials (Wolchok *et al.*, 2017). Combination of nivolumab and ipilimumab raised a 3-year survival rate of melanoma patients to 58%, however, grade 3 to 4 side effects occurred in 46% of patients and treatment was discontinued in around 27% of melanoma patients due to serious adverse events (Gellrich, Beissert and Meier, 2018).

As above, around half of melanoma patients harbour *BRAF* mutations, and another one quarter of patients have *NRAS* mutations. The highly prevalent mutations of *BRAF* and *NRAS* suggested vulnerability in melanomas for inhibitors of the MAPK kinases pathway. Multicenter phase III clinical trials have compared vemurafenib and dabrafenib (small-molecule inhibitors of BRAF) to reference chemotherapy dacarbazine, showing increased benefits on metastatic melanoma (Tsao *et al.*, 2012). Considering the efficient inhibiting of metastatic melanoma by BRAFi, both USFDA and European Medicines Agency (EMA) have approved vemurafenib for metastatic melanoma patients harbouring *BRAF V600* mutations. Moreover, BRAF mutant patients have shown correlation with a highly selective sensitivity to MEKi (Solit *et al.*, 2006), suggesting *BRAF* mutations gain hyper-functions via MAPK pathway. MEK thus can be a potential targeted point for advanced melanoma treatment. Clinical phase II/III trials showed that MEKi presents improvements over cytotoxic chemotherapy in NRAS mutant patients (Ascierto *et al.*, 2013; Dummer *et al.*, 2016). Combination of BRAFi and MEKi is well-tolerated and extends survival compared to single agent BRAFi therapy (Long *et al.*, 2016). Compared to other drugs, BRAFi and MEKi specifically target small molecules and hence should present fewer side effects. Also, they induce higher rates of anti-tumour response compared to immunotherapy and chemotherapy. However, ~80% of patients become resistant to BRAFi and MEKi during treatment (Long *et al.*, 2016).

Although both immunotherapy and targeted therapy display clinical benefit in metastatic melanoma, none of them has provided a cure, and the 5-year relative survival of distantly metastatic melanoma was still estimated to be only 18% in 2017. The causes of this are clear. On the one hand, response rates to treatments remain relatively low; namely, patients present intrinsic resistance to current therapies. On the other hand, the majority of melanoma patients tend to gain drug resistance within one or two years during therapy. Since combination of immunotherapy and kinase inhibitors show increased toxicities during trials (Ribas *et al.*, 2013; Minor *et al.*, 2015), new therapeutic strategies are definitely needed.

1.3 The Hippo pathway in melanoma

The Hippo pathway was first discovered in *Drosophila* two decades ago. Its role in organ control and restriction of tumorigenesis is well accepted, as discussed in section 1.1. Cancers arise from unlimited overgrowth and proliferation of cells that subsequently migrate and cause nearby and distant metastasis. Hence, the Hippo pathway may play an important role in cancers including melanoma. Researchers have discovered several clues to help reveal the association of the Hippo pathway and melanoma progression.

1.3.1 The Hippo pathway and uveal melanoma

UM is the most common intraocular malignancy, occurring in choroid, ciliary body, and iris of the eye. UM is a specialized melanoma, accounting for around 5% of all melanoma cases. Therapeutic options are limited for UM, including surgery and radiation therapy, which are often inadequately effective. Uncontrolled UM has a tendency to spread to the liver, an event that is almost universally and eventually fatal. The majority of UM (around 80%) harbour one of two mutually exclusive activating mutations in *GNAQ* and *GNA11*, which encode homologous subunits Gαq and Gα11 (hereafter referred to as Gαq/11) of G-proteins. As discussed previously, GPCRs are very important regulators of the Hippo pathway, regulating activity of YAP, and finally modulating behaviours of the cell. Nuclear localization of YAP is

correlated with mutant Gαq/11 in UM patient samples. Also, activated YAP is accumulated in nucleus in multiple UM cell lines with Gαq/11 mutations. These findings hint at a potential role of YAP in UM. Recent studies have proved that Gαq/11 promote activity and nuclear localization of YAP by inhibiting LATS1/2 kinase activities. In return, activated YAP also acts as a modulator of the oncogenic activity of mutant Gαq/11 in UM. When YAP is knocked down, tumour growth induced by mutant Gαq in UM cell lines is significantly blocked in nude mice models (Feng *et al.*, 2014; Yu *et al.*, 2014; Yu, Zhang and Guan, 2014).

Current studies indicate a potential application of YAP inhibition in UM treatment. Verteporfin, a USFDA-approved drug for treating abnormal blood vessel formation in the eye, is also a compound that disrupts YAP-TEAD interaction (Liu-Chittenden *et al.*, 2012), and recently showed efficacy in treating small pigmented posterior pole choroidal melanoma in a clinical trial (Fabian *et al.*, 2017). Although whether Verteporfin works in UM by inhibiting YAP remains unknown, this trial highlights the targeting YAP as a potential therapeutic approach against melanoma.

1.3.2 Hippo pathway components in melanoma

Mutations of components of the Hippo pathway are rarely reported in melanoma. Instead, they appear to undergo inactivation or hyperactivation. For example, *RASSF1*, whose protein product RASSF is an upstream regulator of the core kinases cascade, was detected to be inactivated by epigenetic modification in a significant number of melanomas (Spugnardi *et al.*, 2003). Further, *TAZ* mRNA has a high expression in melanoma cell lines than in normal melanocytes (Nallet-Staub *et al.*, 2014).

1.3.3 The Hippo pathway in melanoma tumorigenesis and metastasis

Both *in vivo* and *in vitro* experiments have indicated that overexpression of YAP (Lamar *et*

al., 2012) and decrease of NF2 (Murray, Lau and Yu, 2012) contribute to promotion of melanoma tumorigenesis and invasion. Nallet-Staub et al. first showed experimental evidence that YAP/TAZ induces melanoma cells proliferation, colony formation, and migration *in vitro*, as well as promotion of invasive behaviour *in vivo* (Nallet-Staub *et al.*, 2014). Acquisition of invasive potential in melanoma is a pivotal point of disease progression, associated with a poor prognosis in patients. Thus it is of vital importance to uncover the biological mechanisms that drive it. The first systematic investigation of melanoma cell lines at the gene expression level was reported by Hoek, et al. (2006). 86 melanoma cell lines were divided into three cohorts based on their gene expression profiles, including a cohort of cell lines with proliferative phenotypes and another with invasive phenotypes. Interestingly, in invasive cell line gene expression profiles, several well-known YAP target genes were identified, including *connective tissue growth factor* (*CTGF)*, and other potential YAP target genes such as *THBS1* (Hoek *et al.*, 2006). Transcriptional reprogramming was found to underlie the proliferative or invasive state of melanoma cell lines using regulatory landscapes and in silica analysis, revealing TEADs as pivotal regulators of the invasive state (Verfaillie *et al.*, 2015).

1.3.4 The Hippo pathway in drug resistance

BRAF mutant patients, accounting for ~50% of melanoma, are the majority subpopulation in melanoma (Akbani *et al.*, 2015). The Hippo kinases and effectors have been associated with the oncogenic effector BRAF. For example, it was revealed in papillary thyroid cancer cells that BRAF V600E physically interacts with and inhibits MST1 (Lee *et al.*, 2011). In melanoma cells, RAF1 was found to bind MST2 (Feng *et al.*, 2017). The USFDA has approved BRAFi/MEKi for BRAF V600E melanoma patients, however patients usually acquire drug resistance within one or two years after drug treatment (Chapman *et al.*, 2011; Robert *et al.*, 2015). Unfortunately, the molecular mechanism of BRAFi resistance is not clearly understood. In recent years, association of the Hippo pathway and drug resistance is being gradually uncovered, in which the core effector is YAP. Significantly increased YAP expression is detected in patients with BRAF V600E tumours that have worse initial response and drug

resistance to BRAF/MEK inhibition (Lin *et al.*, 2015). Further, silencing of *YAP* enhanced the response to BRAFi/MEKi of tumour cells encoding BRAF and K- or N-RAS, suggesting combined inhibition of YAP and BRAF or MEK may cause significant lethality in both RAF- and RAS- mutant melanomas (Lin *et al.*, 2015).

1.4 Summary and project rationale

This chapter briefly outlines 1) a newly established molecular signaling pathway, the Hippo pathway, and its biological role in multicellular organisms, 2) the basic introduction of malignant melanoma, and 3) current knowledge of the role of Hippo pathway regulation in melanoma. As mentioned previously, to improve the efficacy of melanoma treatment, a new therapeutic strategy is urgently needed. Since the Hippo pathway performs an important role in cancer progression, investigation on the role of YAP in melanoma may help us develop new therapies for this disease. This project aimed to investigate the role of YAP in melanoma, especially its contribution to melanoma metastasis. We hypothesised that YAP, the crucial downstream effector of Hippo pathway, promotes tumorigenesis and metastasis of melanoma. To address this proposal, firstly I investigated the role of YAP in tumorigenesis of melanoma cell lines *in vitro*. Secondly, melanoma cells with active YAP mutant were introduced to mice as xenograft models in order to examine the role of YAP in melanoma metastasis *in vivo*. Thirdly, molecular mechanisms by which YAP mediates melanoma progression were explored. At last, by using a YAP inhibitor simvastatin, this work demonstrated that YAP is a potential therapeutic target in melanoma.

Chapter 2 Materials and Methods

2.1 Cell Culture

All melanoma cell lines (Appendix 1) were cultured in RPMI 1640 + 20mM HEPES medium (Gibco), supplemented with 10% fetal bovine serum (FBS) (Gibco) and 1% Penicilin Streptomycin (P/S) (Gibco). HEK293T cells were cultured in DMEM medium (Gibco),

supplemented with 10% FBS and 1% P/S. All the cell lines were maintained at 37°C in a CO_2 incubator (Binder) with 5% CO_2.

2.2 SiRNAs transfection

Cells were seeded into 6-well plates at optimised density for 24 hours (hrs) before transfection. Media were removed and replaced with 800 µl of P/S-free fresh RPMI media. 0.8 µl of Lipofectamine RNAiMAX transfection reagent (Invitrogen) and 5 µl of 5µM siRNAs (Appendix 4), were respectively mixed with 100 µl of Opti-MEM Reduced Serum Media (Gibco) for 5 minutes (min) at room temperature (RT). Then they were mixed and incubated for 20 min at RT before applying on cells. Cells were trypsinised and suspended after 24 hrs to set up various assays if necessary or collected for western blots after 48 hrs transfection.

2.3 Establishment of MeWo-RhoA/RhoA-F stable cell lines

Constitutive vectors were introduced to cells via retroviral transduction in order to generate stable cell lines. 1×10^6 HEK293T cells were seeded into 100 mm dishes (CellStar) with 6 ml P/S free DMEM 24 hrs before transfection. 2.5 µg of pLPC-GFP-RhoA^{VIG} or RhoA^{VIG}-F plasmids (donated by Dr. Gianni Del Sal, LNCIB, Trieste, Italy) plus 2.5 µg of amphoteric retroviral packaging vectors were incubated in 200 µl of P/S free DMEM for 5 min at RT. Meanwhile 12.5 µl of FuGENE® HD Transfection Reagent (Promega) were incubated individually in the same conditions. The two types of solutions were mixed and incubated for 20 min at RT, and then were added onto HEK293T cells drop by drop. Cells were refreshed with 6 ml of P/S free DMEM 24 hrs after transfection. Virus-containing media were collected 48 hrs after transfection. The media were filtered, mixed with polybrene (8 µg/µl, 1:1000) (Merck), and applied to MeWo cells seeded one day before. The MeWo cells were incubated with virus-containing media for 24 hrs, and refreshed with complete media for another 24 hrs. Cells were selected with puromycin (1µg/ml) for 7 days to generate a pool with stable transduction.

2.4 Western Blotting

Protein extraction from 6-well plate

Cells were washed with cold phosphate buffered saline buffer (PBS, Appendix 2) twice before lysis buffer was applied. The lysis buffer was the Radioimmunoprecipitation Assay (RIPA) buffer (Appendix 2) freshly supplemented with PhosSTOP phosphatase inhibitor (Roche) and cOmplete protease inhibitor (Roche). Cell lysates were collected into 1.5 ml eppendorfs, incubated on ice for 20 min and centrifuged at 13,500 rpm for 15 min at 4˚C. Supernatants were collected for direct use or stored at -80˚C.

Protein concentration measurement

Protein concentration was measured by Lowry protein assay, using DC protein assay reagent A, reagent B, and reagent S (Bio-Rad). To generate a standard curve for protein concentration, 0.5 µl, 1 µl, 2 µl, 4 µl, and 8 µl of 2 µg/µl bovine serum albumin (BSA) (Roche) solution were loaded into a 96-well plate. 2 µl of cell lysate was loaded into a well to be measured. Reagent A and reagent S were mixed at a ratio of 40:1. 20 µl of the mixture was loaded into each well. Then 200 µl of reagent B was loaded and incubated at RT for 25 min. Absorbance was measured by a VERSAmax microplate reader (Molecular Devices Corporation, Sunnyvale, CA, USA) at 750 nm and converted to protein concentration according to the standard curve.

Protein Gel electrophoresis

The Bolt™ 4-12% Bis-Tris Plus Gels, 15-well (Invitrogen) were used to do gel electrophoresis. Gel electrophoresis was performed with Bolt™ MES SDS Running Buffer (Invitrogen), at a voltage of 150 V for 70 min until proteins were separated. Precision Plus Protein Dual Color Standards (Bio-Rad) were used as protein markers.

Transfer protein from gel to PDVF membrane

The PDVF membrane was cut into a size of around 7.5 × 9 cm^2 and pre-treated with 100% methanol for 15 seconds (sec). A transfer sandwich was setup by putting together one sponge, two filter papers, one PVDF membrane, one protein gel, two filter papers, and one sponge sequentially. Transfer was performed at 110 V for 90 min.

Immunoblotting

The PDVF membrane was incubated with 10% milk in TBST (Appendix 2) for 1 hr at RT. The membrane was incubated with primary antibodies that were diluted with 5% milk in TBST for 1 hr at RT, and then rinsed for 3 × 5 min. Then 1:5000 secondary antibodies were applied to

the membrane for 50 min at RT.

Development

After blotting with secondary antibodies, the membrane was rinsed with TBST, incubated using the ECL™ Prime Western Blotting Detection Reagent Kit (GE Healthcare) for 3 min. The ECL solution was made freshly before use (solution A: B =1: 1). Development was performed in dark room.

2.5 RNA Extraction, Reverse Transcription, and Quantitative Real-Time PCR

2.5.1 RNA isolation

RNAs were collected from cells seeded in 6-well plate. Medium was discarded and 1 ml of TRIzol RNA Isolation Reagent (Invitrogen) was added onto cells in each well. Cells were collected into 1.5 ml eppendorfs. Samples were stored at cold room (at 4˚C) for up to 7 days if not processing immediately. Otherwise samples were incubated at RT for 3 min, then centrifuged at 12,000 × g at 4˚C for 15 min. Samples separated into a lower red phenol-chloroform, and interphase, and a colourless upper aqueous phase. The aqueous phase containing the RNA was transferred into a new eppendorf. Then 500 µl of isopropanol was added into each sample, and incubated for 10 min before centrifuged at 12,000 × g at 4˚C for 10 min. Total RNA precipitate would form a small white pellet at the bottom of the eppendorf. The supernatant was discarded with a sucker. The pellet was resuspended with 1 ml of 75% ethanol and centrifuged for 5 min at 10,000 × g at 4˚C twice. The supernatant was discarded with a sucker. The RNA pellet was dried in air until a gel-like pellet appeared, before resolved in 20 µl of nuclease-free water (Promega).

2.5.2 Reverse transcription

The following components were added into each sample: 1 µg of total RNA, 1µl of Oligo(dT)$_{15}$ Primer (Promega), 1µl of 10 mM dNTP Mix (a set of 10 mM of dATP, dGTP, dCTP and dTTP, Promega), and nuclease-free water up to 13µl in total. The mixture was heated at 65˚C for 5

min and then incubated on ice immediately for at least 1 min. Then the following components were added into each sample: 4 μl of First-Strand Buffer (5×), 1 μl of 0.1 M DTT, 1 μl of RNaseOUT™ Recombinant RNase Inhibitor (Invitrogen), and 1 μl of SuperScript III Reverse Transcriptase (Invitrogen). The mixture was then incubated at 50˚C for 60 min, followed by heating at 70˚C for 15 min to stop the reaction. The productions were used as cDNA template in next step.

2.5.3 Quantitative real-time polymerase chain reaction (qPCR) analysis

QPCR was performed with the Fast SYBR® Green Master Mix (Applied Biosystems). The following were loaded in each sample: 10 μl of Fast SYBR® Green Master Mix (2×), 1 μl of forward primer, 1 μl of reverse primer, 1 μl of cDNA template, and 7 μl of nuclease-free water, to make up to a 20-μl reaction. The PCR was run on a StepOne Plus (Applied Biosystems) instrument, using the StepOne Plus software (Applied Biosystems). The program for running qPCR was set following the instruction on the Fast SYBR® Green Master Mix Quick Reference Card. Data were normalized to *GAPDH* expression. Sequences of primers are listed in Appendix 5.

2.6 Cell Viability Assay

Cell viability assays were performed on 96-well plates. Cells were seeded 24 hrs before applied with drugs (Simvastatin, GGTI, or FTI, Sigma). The next day drugs were added on cells at gradient concentrations and incubated for 3-4 days. The cell viability was measured using an alamar blue reagent (Appendix 2). The medium was discarded, then a reagent mixture of 20 μl of alamar blue and 100 μl of RPMI was added into each well and incubated for 3 hrs. The fluorescent intensity was measured by the BMG POLARSTAR Microplate Reader (gain, 1350) with the excitation wavelength at 579 nm, and emission wavelength at 584 nm.

2.7 Soft agar Assay

Anchorage-independent growth of melanoma cells was assessed using a soft agar colony formation assay. Assays were performed in 96-well plates. Cells were seeded in 50 μl of 0.375% agarose (Bio-Rad) diluted in RPMI media, which was overlaid on 75 μl of 0.75%

agarose in RPMI media. Cells were fed with 10 µl of RPMI media every 3-4 days. To measure the viability, cells were applied with 15 µl of alamar blue for 3 hrs. The fluorescent intensity of alarmar blue was measured as described in section 2.6.

2.8 Invasion Assay

The invasive ability of melanoma cells was measured using invasion assays. The Millicell Hanging Cell Culture Insert with PET 8 µm (Merck) transwell inserts were placed into 24-well plates and coated overnight with 10 µg of Matrigel (Corning) diluted in 100 µl of serum-free RPMI media at 37˚C. MeWo cells were added into the insert of each chamber in 200 µl of serum-free RPMI media at a density of 6×10^4/insert. The lower chamber was loaded with 600 µl of RPMI media supplemented with 10% of FBS. After 48-hrs incubation, inserts were washed with PBS for twice before and after stained in Crystal Violet (CV) (Appendix 2) for 15 min. Non-invaded cells remaining on upper layer of inserts were removed by cotton swabs. Invaded cells were imaged using an inverted microscope (Zeiss Axio Vert. A1; Carl Zeiss AG, Oberkochen, Germany) at a magnification of 100×. Five fields were randomly chosen of each insert. Invaded cells were counted manually.

2.9 Fluorescent Activated Cell Sorting (FACS)

FACS was used to identify transduced cells that express GFP. Cells in culture were prepared by trypsinisation, and coated in PBS supplemented with 2% of FBS. Dissociated tumour cells were prepared as described in the section 2.10.2, and coated in staining media (Appendix 2). Cells to be sorted were maintained on ice. 4',6-diamidino-2-phenylindole (DAPI, Roche) was used at a concentration of 10 µg/ml to identify dead cells. For cells prepared from tumour samples, additional antibodies were applied as described in section 2.10.3 and Appendix 3. Cells were run on BD LSR II flow cytometer (BD Biosciences, San Jose, CA) or BD FACS Canto II flow cytometer (BD Biosciences, San Jose, CA, USA). Cell sorting was performed by technicians from the FACS Facility of Peter MacCallum Cancer Centre (PMCC, Parkville, Melbourne, VIC, Australia) using the BD FACS AriaII Cell Sorter (BD Biosciences, San Jose, CA, USA).

2.10 Animal Experiments

NOD/SCID Il2rg-/- (NSG) mice were used in this study. All mice were housed in a laminar flow room with constant temperature and humidity at the PMCC Animal Facility. Animal husbandry was performed by technicians from the PMCC Animal Facility. All experiments were carried out in accordance with PMCC Animal Ethics and Experimentation Committee protocols (#E526).

2.10.1 Establishment of melanoma xenograft model

NSG mice were subcutaneously transplanted with human melanoma MeWo-Ctrl and MeWo-YAP-5SA cells to generate melanoma xenografts. As MeWo-Ctrl and MeWo-YAP-5SA cells were transfected with plasmids that express GFP with a bi-cistronic promoter, cells were sorted as GFP positive and tested as mycoplasma negative before injection. 1,000 MeWo-Ctrl or MeWo-YAP-5SA cells were suspended in 25 µl of staining media, and mixed with 25 µl of Matrigel to make a 50-µl injection solution. This solution was subcutaneously injected into the right flank of each NSG mouse at day 0. Tumour growth was monitored every week by palpation, and tumour diameter was measured with a vernier caliper. Mice were randomly separated into control group and doxycycline (Dox) treatment group. When Dox treatment started, the treated groups received intra-peritoneal (i.p.) injection with 100 µl of 0.4 mg/ml Dox for two consecutive days. The treated groups also received Dox in drinking water at a concentration of 2 mg/ml until sacrificed.

2.10.2 Dissociation of melanoma cells form solid tumours

The method was adapted from Quintana et al (Quintana *et al.*, 2008). After sacrificing the mice, the xenograft tumours were directly obtained with tweezers and scissors, placed on ice in 50 ml of Hank's Balanced Salt Solution (without Ca^{2+} and Mg^{2+}, HBSS-/-, Sigma). Two small pieces of tumour tissues were cut off and respectively aimed to make frozen tissues and formalin-fixed paraffin-embedded (FFPE) tissues. The rest tissues were chopped by scissors and a McIIwain tissue chopper (Brinkman Instruments, Westbury, NY). The slurry was placed in 50 ml Falcon tube with cold HBSS-/- buffer and weighed, before centrifuged at 220 × g for

4 min at 4˚C. The sediment was resuspended in 10 ml of warmed digest media (Appendix 2) per 1 g of tumour tissue. The tissue slurry was placed in 37°C water bath for 20 min, triturated vigorously every 5 min with disposable pipettes. After digestion, the cell preparation was made up to 50 ml with HBSS-/- buffer and pelleted by centrifugation at 220 × g for 4 min at 4˚C. A secondary enzymatic digestion was performed by resuspending the cell pellets in 100 µl of DNase (10 u/µl) (Sigma) per 1 g of original tissue (final DNase = 200 u/ml after TEG was added in next step). Warmed trypsin-EGTA (TEG, Appendix 2) was added and mixed at 5 ml per 1 g tissue. The mixture was place at 37˚C for 2 min without trituration. Equal volume of cold staining media was added to quench the activity of trypsin. The sample was centrifuged at 220 × g for 4 min at 4˚C, and resuspend in 10 ml of staining media per 1 g of tissue and filtered through 40-µm cell strainers. The sample was cleaned by density centrifugation with OptiPrep™ Density Gradient Medium (Sigma), centrifuged at 800 × g for 20 min at 4˚C, using low deceleration. After centrifuging, the middle phase containing cells was removed with upper layer and transferred to a 50 ml Falcon tube. Then the sample was centrifuged at 220 × g for 4 min at 4˚C, resuspended and cells were counted with a haemocytometer.

2.10.3 Staining and FACS of dissociated tumour cells

Dissociated tumour cells were stained for FACS. General preparation was performed as described in section 2.9. Cells were stained with the following antibodies: HLA (human leukocyte antigen) -ABC (G46-2.6-PE, BD) for detection of human cells, mouse CD45 (30-F11-APC, BD) that detects the leukocyte common antigen ubiquitously expressed in all nucleated hematopoietic cells, mouse Ter119 (TER-119-APC, BD) to detect erythrocytes, and mouse CD31 (390-APC, eBioscience) to detect endothelial cells. After staining, FACS was performed for analysis and sorting. Gating strategies were as follows. Initially, cell populations were identified from the prepared sample by a cell morphology gating based on side-scatter area (SSC-A) and forward-scatter area (FSC-A). Single cells were identified from the morphology gate by side-scatter width (SSC-W) versus side-scatter height (SSC-H) and a second gate of forward-scatter width (FSC-W) versus forward-scatter height (FSC-H). Viable cells were identified from single cells by gating DAPI exclusive populations. Human

melanoma cells were selected from the viable cells through positive HLA selection (PE-A) and exclusion of haematopoietic and endothelial cells (CD45/CD31/Ter119, APC-A). Finally, GFP (FITC-A) intensity was analysed of the gated human melanoma cells.

2.11 Histopathology and Immunochemistry Analysis

2.11.1 Histological and Immunochemical Staining

Fixation, embedding, and section

Tumour and organ tissues were fixed in 10% neutral-buffered formalin (Australian Biostain) overnight at RT. The samples were then embedded in paraffin by Centre for Advanced Histology and Microscopy of PMCC. Section was performed by Dr. Youfang Zhang (Shackleton Laboratory, Monash University, Melbourne, VIC, Australia).

Histological staining

Haematoxylin and eosin (H&E) staining was performed to histologically study the primary tumours. The paraffin sections were dewaxed in histolene (Trajan) for 3 × 5 min, and hydrated through graded alcohols (100%, 95%, and 75%) sequentially and distilled water. Sections were stained with haematoxylin (Amber Scientific) for 5 min, and then washed with tap water for 2 min, followed by incubation in 95% ethanol for 10 dips. Sections were stained with eosin (Sigma) for 1 min, and then dehydrated through graded alcohols (95%, 100%, 100%, and 100%) and then histolene for 3 × 5 min. Sections were mounted in Ajax Finechem D.P.X. neutral mounting medium (Thermo Fisher).

Immunochemical staining

The paraffin sections were pre-dewaxed in an oven at 60˚C for 30 min, dewaxed in histolene, and hydrated through graded alcohols and distilled water. Antigens were retrieved using target retrieval solution (Dako) at 125˚C for 3 min heated by a pressure cooker. The sections were allowed to cool down, and washed in TBS for 3 times. Quenching of endogenous peroxidase was performed in freshly made 3% hydrogen peroxide in methanol for 15 min. The sections were then sequentially washed in TBS for 3 times, incubated in blocking solution (1% BSA in TBST) for 60 min at RT. Excess solution was discarded and the primary antibody (Ki67 or

human mitochondria antibody) diluted in blocking solution was applied at 4˚C overnight. After washing with TBST, the slides were incubated with secondary antibody using an ImmPRESS™ HRP Anti-Rat IgG (Peroxidase) Polymer Detection Kit (Vector) for 60 min at RT. After washing with TBST, the slides were developed using AEC substrate-chromogen (Dako) for 5 min. The samples were sequentially counterstained with haematoxylin for 10 sec, washed with distilled water, and differentiated in Scott's tap water (Appendix 2) for 30 sec. Sections were mounted in ProLong Gold antifade mountant (Invitrogen). Specially, for CD31 staining, antigen was retrieved in specific retrieval solution (Appendix 2) at 37˚C for 20 min. After incubation of anti-CD31 antibody, sections were incubated with a biotinylated rabbit anti-rat IgG antibody (Vector) for 1 hr at RT. Tyramide amplification was conducted using a TSA® biotin detection kit (PerkinElmer). Sections were visualized using AEC, then counterstained with haematoxylin and Scott's tap water, and mounted as described before.

2.11.2 Histological and Immunochemical Quantification

For necrosis analysis, one H&E-stained section was chosen from each sample of primary tumour tissues. Analysis was performed with whole section scanning using the Olympus VS120 Virtual Slide Microscope (Olympus, Tokyo, Japan). Necrotic areas were identified manually. For metastasis analysis, one human mitochondria antibody-stained section was chosen from each sample of lung tissues. The whole sections were scanned by the Olympus VS120 microscope. Files were converted to tagged image file format (TIFF) tiles at a binning of 2 × 2 using the VS-ASW FL software. Ten TIFF files full with lung tissues were randomly chosen and analysed from each section. Metastatic areas, represented by staining of the human mitochondria, were identified and counted. For vascular analysis, one CD31-stained section was chosen from each sample of primary tumour tissues. Images were taken at 200× magnification in bright field using the Olympus BX51 microscope (Olympus, Tokyo, Japan). One field that with the highest vascular density was chosen from each section. For cell proliferation analysis, one Ki67-stained section was chosen from each sample of primary tumour tissues. Images were taken in bright field using the BX51 microscope at a magnification

of 400×. One field full with viable cells was randomly chosen and analysed from each section. Ki67 and CD31 positive areas were identified using FIJI (Fiji Is Image J) version 1.49 (NIH, Bethesda, MD; http://imagej.nih.gov/ij). All quantifications were performed using the FIJI software.

2.12 Statistical Analysis

All data were analysed using t-test or analysis of variance (ANOVA) test performed by GraphPad Prism version 7 (GraphPad Software Inc, California, USA). ns, $P>0.05$; *$P<0.05$; **$P<0.01$; ***$P<0.001$; ****$P<0.0001$.

Chapter 3 Results

3.1 YAP influences melanoma cell colony formation *in vitro*

YAP has been shown to be important in tumorigenesis of various cancers, including UM (Yu *et al.*, 2014). However, YAP has been relatively poorly studied in CM. Previous studies have shown that YAP contributes to proliferation of melanoma cells (Nallet-Staub *et al.*, 2014; Xiong *et al.*, 2017). However, evidence is lacking in regard to YAP and other cancer-associated phenotypes of melanoma cells. Therefore, the soft agar colony formation assay was performed in this project to measure YAP's impact on anchorage-independent growth of melanoma cells.

3.1.1 Growth of ten melanoma cell lines in soft agar

Anchorage-independent growth shows the ability of cells to grow and form single colonies individually in a semi-solid medium, which is considered a hallmark of tumorigenesis. The soft agar assay is a common method to monitor anchorage-independent cell growth. Before testing the function of YAP using soft agar assays, a panel of ten melanoma cell lines was used to characterise the colony formation ability of melanoma parental cells in soft agar. The ten cell lines were A375, IPC-298, HMCB, HT144, SK-MEL-28, SK-MEL-2, CO13, CO67, CO27, and MeWo, which include *BRAF, NRAS* mutations, and cells that are wild-type for these two major melanoma mutations (Appendix 1). The ability of cells to form individual colonies is influenced by experimental conditions such as the density of cells and the time period cells grow. Thus it is important to optimise seeding densities and time period. The growth time should be long enough for cells to grow and proliferate. As a result, ten days was appropriate. Also, the density should not be too high in order to allow the formation of colonies from single cells. Thus, different densities ranging from 1,000 to 20,000 cells/each well were tested (Table 1). Melanoma cells at optimised cell densities were grown in soft agar in 96-well plates for two weeks and were imaged on day 5 and day 10 to record the progression of colony formation (Figure 1). Overall, the majority of melanoma cell lines showed the ability of anchorage-

independent growth. Eight out of ten cell lines formed colonies in two weeks. A375 and HMCB cells formed colonies most quickly, even though they were seeded at lower densities, suggesting higher tumorigenic abilities. SK-MEL-28, SK-MEL-2, HT144, and IPC-298 cells generated middle-sized colonies, whereas MeWo cells formed relatively small colonies. Two cell lines, CO27 and CO67, did not form colonies in soft agar in two weeks. Preliminarily, no strong association between melanoma cell line genotypes and colony formation abilities was found. For more accurate conclusions on this, more cell lines should be tested.

3.1.2 Knockdown of YAP reduces colony formation of melanoma cells

To examine the function of YAP in melanoma, soft agar assays were conducted with several melanoma cell lines bearing vectors that allowed shRNA-mediated knockdown of endogenous YAP. Previously, our lab established melanoma cell lines by stably transfecting with Dox-inducible lentiviral empty vectors (Ctrl) or vectors encoding small-hairpin RNA targeting the *YAP* gene (shYAP). The transcription of shYAP is normally inactive, and is only activated when cells are treated with Dox (Figure 2A). To assess the function of YAP on colony formation of melanoma cells, soft agar assays were performed in 96-well plates with transfected HMCB, MeWo, HT144, and A375 cells. These four cell lines were chosen because their parental cells showed the ability of colony formation, as described in section 3.1. Dox was applied on both Ctrl cells and shYAP cells, labelled as Ctrl+Dox and shYAP+Dox. For untreated control, cells were labelled as Ctrl-Dox and shYAP-Dox. Simultaneously, cells were seeded for western blot using an anti-YAP antibody to measure the protein level of YAP, which showed efficient knockdown of YAP in these cells (Figure 2B). After two weeks in culture, cell numbers were quantified using the alamar blue assay, which is a common method to measure metabolic function and cellular health. In this assay, a blue and non-fluorescent reagent called resazurin is reduced to a pink and highly fluorescent substance called resorufin in a reducing environment produced by viable cells. The readings represent relative cell numbers. As cell colonies are formed because of the proliferation of cells, alamar blue is also an efficient indicator of cell colonies. In four cell lines, knockdown of YAP consistently

reduced cell colonies, whereas their control groups had no significant differences in cell colonies (Figure 2B). In HMCB cells, knock down of YAP caused a reduction of cell colonies at around 65% to that of control cells; in HT144 and A375 cells, knock down of YAP caused around 30% reduction in cell colonies; in MeWo cells, around 50% of cell colonies were inhibited by knocking down YAP (Figure 2B). These results indicate that YAP is required in anchorage-independent cell growth of a wide range of melanoma cells, suggesting a potential role of YAP in melanoma tumorigenesis.

3.1.3 YAP increases colony formation of melanoma cells

As knockdown of YAP reduced colony formation of melanoma cells, it was important to know if overexpressed or hyperactive YAP could increase this phenotype. Therefore, a tet-on system with inducible expression of YAP-5SA was used, where the Dox-inducible empty vectors (pTRE3G-GFP) or vectors encoding YAP-5SA were introduced to MeWo cells. YAP-5SA is a YAP mutant with modifications of five serine residues to alanine, and is resistant to phosphorylation by LATS1/2, thus retaining a high basal activity (Zhao *et al.*, 2007). To investigate the function of YAP-5SA in melanoma cells, colony formation assays were performed with the transfected MeWo-Ctrl and MeWo-YAP-5SA cells. Both Ctrl and YAP-5SA cells were treated either with (+) or without (-) Dox. As the anti-YAP antibody measures the protein level of total YAP, it was used to measure the level of YAP including YAP-5SA in these cells. Western blot analysis confirmed the expression of YAP-5SA in YAP-5SA+Dox cells (Figure 2C). The results showed that MeWo cells expressing YAP-5SA formed more cell colonies, compared to Ctrl+Dox cells. However, the colony number of Ctrl+Dox cells was smaller than that of the Ctrl-Dox cells (Figure 2C). This was likely caused by doxycycline toxicity, since Dox has been reported to induce apoptosis of a variety of tumour cells including melanoma cells (Fife *et al.*, 1997; Onoda *et al.*, 2006; Mouratidis, Colston and Dalgleish, 2007; Shieh *et al.*, 2010). To eliminate this effect, which confounded this experiment, constitutive expression vectors encoding wt-YAP, YAP-2SA, YAP-5SA, or YAP-7SA were used to generate stable transfected MeWo cell lines, which were generated in our lab. YAP-2SA,

similar to YAP-5SA, is an active YAP mutant, bearing 2 mutations of serine to alanine at S127/381 (Zhao *et al.*, 2009). YAP-7SA, found by our collaborators (Zhang et al., unpublished), is a novel mutant of YAP identified in a melanoma patient sample. Again western blots were performed at the same time with soft agar assays (Figure 2D), showing efficient overexpression of wt-YAP, expression of YAP-2SA and YAP-7SA. Cells overexpressing wt-YAP, or expressing YAP-2SA or YAP-7SA, all generated more colonies than control cells when grown in soft agar. However, cells expressing YAP-5SA had no significant elevation of colony number (Figure 2D). One possible explanation is that the protein level of total YAP was only slightly elevated compared to control cells, suggesting a weak expression of YAP-5SA in these cells (Figure 2D) To convince the impacts of YAP-5SA in cultured melanoma cells, more experiments should be done with cells that express enough YAP-5SA.

To conclude, knockdown of endogenous YAP consistently reduced colony growth of different melanoma cell lines, and overexpression of wt-YAP, as well as expression of several forms of active YAP mutants increased melanoma cell colony formation. These results indicate that YAP can influence anchorage-independent growth of melanoma cells, suggesting an important role of YAP in melanoma tumorigensis.

3.2 YAP promotes spontaneous melanoma metastasis

YAP has been shown to promote metastasis in several cancers (Warren, Xiao and Lamar, 2018). However, its role in melanoma metastasis has not been explored thoroughly. Previous research reported that knockdown of YAP causes reduced metastasis in the lung following tail vein injection (Nallet-Staub *et al.*, 2014). As tail vein injection directly seed cells into the vascular system, it is not a robust metastasis assay, and more likely reflects the ability of cells to seed directly in the lung rather than metastasise from a primary cancer growth. Therefore, to better understand YAP's contribution to the intrinsic metastatic ability of melanoma *in vivo*, a spontaneous metastasis model was used in this project.

3.2.1 YAP promotes invasion of melanoma cells in culture

Before the *in vivo* experiment, a potential role of YAP in promoting invasion of melanoma cells was assessed *in vitro*. To examine the role of YAP in melanoma cell invasion, a transwell invasion assay was performed with Dox-inducible MeWo-Ctrl and MeWo-YAP-5SA cells. The invasion assay utilises a permeable transwell insert, which separates the 24-well chamber into upper and lower layers. Matrigel is added onto the upper layer of the insert, and therefore the system roughly mimics the physical microenvironment of a tissue. Cells whose invasive ability is to be examined are seeded into the upper layer and attracted by a chemoattracting solution (e.g. medium supplemented with higher concentration of FBS) placed in the lower layer of the chamber. After a short period of incubation, cells with invasive ability will pass through the Matrigel, move down to the lower side of the insert via pores on the insert membrane (Figure 3A). Thus the number of invaded cells allows quantification of their invasive ability.

MeWo-Ctrl and MeWo-YAP-5SA cells were seeded at optimised densities into transwell inserts that were pre-coated with Matrigel. After incubation for 48 hours, cells were stained with CV solution. Non-invaded cells remaining on the upper layer of the insert were removed,

and invaded cells on the lower layer of the insert were imaged. As shown in Figure 3BC, more YAP-5SA+Dox cells were found at the lower side of the transwell membrane, suggesting that they are highly invasive. In contrast, control cells that did not express YAP-5SA showed little invasive ability (Figure 3BC). Simultaneously, cells were seeded in 96-well plates at the same density for cell viability measurements (Figure 3D). There was no significant change in cell viabilities among each group of cells, indicating the increased cell invasion was not caused by changes in cell number. These results indicate that expression of YAP-5SA promotes the invasive ability of melanoma cells, suggesting a potential role of YAP in melanoma metastasis.

3.2.2 Establishment of a spontaneous murine metastasis xenograft model

In order to investigate the role of YAP in melanoma metastasis *in vivo*, a xenograft mouse model with spontaneous metastasis was established. Tail vein injections are a widely used way to examine the metastatic ability of cells but these are limited because cells are directly placed into the bloodstream. Patient tumour metastasis is a more complicated process in which the invading cells have to evade the in situ tumour, invade the ECM, penetrate the endothelial barrier, and entry the circulatory system, before they extravasate and seed a secondary organ. Therefore, the spontaneous metastatic xenograft model is a better mimic of the pathophysiological behaviour of metastasis, which provides more robust information on the intrinsic metastatic ability of cancer cells.

In this model, NSG mice were used. NSG mice are immunodeficient, as they lack mature T cells, B cells, and natural killer (NK) cells (Shultz *et al.*, 2005; Shultz, Ishikawa and Greiner, 2007). NSG mice are also deficient in many cytokine pathways as well as innate immunity (Shultz *et al.*, 1995, 2005).Therefore, NSG mice allow the generation of various human tumours without immune rejection. A previous report has shown successful tumour formation of single human melanoma cell in NSG mice (Quintana *et al.*, 2008), which provides evidence of using few human melanoma cells for each mouse in this project. As a result, all mice successfully generated in situ tumours within three months (Figure 4A). Spontaneous

metastases were observed in multiple organs including lungs, livers, kidneys, hearts, and lymph nodes (Figure 4B). The lung was the organ that displayed most metastases, with the liver as the second, followed by the kidney and the heart. Lymph nodes also showed high levels of metastases, whilst the muscle, pleura, and mesenteric system also did so, although rarely.

3.2.3 YAP promotes melanoma metastases *in vivo*

Examination of the macrometastasis

Using the spontaneous metastasis xenograft model, the metastatic ability of MeWo-Ctrl and MeWo-YAP-5SA cells was examined *in vivo*. To induce expression of YAP-5SA, Dox was applied on mice by i.p injection for two consecutive days, and drinking water was replaced with Dox water until sacrifice. Dox treatment started when the diameter of tumours reached 5 mm, and mice were sacrificed individually when tumour diameter reached 20 mm (Figure 5A). To analyze metastasis, autopsies were performed. Figure 5B shows the representative organs generated from the autopsy. All mice with expression of YAP-5SA generated metastases, among which 7 out of 8 mice were burdened with heavy metastasis (Figure 5C). Consistently, mice bearing primary tumours that expressed YAP-5SA had many more metastases in multiple organs including lungs, livers, kidneys, hearts, and lymph nodes (Figure 5D). In contrast, at least half of control mice did not generate metastases in any organs. These results suggested that YAP plays an important role in promoting melanoma metastasis *in vivo*. However, the growth time of primary tumours was significantly prolonged in YAP-5SA+Dox mice than in others (Figure 7B), which raised the possibility that the increased metastases were caused by the prolonged growth time of YAP-5SA+Dox tumours rather than enhanced metastatic capacity.

To eliminate the difference of tumour growth time and to avoid its potential influence on metastasis, a second *in vivo* experiment was performed. All mice were treated with Dox for the same period of time and were sacrificed at the same time point (Figure 5E). 6 out of 24 mice were not treated with Dox, among which 3 were injected with MeWo-Ctrl and the other 3 were

MeWo-YAP-5SA. 18 out of 24 mice were treated with Dox, in which 9 were injected with MeWo-Ctrl and the other 9 were with MeWo-YAP-5SA. Dox treatment started when the biggest tumour reached 10 mm, and all mice were sacrificed in two weeks when the biggest tumour reached 20 mm. 24 mice were sacrificed in 3 batches within two weeks, and at each time experimental mice were sacrificed together with a same ratio of control mice. Upon this method, the time effect was completely eliminated.

Upon autopsy, macrometastases were observed in lungs, livers, kidneys, and lymph nodes. All mice in the YAP-5SA+Dox group had macrometastases in distant organs. In contrast, only 2 out of 9 mice in Ctrl+Dox group had generated distant metastases. Additionally, half of the mice without Dox treatment showed no macrometastasis (Figure 5G). YAP-5SA+Dox mice displayed macrometastases in multiple organs including lungs, livers, kidneys, and lymph nodes. Contrastively, macrometastases of Ctrl+Dox mice were limited to one organ, the lung. Ctrl/YAP-5SA mice without Dox treatmentalso displayed macrometastases in lungs, livers, and lymph nodes, but not in kidneys (Figure 5H). In lungs, macrometastases were observed in 77.78% of 5SA+Dox mice, 22.22% of Ctrl+Dox mice, and 16.67% of Ctrl/YAP-5SA-Dox mice. In livers, 66.67% of 5SA+Dox mice and 16.67% of Ctrl/YAP-5SA-Dox mice were observed with macrometastases, while no Ctrl+Dox mice had macrometastases. In kidneys, only YAP-5SA+Dox mice had macrometastases, with a percentage of 11.11% (Figure 5H). These phenotypes indicate that more macrometastases were caused by expression of YAP-5SA.

Examination of the micrometastasis in lungs

As all mice in this second *in vivo* experiment were sacrificed together when the biggest tumour reached 20 mm, the overall growth time of tumours was shorter than the first *in vivo* experiment, resulting in smaller and fewer macrometastases that were hard to distinguish with naked eyes (Figure 5F). Hence, for more accurate analysis, micrometastasis was assessed using immunohistochemistry (IHC) staining. Lung tissues were used in this analysis as the lung was the most invaded organ. An anti-human mitochondria antibody was used to identify all human cells in mice lung tissues, providing more precise evidence of micrometastasis from in situ

melanomas, as compared to H&E staining (Figure 6A). In the YAP-5SA expression group, micrometastases in lungs were observed in all 9 mice. In contrast, only around half of control mice (2/3 of Ctrl/YAP-5SA-Dox mice, and 5/9 of Ctrl+Dox mice) had lung micrometastases (Figure 6B). Although micrometastases were observed in control mice, their abundance was less than that in YAP-5SA+Dox mice. Quantifications were conducted with stained lung tissues. Strikingly, the density of micrometastases of the YAP-5SA+Dox group, which was defined as number of micrometastases per mm^2 lung tissues, was substantially higher (Figure 6C). When quantified, the YAP-5SA expressing group had a mean number of micrometastases of 15.19 per mm^2 lung tissues. In contrast, that of control groups were 0.97 for Crol-Dox, 0.30 for YAP-5SA-Dox, and 0.56 for Ctrl+Dox. Similarly, the percentage of micrometastatic area, defined as human mitochondria positive areas divided by total area, was increased in YAP-5SA+Dox group, at 10.03% (Figure 6D). In contrast, the percentage of micrometastatic area in control groups was 0.51% for Ctrl-Dox group, 0.01% for YAP-5SA-Dox group, and 0.06% for Ctrl+Dox group. Moreover, the sizes of micrometastases were also significantly enlarged in the YAP-5SA+Dox group, with a mean size of each micrometastatic lesion at 5510 μm^2, whereas that of control groups was 4455 μm^2 for Crol-Dox group, 108.7 μm^2 for 5SA-Dox group, and 504.1 μm^2 for Ctrl+Dox group (Figure 6E). Unexpectedly, mice in the Ctrl-Dox group also generated enlarged micrometastases compared to the other two control groups. This could be because the number of mice in this group (n=3) was small, increasing the impact of outlier data. To conclude, more mice bearing primary tumours with expression of YAP-5SA had more metastases in multiple organs, with the density, area, and mean size of micrometastases in lungs all increased. These results indicate a strongly enhanced metastatic burden in YAP-5SA expressing mice, suggesting that YAP is likely to promote metastasis of melanoma *in vivo*.

3.2.4 YAP-5SA causes primary tumours to grow slower

Unexpectedly, YAP-5SA+Dox tumours grew slower than control tumours, and this phenotype was consistent in both *in vivo* experiments (Figure 7AC). In the first experiment, when tumours were collected at a size of 20 mm, it took longer for YAP-5SA expressing tumours to grow from 5 mm to 20 mm (Figure 7B). In the second experiment, when all tumours were collected at the same time, YAP-5SA expressing tumours were significantly smaller than control tumours (Figure 7C). These results suggested that expression of YAP-5SA could cause primary tumours to grow slower while promoting their metastasis.

3.2.5 YAP-5SA promotes necrosis of primary tumours

In the examination of primary tumours, necrosis was assessed using H&E staining. Histologically, proteins are acidophilic and can be stained in light pink by an acidic dye eosin, while the nucleus can be stained by haematocxylin in blue. Necrosis is mainly initiated by environmental death factors, in which cells display a progression of chromatin condensation, and finally end in nucleus degradation and cell lysis. Therefore, necrotic areas can be easily identified with H&E staining. By measuring the area of light pink, necrosis was identified and quantified (Figure 8A). YAP-5SA expressing tumours had strikingly increased necrotic area (Figure 8B). The necrotic area had a mean value of 39.38% in YAP-5SA+Dox tumours, whereas it was 11.35% in Ctrl-Dox tumours, 5.14% in 5SA-Dox tumours, and 3.37% in Ctrl+Dox tumours. This result suggested that YAP-5SA expression induced necrosis of primary melanoma tumours. As apoptosis and necrosis can share some similarities (Coleman, 2010), it's hard to morphologically differentiate apoptotic cells from necrotic cells in progress. Further investigation of apoptosis in primary tumours could be performed using IHC staining with specific markers such as terminal deoxynucleotidyl transferase dUTP nick end labeling (TUNEL) and Cleaved Caspase-3 (Asp175).

3.2.6 YAP-5SA increases vascular components of primary tumours

Angiogenesis is another hallmark of tumour progression. To examine vascularity in primary tumours, IHC was performed using an anti-CD31 antibody, as CD31 is a commonly used marker of endothelial cells. The tumour field with highest CD31+ density was imaged and analysed in each sample (Figure 9A). Chosen fields did not contain necrotic elements. Both density and area of vascular components were significantly increased in YAP-5SA expressing tumours (Figure 9BC). Vascular components density was defined as the number of vascular components per mm^2. For the YAP-5SA+Dox group, the mean value of vascular components density was 215.6, whereas for Ctrl-Dox, YAP-5SA-Dox, and Ctrl+Dox groups, the mean densities were 75.19, 108, and 67.65, respectively. In addition, the percentages of CD31+ area in total area were 1.56%, 2.33%, 1.57%, and 3.21% for Ctrl-Dox, YAP-5SA-Dox, Ctrl+Dox, and YAP-5SA+Dox groups respectively. As for the mean size of vascular components, there was no significant difference among groups (Figure 9D). These results show increased vascularity in YAP-5SA expressing tumours, suggesting that YAP-5SA promotes angiogenesis in melanoma tumours, which could enhance metastasis of these tumours.

3.2.7 Investigation of YAP in depigmentation of melanoma cells

An interesting phenotype observed in the above mouse tumour experiments was that tumours bearing YAP-5SA expression were less pigmented. In comparison, control tumours were much darker. This phenotype was consistent in two independent *in vivo* experiments (Figure 10A).

To decipher whether depigmentation could be directly caused by expression of YAP in melanoma cells, *in vitro* experiments were performed. Two pigmented cell lines, C006 and LM28, were transfected with either empty vectors or constitutive vectors encoding wt-YAP or YAP-7SA. Colours were recorded by imaging cell pellets in 15 ml Falcon tubes. Cell pellets were centrifuged from populations of 100 million or 600 million cells. After cells were passaged for ≥10 generations, YAP-7SA expressed in both cell lines caused a loss of pigmentation, while wt-YAP induced a subtle reduction in pigment (Figure 10B). In pigmentation biochemistry, tyrosinase activity is considered rate limiting. The human

tyrosinase is encoded by the *TYR* gene. Additionally, MITF is an essential transcription factor in pigmentation as it controls many of the enzymes of key steps in the melanin synthesis. Therefore, to investigate the mechanism of YAP-induced depigmentation of melanoma cells, mRNA levels of *TYR* and *MIFT* were measured. YAP-7SA caused a clear decrease in *TYR* and *MIFT* mRNA levels in both C006 and LM28 cell lines. In contrast, wt-YAP had no effect compared to control cells (Figure 10C). It should be noted that, owing to time limitations, these experiments were only performed in duplicate and, to confirm the result, should be repeated again. In conclusion, these preliminary data suggested that expression of YAP-7SA could cause depigmentation of melanoma, at least partly through down-regulating *MITF* and *TYR*.

3.3 Identification of YAP target genes

YAP has a strong ability to promote melanoma metastasis, as described above. As YAP is a key transcriptional co-activator of the Hippo pathway, controlling transcription of a wide range of downstream target genes, it is of importance to identify specific target genes of YAP that mediate invasion of melanoma cells. In addition, it is important to define the TFs that bind to YAP and mediate transcription of genes that promote invasion.

3.3.1 Validation of RNA-sequencing

To identify YAP target genes in melanoma cells, our lab performed RNAseq on MeWo-5SA and control cells. Cells were treated with Dox for 16 hours to induce genes transcribed immediately after YAP induction. Bioinformatics analysis was performed by Jason Li and Amarasinghe Kaushalya from the Bioinformatics Core Facility of PMCC. As a result, 146 genes were identified to be upregulated in YAP-5SA expressing MeWo cells, which were defined as potential YAP target genes. To validate these data, mRNA levels of 20 genes were measured by qPCR with MeWo-5SA and control cells. *GAPDH* was used as the internal control. Of these genes, the mRNA level of *ITGB2* was the most elevated (93.5 fold), followed by *CYR61* (38.2 fold), *CTGF* (15.4 fold), *THBS1* (8.0 fold), *TGFB2* (6.8 fold), and *IL6* (5.2 fold) (Figure 11). Conclusively, mRNA levels measured by qPCR were consistent with RNAseq data (Table 2), indicating reliable results of gene transcription changes generated by RNAseq.

3.3.2 Identification of four candidate target genes of YAP

As RNAseq data were validated to be reliable, target genes that might mediate the YAP-promoted invasion of melanoma cells were chosen from the upregulated gene list. Previously, Hoek and colleagues reported two gene signatures of melanoma cells, the proliferation signature and invasion signature, which could be used to predict the phenotype of melanoma

cells (Hoek *et al.*, 2006). When comparing the Hoek invasion signature and the YAP signature generated in our lab, several genes were found to be shared by both. In reviewing the literature, we found that several genes in this overlapping group were reported to be relevant to metastasis and be targets of YAP. For example, *AXL* is a gene encoding AXL receptor tyrosine kinase that transduces signals from the ECM to the cytoplasm. Previous studies reported that elevated *AXL* expression is linked to poor prognosis of melanoma, as well as contributing to invasion and metastasis in MITF-lacking melanomas (Sensi *et al.*, 2011). *THBS1* encodes a protein called Thrombospondin 1, abbreviated as TSP-1, which is an adhesive glycoprotein that mediates cell-to-cell and cell-to-matrix interactions. TSP-1 was also demonstrated to promote invasion of melanoma cells through epithelial-to-mesenchymal transition (Jayachandran *et al.*, 2014). Additionally, *CYR61*, also known as *CCN1*, encodes a protein called cysteine-rich angiogenic inducer 61 (CYR61), which is a well-characterised YAP target. Moreover, cysteine-rich motor neuron 1 protein (CRIM1), a transmembrane protein encoded by the *CRIM1* gene, was recently discovered to regulate migration of cancer cells (Zeng *et al.*, 2015). Hence, four candidate YAP target genes that have been linked to metastasis, *AXL*, *THBS1*, *CYR61*, and *CRIM1*, were chosen for further studies.

3.3.3 *AXL, THBS1, CYR61,* and *CRIM1* mediate YAP-induced invasion of melanoma cells

To investigate whether these candidate YAP target genes mediated invasion of melanoma cells, each gene was individually knocked down in YAP-5SA overexpressing cells by transient transfection using small interfering RNA (siRNA) targeting specific genes or Orthopedia Homeobox (OTP) as control. In order to introduce knockdown of the genes in a YAP-hyperactive condition, Dox was used to induce expression of YAP-5SA 24 hrs before the transfection was conducted. The efficiencies of knockdown were validated using western blot analysis (Figure 12B) and to measure the invasive abilities of cells, transwell invasion assays were performed. Consistent with section 3.2.1, cells with expression of YAP-5SA were more invasive than control cells. In YAP-5SA expressing cells, individual knockdown of the four

candidate genes reduced the invasive ability of melanoma cells (Figure 12AC). In comparison to YAP-5SA expressing MeWo cells that were treated with OTP as control, knockdown of *AXL*, *THBS1*, *CYR61*, and *CRIM1* reduced invaded cells to 26.3%, 35.8%, 45.4%, and 41.2%, respectively. Simultaneous cell viability assays were performed, and no decrease was observed in cell viability among each group of cells, indicating no reduction of cell proliferation (Figure 12D). These results suggest that the four candidate genes, *AXL*, *THBS1*, *CYR61*, and *CRIM1* are all crucial target genes that mediate YAP-induced invasion of melanoma cells.

3.3.4 YAP promotes melanoma invasion in a TEAD-dependent manner

TEAD family proteins (TEAD1-4) are the most important TFs that bind to YAP and mediate transcription of target genes that regulate proliferation, survival and cell adhesion. Therefore, TEADs could also be crucial in promotion of melanoma metastasis. To investigate this idea, TEAD1-4 were simultaneously knocked down in MeWo-5SA cells, by transient transfection, conducted after Dox treatment. The efficiency of knockdown was confirmed using a pan-TEAD antibody that detects TEAD1-4 protein levels (Figure 12B). In YAP-5SA expressing cells, knockdown of TEAD1-4 reduced melanoma cell invasion induced by YAP-5SA (Figure 12AC). TEAD1-4 knockdown reduced cell invasion to 39.8% compared to YAP-5SA expressing only. Again, the simultaneous cell viability assay confirmed that the reduction in cell invasion was not caused by decreased cell viability (Figure 12D). These results indicated that TEAD1-4 knockdown inhibited the ability of YAP to induce melanoma cell invasion, suggesting that YAP promotes invasion in a TEAD-dependent manner.

3.4 Investigation of statin-induced YAP inactivation in melanoma cells

3.4.1 Introduction

Statins are inhibitors of the hydroxymethylglutaryl-CoA (HMG-CoA) reductase enzyme, and block an early key step in the mevalonate pathway, thereby inhibiting the biosynthesis of sterols and cholesterol. The mechanism of how statins inhibit the mevalonate pathway can be schematically described as Figure 13. Isopentenyl pyrophosphate (IPP), an intermediate in the pathway, synthesises Geranylgeranyl- and farnesyl pyrophosphate (GGPP and FPP), two isoprenoid intermediates in the pathway. GGPP is able to modify specific proteins through a post-translational modification called geranylgeranylation, which is mediated by geranylgeranyl transferase I (GGTase I); while FPP can modify proteins through farnesyl transferase-mediated farnesylation. Simvastatin inhibits the mevalonate pathway by suppressing HMG-CoA reductase, thus limiting both GGPP and FPP, and their functions in geranylgeranylation and farnesylation. GGTase I inhibitor (GGTI) and farnesyl transferase inhibitor (FTI) block the abundance of geranylgeranylated proteins and farnesylated proteins, respectively (Figure 13).

Statins are lipid-lowering drugs that are widely used in patients with hypercholesterolemia, and are also recommended as long-term cardiovascular plaque stabilization agents. In the *2013 ACC/AHA Guideline on the Treatment of Blood Cholesterol to Reduce Atherosclerotic Cardiovascular Risk in Adults*, statin treatment is recommended as a primary and secondary prevention for cardiovascular diseases (Stone *et al.*, 2014). In recent years, an increasing amount of preclinical research has reported the anti-cancer effect of statins *in vitro* and in animal models. The anti-cancer function of statins includes different types of leukemia and different solid cancers such as breast cancer, colon cancer, prostate cancer, gastrointestinal cancer, lung cancer, liver cancer, kidney cancer, pancreas cancer, bladder cancer, as well as melanoma (Stryjkowska-Góra *et al.*, 2015). The major anti-tumor effect of statins has been linked to reducing cell proliferation and inducing apoptosis. Despite much preclinical research, the clinical trials and clinical database analyses showed inconsistency on the anti-tumor effects

of statins in various cancers (Chae *et al.*, 2015). Therefore, their potential as anti-cancer agents remains controversial.

Given that the anti-cancer effect of statins is still debated, it is worthwhile to understand the mechanism by which statins exhibit inhibition of cancer cell viability and proliferation. A paper published in 2014 using drug screening in a breast cancer cell line reported statins as inhibitors of YAP (Sorrentino *et al.*, 2014). To decipher YAP's potential as a drug target in melanoma, I studied the inhibition of YAP by simvastatin and the underlying mechanism in melanoma cells.

3.4.2 Results

3.4.2.1 Simvastatin inhibits melanoma cell viability

To investigate whether statin-induced inhibition of YAP occurs in melanoma cells, cell viability assays were performed with a panel of melanoma cell lines treated with different concentrations of simvastatin. Melanoma cell lines used were IPC-298, A375, CO67, MeWo, CO13, and HT144. Overall, the maximum concentration of simvastatin used was 40 μM and the minimum was 0.046 μM. The gradients of concentrations were optimised for each cell line to generate precise dose-response curves. DMSO was the solvent of simvastatin; thus for controls, cells were treated with DMSO that was equivalent to the maximum concentration of simvastatin (40 μM or 20 μM depending on the cell line). Cell viabilities were measured by alamar blue assays after 72-hrs treatment. Relative cell viability was identified by normalising the value of cell number measurements to that of control cells. As most of the concentrations were between 0 to 10 μM, the values of concentrations were transformed to log[μM]. As shown in Figure 14A, all melanoma cell lines were responsive to simvastatin. The dose-response curves showed that the half maximal effective concentrations (EC50s) of melanoma cell lines ranged between around 0.7 to 6.7 μM. MeWo and A375 were the most sensitive, with EC50s smaller than 1 μM. IPC-298 and HT144 were moderately sensitive, with EC50s at around 2 μM, while CO67 and CO13 have relatively less sensitivities, with EC50s at around 5 μM. Hence, all melanoma cell lines used in this work were highly susceptible to simvastatin.

3.4.2.2 Simvastatin inhibits activity of YAP

Given that all melanoma cell lines were responsive to simvastatin, it could be an effective drug for melanoma, and the mechanism by which it acts is worthwhile of study. Statins have been reported to regulate the subcellular localisation and activity of YAP in breast cancer cells (Sorrentino *et al.*, 2014). Therefore, it is likely that the simvastatin-induced decrease of melanoma cell viability is via suppression of YAP activity. To address this hypothesis, western blot and qPCR were used to analyse the expression level and transcriptional activity of YAP. MeWo and IPC-298 cell lines were used as representative cell lines for further investigation, given that they were, respectively, the most and less but not the least sensitive cell lines to simvastatin. As there is currently no direct method to measure YAP activity, the ratio of phosphorylated YAP (p-YAP) and total YAP is normally used to evaluate YAP activity. Total YAP and p-YAP level were measured using an anti-YAP antibody and an anti-YAP-S127 antibody, respectively. Western blot analysis showed that the p-YAP level was increased in both MeWo and IPC-298 cells treated with simvastatin. By contrast, the total YAP level remained unchanged in cells treated with simvastatin (Figure 14B). This suggests that the Hippo pathway was induced by simvastatin that would normally correspond with decreased YAP activity. To examine this further, qPCR was performed with MeWo cells. *CYR61* and *CTGF* are well-established transcriptional targets of *YAP*, and therefore they were used as indicators of YAP activity. Both *CYR61* and *CTGF* mRNAs levels were decreased in cells treated with simvastatin, indicating suppressed transcriptional activity of YAP (Figure 14C). These results suggest that simvastatin inhibits YAP in melanoma cells by promoting Hippo pathway-dependent phosphorylation of YAP, although this requires further study such as rescue experiments to be sure.

3.4.2.3 Simvastatin inhibits melanoma cell viability through suppression of GGPP

As described above, the statin-inhibited mevalnonate pathway has two main ways to synthesise specific proteins, which can be respectively blocked by GGTI and FTI. To examine the effect of GGTI and FTI on melanoma cells, cell viability assays were performed with IPC-298, A375, MeWo, and CO67 cell lines. Again the concentration gradients were optimised for each cell line, with the maximum at 20 μM and minimum at 0.001 μM. As GGTI was dissolved in

DMSO, and FTI in dH_2O, DMSO and dH_2O were used as controls to normalise measurements. The drug-response curves showed that the EC50s of GGTI of most melanoma cell lines were relatively low, in a range from 2 to 5 μM, whereas that of CO67 cells was above 5 μM (Figure 15A). For each cell line, the EC50 of GGTI was higher than that of simvastatin, implying that simvastatin is a more effect drug in this context. Importantly, all cell lines showed largely reduced viabilities close to 0% at a concentration of 20 μM of GGTI (Figure 15A). In contrast, four cell lines all retained viabilities higher than 20% when treated with 20 μM FTI, especially A375, MeWo, and CO67 cells whose viabilities were higher than 50% (Figure 15B). Thus GGTI had a strong inhibitory effect on all of the melanoma cell lines, whereas FTI showed only slight inhibition. In conclusion, the dose-response curves of GGTI and FTI suggest that GGPP was more crucial to statin-reduced melanoma cell viability. To further test this, rescue experiments were employed with MeWo cells using GGTI, FTI, and simvastatin. Cells were treated with DMSO as a control for simvastatin, and treated with methanol as controls for GGPP and FPP, since these were dissolved in methanol. Strikingly, GGPP largely rescued the inhibition of cell viability induced by simvastatin, whereas FPP had a significant but only modest rescue (Figure 15C). This result, together with the dose-response curves, suggest that GGPP in the mevalonate pathway is a crucial intermediate for melanoma cell survival.

3.4.2.4 GGPP is the key to simvastatin-induced inactivation of YAP

As YAP is not a direct product of the mevalonate pathway, internal regulators must exist that mediate statin-induced inactivity of YAP. Therefore, it is important to know whether geranylgeranylated proteins or farnesylated proteins are regulators of YAP. To address this, western blot and qPCR assays were used to examine the protein level and transcriptional activity of YAP in MeWo and IPC-298 cells. As showed in Figure 16C, neither GGTI nor FTI impacted total YAP levels, whereas GGTI enhanced the p-YAP level, similar to simvastatin. In contrast, FTI had no effect on p-YAP. These results suggest induction of Hippo pathway-mediated phosphorylation of YAP by GGTI, but not by FTI. *CYR61* and *CTGF* again were used as transcriptional indicators of YAP in qPCR analysis. mRNA of *THBS1*, a YAP target gene described in section 3.3, was also analysed. The result indicated a significant inhibition

of transcriptional activity of YAP by GGTI (Figure 16A). In contrast, FTI had no significant influence on levels of YAP target genes (Figure 16B). Rescue experiments were performed with MeWo cells treated with simvastatin or a combination of simvastatin and GGPP or FPP, and the results were consistent with cell viability assays. mRNA levels of *CYR61*, which were decreased by simvastatin, was almost fully rescued by GGPP. In contrast, FPP only slightly rescued them (Figure 16D). It should be noted that this rescue experiment was only performed once; triplicate repeats should be conducted. To conclude, GGPP, but not FPP, was essential in mediating the inactivation of YAP induced by simvastatin in melanoma cells.

3.4.2.5 Investigation of RhoA in statin-induced YAP inactivation

The above data suggested that geranylgeranylated proteins could regulate YAP activity, and mediated statin-induced YAP inactivation in melanoma cells. Importantly, geranylgeranylated proteins, which are involved in proliferation, include GTPases such as Rac-1, Cdc42, and RhoA. The Rho family of small GTPases can regulate YAP activity and have oncogenic functions. For example, RhoA is an activator of YAP, inhibiting phosphorylation and promoting nuclear accumulation of YAP in breast cancer cells (Sorrentino *et al.*, 2014). Therefore, RhoA was hypothesized as the regulator of YAP that mediated statin-induced YAP inactivation.

To address this idea, a RhoA mutant was used, which was kindly donated by donated by Dr. Gianni Del Sal. As wild-type RhoA undergoes geranylgeranylation, a posttranslational modification involving transfer of a geranylgeranyl group to the sulphydryl group of Cys residues (near C-termini) of target proteins, the RhoA mutant was established to bear a farnesylation motif (RhoA-F) instead of a geranylgeranylation motif in wild-type RhoA. Thus RhoA-F was used as a bypass of the requirement of the geranylgeranylation for RhoA to be biologically functional (Figure 17A). In theory, the RhoA-F can be inactivated by FTI while wild-type RhoA is inactivated by GGTI. MeWo cells transfected with vectors encoding either RhoA or RhoA-F were thus treated with FTI, followed by measurement using qPCR of *CYR61, CTGF,* and *THBS1* mRNA levels. These mRNA levels were reduced in MeWo-RhoA-F cells

after treatment with FTI (Figure 17C), indicating decreased transcription activity of YAP. However, in RhoA cells, mRNA levels were increased after treatment of FTI. This could be because FTI blocked synthesis of farnesylated proteins and therefore enhanced the dependence of cells on geranylgeranylated proteins, e.g. RhoA, thereby promoting YAP activation. Additionally, when Rho A and RhoA-F cells were treated with GGTI, the mRNA levels were decreased in both cell lines (Figure 17D). This suggests that RhoA is not the only geranylgeranylated protein that mediates simvastatin-induced YAP inactivation; other geranylgeranylated proteins must be important in this process.

To confirm these results, more experiments should be conducted. For example, activities of RhoA/A-F should be confirmed after transfection using methods such as identification of membrane attachment of RhoA/A-F by immunofluorescence or using a RhoA activation assay kit. Also, inactivation of RhoA/A-F by GGTI/FTI should be confirmed using methods mentioned above. To further confirm the indications described in last paragraph, more direct targets of YAP should be included as transcriptional indicators. In addition, rescue experiments using FPP in FTI-treated MeWo-RhoA-F cells could be performed. In conclusion, these preliminary data suggest RhoA as an important geranylgeranylated protein that mediates inactivation of YAP by simvastatin in melanoma cells (Figure 17B).

Chapter 4 Discussion

4.1 The potential role of YAP in melanoma tumorigenesis

YAP/TAZ are able to induce melanoma cells proliferation, colony formation *in vitro* (Nallet-Staub et al., 2014.). Recent studies provided evidence that knockdown of YAP was able to inhibit cell proliferation of melanoma cells (Xiong *et al.*, 2017). However, a potential impact of YAP hyperactivity on other cancer-associated phenotypes of melanoma cells had not been studied when I commenced my Master's studies. In this project, effects of knockdown of endogenous YAP and overexpression of YAP (wild type or mutant) were assessed in a panel of melanoma cell lines using the soft agar assay, since this assay represents the ability of cells to grow independently of a solid surface, which is a hallmark of tumorigenesis (Borowicz *et al.*, 2014). As shown in Figure 2, knockdown of YAP consistently inhibited colony formation of several melanoma cell lines, and overexpression of either wild type YAP or mutant YAP promoted colony formation of melanoma cells. These results indicated that YAP is important for melanoma cells to grow in soft agar, suggesting a requirement of YAP in promoting tumorigenic ability of melanoma cells. To further investigate this, additional cancer-related phenotypes, such as limitless proliferation and resistance to apoptosis, as well *in vivo* mouse studies, could be assessed with melanoma cells bearing either YAP knockdown, overexpression, or hyperactivity. Because YAP is a transcriptional co-activator, it is also important to find its co-operating transcription factors, their downstream target genes and how they work together in regulating melanoma tumorigenesis.

4.2 The potent capacity of YAP in promoting melanoma progression

4.2.1 Invasion and metastasis

Multiple tumour metastasis has been proved to be partly promoted by inappropriately upregulated YAP/TAZ (Janse van Rensburg and Yang, 2016.). YAP promotes cell proliferation and migration in pancreatic cancer (Kapoor et al., 2014.), and Lamar et al. showed

that activation of YAP stimulates metastasis in both mammary carcinoma and melanoma (Lamar et al., 2012.). YAP knockdown was reported to inhibit melanoma cell invasion *in vitro* and lung metastasis *in vivo* following tail vein injection (Nallet-Staub *et al.*, 2014; Xiong *et al.*, 2017). However, little is known about the role of YAP in contributing to melanoma progression such as spontaneous metastasis and angiogenesis *in vivo*. In this study, in situ melanoma was introduced using xenograft models, and thereby spontaneous metastasis was assessed. YAP-5SA greatly promoted melanoma metastasis, not only when primary tumours were controlled to be at same size, but also when primary tumours were significantly smaller than control tumours (Figure 5). When harbouring primary tumours that expressed YAP-5SA, more mice displayed metastasis, as well as a heavier metastatic burden in more organs. These results highly suggest a potent promotion of spontaneous metastatic ability by YAP. Interestingly, the YAP transcriptional signature generated in our lab overlaps strongly with the Hoek invasive melanoma cell signature but not the proliferative melanoma cell signature (data not shown). This shows evidence that YAP expression, activity, and/or expression of its target genes could possibly be used as markers of invasive melanoma. To confirm this, more experiments are needed. For example, to decipher whether YAP drives metastatic melanoma in patients, YAP activity and expression could be measured in a wide range of melanoma patient samples, as well as by using online databases.

4.2.2 Necrosis and angiogenesis

In my study of primary tumours, a large increase in necrosis was found in YAP-5SA expressing tumours (Figure 8), indicating more tumour cell death was induced by YAP-5SA. At face value, this finding appears inconsistent with the finding that YAP-5SA promotes melanoma cell growth in soft agar. As growth conditions are different for cells in culture and *in vivo*, the increased necrosis could be caused by the several reasons. Firstly, YAP was reported to bind with the p73 transcription factor and initiate transcription of pro-apoptosis genes (Strano *et al.*, 2001, 2005; Basu *et al.*, 2003), providing a potential mechanism by which YAP-5SA induced cell death in primary tumours. Secondly, although tumour necrosis is a process in which tumour cells are dying, excessive spontaneous necrosis during tumour development may result in more

aggressive tumours because of necrosis-induced inflammation (Proskuryakov and Gabai, 2010). On the other hand, disordered and irregular necrotic cell deaths were reported to lead to suppressed immunity in tumours (Vakkila and Lotze, 2004). Although the NSG mice are immune deficient, the immune system is not totally lost in these mice. For example, neutrophils and monocytes are still detectable in the mouse peripheral blood (the Jackson Laboratory). As such, YAP-5SA induced necrosis in primary melanomas could be caused by an induction of inflammation.

In addition to controlling proliferation and metastasis of cells, YAP/TAZ have been shown crucial in sprouting angiogenesis (Kim *et al.*, 2017), which is hypothesized by the investigator to be a potential mechanism of angiogenesis during tumorigenesis. Increased densities of vascular components were observed in tumours bearing expression of YAP-5SA (Figure 9), suggesting that YAP could promote angiogenesis in melanoma. Angiogenesis induction is one of the hallmarks of cancers (Hanahan and Weinberg, 2011), and the growth of primary tumours and metastases of various cancers are believed to be dependent on angiogenesis (Carmeliet and Jain, 2000). Interestingly, *CYR61* is an angiogenic factor that might contribute to the angiogenic phenotype in UM (Walker *et al.*, 2002). In my study, *CYR61* was also identified as an important downstream gene in YAP-induced melanoma invasion (section 3.3). Therefore, my study provides another potential tumour-promoting effect of YAP, i.e. angiogenesis.

Angiogenesis of tumours can be induced by hypoxia (Chen, Endler and Shibasaki, 2009). In many multicellular organisms, the vascular system is very important as the blood vessels supply nutrients and oxygen to tissues. Hypoxia is toxic to normal cells, but tumour cells can survive and continue proliferation in hypoxic microenvironments, mainly through a progression called hypoxia-induced angiogenesis (Chen, Endler and Shibasaki, 2009)**.** During tumour growth, cells that are far from the blood supply become necrotic because of a lack of oxygen and nutrition, whereas cells closer to the blood supply can sense hypoxia and secrete angiogenic factors. As a result, neo-vessels appear in tumours; this is how neoangiogenesis is induced by hypoxia. Tumour necrosis is considered as a morphologic marker of tumour hypoxia, which is a feature of aggressive cancers (Hanahan and Weinberg, 2011). Notably,

increased necrosis is associated with vascular invasion, higher cell proliferation, and poor prognosis in melanoma (Bachmann *et al.*, 2008). Because I observed both increased necrosis and vascular components in YAP-5SA tumours, it is likely that the promoted angiogenesis is linked with increased necrosis. Moreover, YAP might play a role in hypoxia-induced angiogenesis.

Vascular endothelial growth factor (VEGF) is a crucial factor for angiogenesis. VEGF was firstly known for its angiogenic effects in endothelial cells. Recent reports describe YAP/TAZ as central mediators of VEGF signaling: VEGF activates YAP/TAZ and deletion of YAP/TAZ resulted in an impaired vascular response to VEGF. In succession, enhanced YAP/TAZ activity contributes to retaining VEGFR2 on the cell surface and promoting a feedforward loop that involved in developmental angiogenesis (Wang *et al.*, 2017). Another study revealing that VEGF activates YAP/TAZ in endothelial cells focused more on how YAP/TAZ influence angiogenesis in terms of cell biology (Kim *et al.*, 2017). However, the study is lacking on the links of YAP and VEGF in endothelial cells during tumorigenesis and metastasis, though VEGF signaling has been shown effects in cancer stem cells (Elaimy and Mercurio, 2018).

4.2.3 Tumour growth

As described in section 3.1.3, YAP-5SA increased colony formation of melanoma cells in culture, so it is surprising that YAP-5SA expression resulted in smaller tumours *in vivo* (section 3.2.4). Tumour size depends largely on both cell proliferation and cell death. To understand why expression of YAP-5SA resulted in smaller tumours *in vivo*, both cell proliferation and cell death should be examined. As discussed previously, tumour necrosis was increased in YAP-5SA tumours. As for cell proliferation, cells in YAP-5SA expressing tumours could be either more or less proliferative or without change. In my study, proliferative cells were identified in tumours samples via IHC staining using an anti-Ki67 antibody, as Ki67 is a commonly used marker of proliferative cells. However, because of the large area of necrosis in YAP-5SA expressing tumours, it was hard to identify viable regions in Ki67-stained samples. Furthermore, I observed substantial variability of Ki67 staining in different tumour

regions, which made it more difficult to measure and quantify the ratio of Ki67 positive cells in all viable cells. Because of time limitations, only one field of viable cells per tumour was assessed and no significant difference in the percentage of Ki67 positive cells was found (Figure 7DE). However, as the data were variable, a more extensive analysis is needed.

Slower growth of primary tumours and increased metastasis occurred simultaneously in this study, which conflicts a prevailing view that rapidly growing tumours are more likely to be metastatic and lethal than slower-growing tumours (Adami *et al.*, 2017). This view, however, lacks supporting evidence. A recent study reviewed all available data of three types of cancers, indicating that the molecular events of rapid growth and metastasis are often different, providing no evidence that rapidly growing tumours are more aggressive (Adami *et al.*, 2017). In addition, slow proliferation was reported as a biological feature of metastatic colorectal tumours (Anjomshoaa *et al.*, 2009). My study provides evidence for these findings in melanoma.

4.2.4 Depigmentation

Melanoma is caused by abnormal proliferation of mutated melanocytes, and is also highly aggressive. As dedifferentiation has been regarded as an important step of tumour progression, especially in metastasis (Gabbert *et al.*, 1985), it is of interest to understand whether and how dedifferentiation occurs in melanoma. In this study, depigmentation induced by YAP-5SA and wt-YAP/YAP-7SA was observed in both melanoma tumours and melanoma cells in culture, respectively, suggesting loss of melanocytic dedifferentiation of these cells. To further decipher this, dedifferentiation and stem cell-like phenotypes should be examined using more experiments. For example, the enrichment and characterization of cells to survival and self-renew in serum-free, non-adherent conditions could be measured using a tumoursphere formation assay, because only cancer stem/progenitor cells can grow in these conditions (Johnson, Chen and Lo, 2013). In addition, expression of pluripotency-associated stem cell markers such as *OCT4*, *SOX2*, and *NANOG* could be measured using qPCR, western blot, or

immunofluorescence staining. These experiments would be able to show whether stem cell-like phenotypes occur on these depigmented cells. Mechanically, the YAP-induced depigmentation could be mediated by downregulation of *MITF* and *TYR* (Figure 10C). This finding is in line with previous reports that MITF is an essential regulator of the melanoma phenotype switch (Carreira *et al.*, 2006; Hoek and Goding, 2010), as discussed in chapter 1. Moreover, the depigmentation and phenotype switching of melanoma indicate epithelial-to-mesenchymal transitioning (EMT), a process in which cells reduce cell-cell adhesion, becoming invasive and mesenchymal-like. Many signalling pathways have been reported to be linked with EMT (Pearlman *et al.*, 2017). However, the detail mechanism of EMT in melanoma is not yet fully understood. A previous study showed that YAP-S127A, a YAP mutant that reduces Hippo pathway-mediated repression, is not sufficient for a full EMT in melanoma cells (Lamar *et al.*, 2012). My study provides proof that YAP-7SA and YAP-5SA are more potent in inducing depigmentation compared to wt-YAP, suggesting a gradient of effects of YAP on EMT.

4.2.5 YAP as a prognostic marker in melanoma

There is accumulating evidence suggesting YAP as a transcriptional effector in diseases. Few of them showed the potential impact of YAP as a prognostic marker. Indeed, high YAP1 expression was found to be positively correlated with TEAD4 expression in ovarian cancer, and the co-expression of YAP1 and TEAD4 was a prognostic marker for poor ovarian cancer survival (Yuan *et al.*, 2015). Similar studies have not been performed in melanoma, although one study using IHC staining found that YAP showed similar expression levels in both benign nevi and metastatic melanoma (Nallet-Staub *et al.*, 2014). In this study, YAP-5SA showed a highly potent ability to promote melanoma metastasis and angiogenesis. As metastasis and angiogenesis are two well-established hallmarks of cancer, my study remarks YAP as a potential biomarker of melanoma progression. Clearly, further studies are required to determine whether YAP could serve as a prognostic marker of melanoma. For example, YAP expression and activity are two independent indicators that could be measured and correlated

with different outcomes of melanoma including patient survival and pathological characteristics such as tumour thickness, ulceration, mitotic rate and vascular involvement.

4.3 The mechanism of YAP-promoted melanoma invasion

Many genes have been shown to promote invasiveness of melanoma, including *TSPAN8* (Berthier-Vergnes *et al.*, 2011), *THBS1* (Jayachandran *et al.*, 2014), and *NEDD9* (Kim *et al.*, 2006). MITF was reported to be down-regulated during cell invasion, and required for melanoma proliferation (Carreira *et al.*, 2006) Jeffs et al., 2009.). YAP, a transcriptional co-activator, has shown the ability to promote metastasis of melanoma either in a tail vein-injection mouse model (Lamar et al., 2012.) or a spontaneous metastasis model as in this study. However, downstream effectors of YAP that contribute to invasion and metastasis of melanoma are not well known. In this study, four genes, *AXL, THBS1, CYR61*, and *CRIM1*, were identified as important YAP target genes that mediate YAP-induced melanoma invasion (Figure 12). These target genes were identified by RNAseq from YAP-5SA expressing MeWo cells, so it is unclear if they are direct targets of YAP. To assess this, further experiments such as chromatin immunoprecipitation and luciferase reporter assays should be performed. In addition, how these genes mediate YAP-promoted invasion has not been explored. According to past research, two of the four genes, *THBS1* and *CYR61,* encode secretory proteins, and the other two, *AXL* and *CRIM1*, encode membrane proteins. As such, these four genes are unlikely to share the same pathway to stimulate invasion of melanoma cells. This suggests that YAP promotes melanoma invasion and metastasis through a wide range of effectors and different mechanisms. AXL promotes invasion and metastasis by stimulating expression of matrix metalloproteinases (MMPs) in response to PI-3K/AKT and ERK pathway signalling (Tai *et al.*, 2008), which are commonly reported pathways involved in invasion of several cancers including melanoma (Ruth *et al.*, 2006; Chen *et al.*, 2009; Xu *et al.*, 2013; Li *et al.*, 2017). Similarly, TSP-1, encoded by the *THBS1* gene, can also stimulate expression of MMPs (Pal *et al.*, 2016). CYR61 promotes MEK/ERK pathway activity and EMT, leading to cell migration (Hou *et al.*, 2014). CRIM1 was recently found as a target of YAP in lung cancer cells, and found to promote cell migration and adhesion, as well as increasing expression of both N-

cadherin and E-cadherin (Zeng *et al.*, 2015). Another research group reported that reduction of CRIM1 decreased E-cadherin and increased MMPs, thus enhancing migration and invasion of renal carcinoma cells (Ogasawara *et al.*, 2018). Indeed, little has been explored about the role of CRIM1 in cancers. My findings provide evidence of *CRIM1* as a target of YAP, which promotes invasion of melanoma cells. Further studies are required to determine the precise mechanism by which YAP and its target genes drive melanoma invasion and metastasis.

4.4 YAP as a therapeutic target in melanoma

Life-threatening as it is, melanoma is a common malignant cancer that needs efficient treatments urgently. The anti-PD-1 monoclonal antibody, a newly identified immunotherapy, was first investigated and proved effective in treating patients with melanoma (Hodi et al., 2010.). Other major melanoma treatments are anti-CTLA-4 monoclonal antibodies, high-dose IL-2, BRAFi and MEKi. A combination of BRAFi and MEKi is well-tolerated and extends survival of melanoma patients (Long *et al.*, 2016). Despite the use of these new treatments, long-term survival rate of melanoma patients remains extremely low. Moreover, drug resistance is becoming a problem. For instance, ~80% of patients become resistant to BRAFi and MEKi during treatment (Long *et al.*, 2016). Therefore, new therapeutic targets are urgently needed. This study provides evidence that YAP is likely to stimulate melanoma progression by regulating metastasis, necrosis, and vascular appearance, suggesting a possibility of targeting YAP to treat melanoma. As such, statins were used to assess the potential of YAP as a drug target in melanoma cells. My findings indicated that statins could induce the phosphorylation of YAP, which is inhibitory (Figure 14). All melanoma cell lines showed sensitivity to simvastatin, suggesting a wide response of melanoma cells to statins, although more cell lines should be included to substantiate this conclusion. To understand a selective toxicity to melanoma cells, normal cell lines should be treated with simvastatin as well to compare the effect and that of melanoma cell lines. YAP protein activity (represented by the ratio of phosphorylated to non-phosphorylated YAP and by expression of three YAP target genes) was inhibited by simvastatin in two melanoma cell lines (Figure 14), indicating that YAP is a molecular target of simvastatin. Moreover, the statin-induced melanoma cell death and YAP

inactivation were found to share the same pathway, i.e. suppression of GGPP, an intermediate of the mevalonate pathway (Figure 13-16). These findings suggested that YAP could be an effector of statins in melanoma cells, and YAP repression might mediate statin-induced melanoma cell death. To further confirm this, rescue experiments could be performed by overexpressing YAP in statin-treated cells. Also, the correlation of YAP and cell sensitivity to statins could be investigated by measuring YAP levels (expression and activity) of different cell lines that have different sensitivity of statins. Overall, these results provide evidence that YAP is a potential drug target in melanoma treatment. Future drugs could be designed to target YAP through phosphorylation or inhibition of its transcriptional activity.

The mechanism of induction of phosphorylation of YAP by statins is likely to be via the central Hippo pathway kinases LATS1/2. To test this, the YAP-S127A mutant could be introduced into melanoma cells to measure whether YAP transcriptional activity can still be inhibited by statins. Also, YAP phosphorylation and transcriptional activity could be measured to find whether efficient rescue would occur by knockdown of *LATS1/2* on statin-treated cells. These experiments could tell us if the statin-induced YAP inactivation is Hippo-dependent. A previous study revealed that the statin-induced YAP phosphorylation and cytoplasmic sequestration was independent of LATS1/2 kinases in breast cancer cells (Sorrentino *et al.*, 2014), which is unsupportive of my hypothesis. Therefore, such mentioned experiments should be carefully conducted before any inference could be drawn. In addition to LATS1/2, direct regulators of YAP that mediate this phenotype could be other kinases, such as NDR1/2 which also phosphorylate YAP at S127 site (Zhang *et al.*, 2015). What I can conclude is that the mechanism by which simvastatin inhibites YAP activity is through geranylgeranylated proteins (Figure 17B). RhoA is one potential geranylgeranylated protein that regulates YAP activity (Figure 17). Other geranylgeranylated proteins such as RAC1 and CDC42 could be potential activators of YAP in melanoma cells that require further investigation.

Statins inhibit the mevalonate pathway and limit its downstream products, which has a wide range of effects on critical cell functions. The effect of statins on tumour cells are mediated by many molecules, and is not specific to the HIPPO/YAP pathway, many of them are linked to

melanoma or HIPPO though. Statins post translationally regulate proteins by the prenylation modification. The Raf, Ras and Rho families, are post translationally modified and can be inhibited by statins, and regulate pivotal cell functions such as apoptosis, cell proliferation, and metastasis (Ahmadi, Ghorbanihaghjo and Argani, 2017). In melanoma, *BRAF* is frequently mutated (52%), as is *NRAS* (28%) (Akbani *et al.*, 2015). As such, expression level and activity of YAP deserve to be measured in *BRAF* and *NRAS* mutant melanoma cell lines to understand if YAP is linked to the major gene mutations of melanoma. Sorrentino et al. showed RhoA inhibits phosphorylation and promotes nuclear accumulation of YAP in breast cancer cells (Sorrentino *et al.*, 2014). Rho family members, best known for their role in cytoskeleton remodeling, mediate a wide range of signaling pathways that regulate cell polarity, cell cycle, cell motility, transcriptional activities and numbers of enzymatic activities such as NADPH-oxidase (Van Aelst and D'Souza-Schorey, 1997; Shitara and Sugiyama, 2006).

NADPH oxidase, a membrane-bound enzyme complex, has been shown to perform a critical role in VEGF-induced angiogenesis (Ushio-Fukai *et al.*, 2002). Statin has anti-VEGF effect, reported by several groups of researchers. Statin treatment prevents the increase of VEGF and ICAM-1 expression induced by diabetes or high glucose and blocks NADPH oxidase-mediated activation of STAT3 (Al-Shabrawey *et al.*, 2008). In non-diabetic rats, statin decreased in VEGF levels in all vascular area. A systematic review and meta-analysis revealed a significant reduction in human plasma VEGF following statin therapy (Sahebkar *et al.*, 2015). Interestingly, acting Raf at various levels on the Ras signaling pathway can induce upregulation of VEGF and angiogenesis (Rak *et al.*, 2000). As such, statin-induced inactivation of YAP could play a role in VEGF-mediated angiogenesis of tumours. Thus the impacts of YAP following statin treatment, and that of angiogenesis need further investigation.

4.5 Conclusions, limitations and future directions

In this study, the important role of YAP was demonstrated in melanoma cell proliferation, metastasis, necrosis, and angiogenesis. Importantly, hyperactive YAP displayed a potent ability to enhance melanoma metastasis *in vivo*, indicating a potential contribution of YAP

hyperactivity in metastatic melanoma. Of note, activating metastasis and inducing angiogenesis are two hallmarks of cancer, thus YAP is possibly a biomarker of melanoma progression, an idea that requires further studies. In addition to the investigation of YAP in melanoma, four target genes of YAP were identified that mediate melanoma cell invasion. The four genes, *AXL*, *THBS1*, *CYR61,* and *CRIM1,* are unlikely to share the same pathway, thus indicating that YAP-promoted melanoma invasion and metastasis involve multiple modes. Preliminary evidence was also found for the use of statins as a new melanoma therapy.

Weaknesses and shortcomings exist in this study due to limited knowledge of the author and time limitation. Expression level of endogenous YAP and p-YAP should be measured in all melanoma cell lines I worked on to get a better sense of YAP and Hippo activity. Besides, TAZ, YAP's paralog, should also be studied as YAP/TAZ have been reported to have similar impacts on cells and may have redundant functions in some cell lines. A total of 10 melanoma cell lines were utilised in this study. For some of experiments including the invasion assay and animal experiment, only MeWo cell line was used. To make conclusions with more confidence, more melanoma cell lines should be included.

The important role of YAP in melanoma growth and metastasis was revealed in this study, which provides a potential therapeutic strategy of melanoma by targeting YAP. To achieve this purpose, more investigation must be performed. In the future, systematic analysis of YAP activity and expression could be measured in a wide range of melanoma patient samples. Expression level of wt-YAP and mutated YAP should be analysed independently, thus giving a clear understanding of the effects linked to either type of YAP. Results of soft agar assays suggested that YAP likely contributes to melanoma tumorigenesis; invasion assays demonstrated a potent ability of YAP to promote invasion of melanoma cells *in vitro* as well as melanoma metastasis *in vivo*; mice with primary tumours that express hyperactive YAP that is resistant to Hippo pathway-mediated repression (YAP-5SA) had more and larger metastases in multiple organs. The mechanism by which YAP promotes melanoma progression should be better explored. Many questions remain unknown. For example, how YAP and its target gene contribute to the promotion of melanoma metastasis? What is the impact of enhanced wt-YAP

on melanoma cells? As mutated YAP is hyperactivated, is the strength of activity of YAP or mutated YAP linked to their biological effects? Mechanistically, the key YAP transcription factor partners TEAD1-4, as well as four YAP/TEAD target were found to mediate YAP-induced invasion of melanoma cells. The TEAD family have been reported as the most important TFs binding to YAP. Whether TEADs are required to bind to YAP in the regulation of invasion of melanoma cells could be measured. How YAP regulates expression of the four target genes could be checked using chromatin immunoprecipitation. Additionally, YAP-5SA expressing primary tumours were more necrotic and had enhanced vascularity. VEGF signalling should be checked following enhanced YAP activation using western blot and qPCR. The inhibition of VEGF-mediated angiogenesis is possibly caused by statin-induced inactivation of YAP. As such, statin treatment could be conducted on mice, checking whether vascularity occurs less frequently and if the impact could be rescued by activating YAP. Such efforts should clarify the role of YAP in melanoma and ultimately establish a way to treat melanoma by targeting YAP.

Acknowledgements

First and foremost, I would like to thank my supervisors Prof. Kieran Harvey, Prof. Mark Shackleton, and Dr. Xiaomeng Zhang. Thank you for providing such an interesting and meaningful project to me, which perfectly combines my interests of cell biology and animal models. Kieran, thank you for all of the ongoing support and kind guidance during the two years. I've learned much from you about being critical, precise, and determined in scientific research. I appreciate all the knowledge and skills you've imparted to me. Mark, thank you for the invaluable suggestions on this project. Thank you for setting an excellent example for me as being a medical doctor and a scientist at the same time, which is likely the direction of my future career. A big thank you must go to Xiaomeng, who has provided me with invaluable guidance throughout my Masters. Thank you for all of your kind instructions, great insights, endless patience, encouragements and suggestions to me. You've left me with the very first understanding and feeling about scientific research. I wouldn't have been able to done these without you.

I would like to sincerely thank other members from the Harvey lab. Thank you all for the enjoyable and friendly atmosphere. I appreciate all the kind help and suggestions on both experiments and life in Australia from you guys.

Thanks and appreciation must also go to the Shackleton lab. Especially to Pacman, thank you for all the kind and patient instructions on the mice work. To Youfang, thanks for your excellent guidance on the histological and IHC staining. I've learned much amazing knowledge and tips of staining from you. The two months I spent learning and working with you have really been a very enjoyable and excellent time for me.

Thanks especially to Catriona Mclean, a great pathologist always filled with enthusiasm, who gave me many appreciated suggestions on the quantifications and analysis of stained tissues.

Thanks must also go to the teachers and administrators from Tsinghua University and the University of Melbourne, who have contributed a lot in the collaboration program between the two universities. I would like to especially thank China Scholarship Council for the financial support throughout the two years.

I'd also like to thank my Tsinghua classmates who came here together with me. Special thanks go to the girls living with me during the two years, Mai and Zixuan. It has been a wonderful time living with you guys. Thanks a lot for all the laughter and funny we made together.

Last but by no means least, I'd like to thank my beloved family. Thank you to my parents for your selfless devotion and lifelong love. Words cannot explain how I acknowledge, appreciate, and love you. I just cannot thank you enough.

-Lie

References

Adami, H.-O. *et al.* (2017) 'Are rapidly growing cancers more lethal?', *European Journal of Cancer*, 72, pp. 210–214. doi: 10.1016/j.ejca.2016.11.011.

Adler, J. J. *et al.* (2013) 'Serum deprivation inhibits the transcriptional co-activator YAP and cell growth via phosphorylation of the 130-kDa isoform of Angiomotin by the LATS1/2 protein kinases', *Proceedings of the National Academy of Sciences*, 110(43), pp. 17368–17373. doi: 10.1073/pnas.1308236110.

Van Aelst, L. and D'Souza-Schorey, C. (1997) 'Rho GTPases and signaling networks', *Genes & Development*, 11(18), pp. 2295–2322. doi: 10.1101/gad.11.18.2295.

Ahmadi, Y., Ghorbanihaghjo, A. and Argani, H. (2017) 'The balance between induction and inhibition of mevalonate pathway regulates cancer suppression by statins: A review of molecular mechanisms', *Chemico-Biological Interactions*, 273, pp. 273–285. doi: 10.1016/j.cbi.2017.06.026.

AIHW (2017) *Australian Cancer Incidence and Mortality (ACIM) books: Melanoma of the skin*. Available at: https://www.aihw.gov.au/reports/cancer/acim-books/contents/acim-books (Accessed: 11 May 2018).

Akbani, R. *et al.* (2015) 'Genomic Classification of Cutaneous Melanoma', *Cell*, 161(7), pp. 1681–1696. doi: 10.1016/j.cell.2015.05.044.

Al-Shabrawey, M. *et al.* (2008) 'Role of NADPH Oxidase and Stat3 in Statin-Mediated Protection against Diabetic Retinopathy', *Investigative Opthalmology & Visual Science*, 49(7), p. 3231. doi: 10.1167/iovs.08-1754.

Anjomshoaa, A. *et al.* (2009) 'Slow proliferation as a biological feature of colorectal cancer metastasis', *British Journal of Cancer*, 101(5), pp. 822–828. doi: 10.1038/sj.bjc.6605229.

Ascierto, P. A. *et al.* (2013) 'MEK162 for patients with advanced melanoma harbouring NRAS or Val600 BRAF mutations: a non-randomised, open-label phase 2 study', *The Lancet Oncology*, 14(3), pp. 249–256. doi: 10.1016/S1470-2045(13)70024-X.

Atkins, M. B. *et al.* (1999) 'High-Dose Recombinant Interleukin 2 Therapy for Patients With Metastatic Melanoma: Analysis of 270 Patients Treated Between 1985 and 1993', *Journal of Clinical Oncology*, 17(7), pp. 2105–2105. doi: 10.1200/JCO.1999.17.7.2105.

Azzolin, L. *et al.* (2014) 'YAP/TAZ Incorporation in the β-Catenin Destruction Complex Orchestrates the Wnt Response', *Cell*. Elsevier, 158(1), pp. 157–170. doi: 10.1016/j.cell.2014.06.013.

Bachmann, I. M. *et al.* (2008) 'Tumor necrosis is associated with increased alphavbeta3integrin expression and poor prognosis in nodular cutaneous melanomas', *BMC Cancer*, 8(1), p. 362. doi: 10.1186/1471-2407-8-362.

Barry, E. R. *et al.* (2012) 'Restriction of intestinal stem cell expansion and the regenerative response by YAP', *Nature*. Nature Publishing Group, 493(7430), pp. 106–110. doi: 10.1038/nature11693.

Bashyam, M. D. *et al.* (2005) 'Array-based comparative genomic hybridization identifies localized DNA amplifications and homozygous deletions in pancreatic cancer.', *Neoplasia (New York, N.Y.)*, 7(6), pp. 556–62. Available at: http://www.ncbi.nlm.nih.gov/pubmed/16036106.

Berthier-Vergnes, O. *et al.* (2011) 'Gene expression profiles of human melanoma cells with different invasive potential reveal TSPAN8 as a novel mediator of invasion', *British Journal of Cancer*, 104(1), pp. 155–165. doi: 10.1038/sj.bjc.6605994.

Beyer, T. A. *et al.* (2013) 'Switch enhancers interpret TGF-β and hippo signaling to control cell fate in human embryonic stem cells', *Cell Reports*. The Authors, 5(6), pp. 1611–1624. doi: 10.1016/j.celrep.2013.11.021.

Bianchi, A. B. *et al.* (1995) 'High frequency of inactivating mutations in the neurofibromatosis type 2 gene (NF2) in primary malignant mesotheliomas.', *Proceedings of the National Academy of Sciences of the United States of America*, 92(24), pp. 10854–8. doi: 10.1146/annurev.mi.33.100179.002213.

Bilder, D. and Perrimon, N. (2000) 'Localization of apical epithelial determinants by the basolateral PDZ protein Scribble', *Nature*, 403(6770), pp. 676–680. doi: 10.1038/35001108.
Bishop, J. N. *et al.* (2007) 'The prevention, diagnosis, referral and management of melanoma of the skin: concise guidelines', *Clinical Medicine*, 7(3), pp. 283–290. doi: 10.7861/clinmedicine.7-3-283.
Boggiano, J. C., Vanderzalm, P. J. and Fehon, R. G. (2011) 'Tao-1 Phosphorylates Hippo/MST Kinases to Regulate the Hippo-Salvador-Warts Tumor Suppressor Pathway', *Developmental Cell*. Elsevier Inc., 21(5), pp. 888–895. doi: 10.1016/j.devcel.2011.08.028.
Borowicz, S. *et al.* (2014) 'The Soft Agar Colony Formation Assay', *Journal of Visualized Experiments*, (92). doi: 10.3791/51998.
Bratt, A. *et al.* (2005) 'Angiomotin Regulates Endothelial Cell-Cell Junctions and Cell Motility', *Journal of Biological Chemistry*, 280(41), pp. 34859–34869. doi: 10.1074/jbc.M503915200.
Briso, E. M. *et al.* (2013) 'Inflammation-mediated skin tumorigenesis induced by epidermal c-Fos', *Genes & Development*, 27(18), pp. 1959–1973. doi: 10.1101/gad.223339.113.
Cai, J. *et al.* (2010) 'The Hippo signaling pathway restricts the oncogenic potential of an intestinal regeneration program', *Genes & Development*, 24(21), pp. 2383–2388. doi: 10.1101/gad.1978810.
Camargo, F. D. *et al.* (2007) 'YAP1 Increases Organ Size and Expands Undifferentiated Progenitor Cells', *Current Biology*, 17(23), pp. 2054–2060. doi: 10.1016/j.cub.2007.10.039.
Cancer Australia (2018) *Cancer in Australia statistics*. Available at: https://canceraustralia.gov.au/affected-cancer/what-cancer/cancer-australia-statistics (Accessed: 11 May 2018).
Cao, X., Pfaff, S. L. and Gage, F. H. (2008) 'YAP regulates neural progenitor cell number via the TEA domain transcription factor', *Genes & Development*, 22(23), pp. 3320–3334. doi: 10.1101/gad.1726608.
Carmeliet, P. and Jain, R. K. (2000) 'Angiogenesis in cancer and other diseases', *Nature*, 407(6801), pp. 249–257. doi: 10.1038/35025220.
Carreira, S. *et al.* (2006) 'Mitf regulation of Dia1 controls melanoma proliferation and invasiveness', *Genes & Development*, pp. 3426–3439. doi: 10.1101/gad.406406.changes.
Chae, Y. K. *et al.* (2015) 'Statins as anti-cancer therapy; Can we translate preclinical and epidemiologic data into clinical benefit?', *Discovery medicine*, 20(112), pp. 413–27. Available at: http://www.ncbi.nlm.nih.gov/pubmed/26760985.
Chan, S. W. *et al.* (2011) 'Hippo Pathway-independent Restriction of TAZ and YAP by Angiomotin', *Journal of Biological Chemistry*, 286(9), pp. 7018–7026. doi: 10.1074/jbc.C110.212621.
Chapman, P. B. *et al.* (2011) 'Improved Survival with Vemurafenib in Melanoma with BRAF V600E Mutation', *New England Journal of Medicine*, 364(26), pp. 2507–2516. doi: 10.1056/NEJMoa1103782.
Chen, J. *et al.* (2009) 'Involvement of PI3K/PTEN/AKT/mTOR pathway in invasion and metastasis in hepatocellular carcinoma: Association with MMP-9', *Hepatology Research*, 39(2), pp. 177–186. doi: 10.1111/j.1872-034X.2008.00449.x.
Chen, L., Endler, A. and Shibasaki, F. (2009) 'Hypoxia and angiogenesis: regulation of hypoxia-inducible factors via novel binding factors', *Experimental and Molecular Medicine*, 41(12), p. 849. doi: 10.3858/emm.2009.41.12.103.
Chen, Q. *et al.* (2015) 'Homeostatic control of Hippo signaling activity revealed by an endogenous activating mutation in YAP', *Genes and Development*, 29(12), pp. 1285–1297. doi: 10.1101/gad.264234.115.
Chen, S. N. *et al.* (2014) 'The Hippo Pathway Is Activated and Is a Causal Mechanism for Adipogenesis in Arrhythmogenic Cardiomyopathy', *Circulation Research*, 114(3), pp. 454–468. doi: 10.1161/CIRCRESAHA.114.302810.

Codelia, V. A., Sun, G. and Irvine, K. D. (2014) 'Regulation of YAP by Mechanical Strain through Jnk and Hippo Signaling', *Current Biology*. Elsevier Ltd, 24(17), pp. 2012–2017. doi: 10.1016/j.cub.2014.07.034.
Coleman, J. . (2010) *Robbins and Cotran's Pathologic Basis of Disease*.
Cordenonsi, M. *et al.* (2011) 'The Hippo Transducer TAZ Confers Cancer Stem Cell-Related Traits on Breast Cancer Cells', *Cell*. Elsevier Inc., 147(4), pp. 759–772. doi: 10.1016/j.cell.2011.09.048.
Creasy, C. L. and Chernoff, J. (1995a) 'Cloning and Characterization of a Human Protein Kinase with Homology to Ste20', *Journal of Biological Chemistry*, 270(37), pp. 21695–21700. doi: 10.1074/jbc.270.37.21695.
Creasy, C. L. and Chernoff, J. (1995b) 'Cloning and characterization of a member of the MST subfamily of Ste20-like kinases', *Gene*, 167(1–2), pp. 303–306. doi: 10.1016/0378-1119(95)00653-2.
Dai, Z. *et al.* (2003) 'A comprehensive search for DNA amplification in lung cancer identifies inhibitors of apoptosis cIAP1 and cIAP2 as candidate oncogenes.', *Human molecular genetics*, 12(7), pp. 791–801. Available at: http://www.ncbi.nlm.nih.gov/pubmed/12651874.
Danovi, S. A. *et al.* (2008) 'Yes-Associated Protein (YAP) is a critical mediator of c-Jun-dependent apoptosis', *Cell Death & Differentiation*, 15(1), pp. 217–219. doi: 10.1038/sj.cdd.4402226.
Davies, H. *et al.* (2002) 'Mutations of the BRAF gene in human cancer', *Nature*, 417(6892), pp. 949–954. doi: 10.1038/nature00766.
Dummer, R. *et al.* (2016) 'Results of NEMO: A phase III trial of binimetinib (BINI) vs dacarbazine (DTIC) in NRAS-mutant cutaneous melanoma.', *Journal of Clinical Oncology*, 34(15_suppl), p. 9500. doi: 10.1200/JCO.2016.34.15_suppl.9500.
Dupont, S. *et al.* (2011) 'Role of YAP/TAZ in mechanotransduction', *Nature*. Nature Publishing Group, 474(7350), pp. 179–183. doi: 10.1038/nature10137.
Elaimy, A. L. and Mercurio, A. M. (2018) 'Convergence of VEGF and YAP/TAZ signaling: Implications for angiogenesis and cancer biology', *Science Signaling*, 11(552), p. eaau1165. doi: 10.1126/scisignal.aau1165.
Elbediwy, A. *et al.* (2016) 'Integrin signalling regulates YAP and TAZ to control skin homeostasis', *Development*, 143(10), pp. 1674–1687. doi: 10.1242/dev.133728.
Elwood, J. M. and Jopson, J. (1997) 'Melanoma and sun exposure: An overview of published studies', *International Journal of Cancer*, 73(2), pp. 198–203. doi: 10.1002/(SICI)1097-0215(19971009)73:2<198::AID-IJC6>3.0.CO;2-R.
Fabian, I. D. *et al.* (2017) 'Primary photodynamic therapy with verteporfin for small pigmented posterior pole choroidal melanoma', *Eye*. Nature Publishing Group, 31(4), pp. 519–528. doi: 10.1038/eye.2017.22.
Facts, C. (2017) 'Cancer Facts & Figures 2017'.
Feng, R. *et al.* (2017) 'MAPK and Hippo signaling pathways crosstalk via the RAF-1/MST-2 interaction in malignant melanoma', *Oncology Reports*, 38(2), pp. 1199–1205. doi: 10.3892/or.2017.5774.
Feng, X. *et al.* (2014) 'Hippo-Independent Activation of YAP by the GNAQ Uveal Melanoma Oncogene through a Trio-Regulated Rho GTPase Signaling Circuitry', *Cancer Cell*. Elsevier Inc., 25(6), pp. 831–845. doi: 10.1016/j.ccr.2014.04.016.
Ferrigno, O. *et al.* (2002) 'Yes-associated protein (YAP65) interacts with Smad7 and potentiates its inhibitory activity against TGF-β/Smad signaling', *Oncogene*, 21(32), pp. 4879–4884. doi: 10.1038/sj.onc.1205623.
Fife, R. S. *et al.* (1997) 'Inhibition of proliferation and induction of apoptosis by doxycycline in cultured human osteosarcoma cells', *Journal of Laboratory and Clinical Medicine*, 130(5), pp. 530–534. doi: 10.1016/S0022-2143(97)90130-X.

Fossdal, R. (2004) ‘A novel TEAD1 mutation is the causative allele in Sveinsson’s chorioretinal atrophy (helicoid peripapillary chorioretinal degeneration)’, *Human Molecular Genetics*, 13(9), pp. 975–981. doi: 10.1093/hmg/ddh106.
Fu, V., Plouffe, S. W. and Guan, K.-L. (2017) ‘The Hippo pathway in organ development, homeostasis, and regeneration’, *Current Opinion in Cell Biology*. Elsevier Ltd, 49, pp. 99–107. doi: 10.1016/j.ceb.2017.12.012.
Fujii, M. *et al.* (2012) ‘TGF-β synergizes with defects in the Hippo pathway to stimulate human malignant mesothelioma growth’, *The Journal of Experimental Medicine*, 209(3), pp. 479–494. doi: 10.1084/jem.20111653.
Gabbert, H. *et al.* (1985) ‘Tumor dedifferentiation: An important step in tumor invasion’, *Clinical & Experimental Metastasis*, 3(4), pp. 257–279. doi: 10.1007/BF01585081.
Garcia-Rendueles, M. E. R. *et al.* (2015) ‘NF2 loss promotes oncogenic RAS-induced thyroid cancers via YAP-dependent transactivation of RAS proteins and sensitizes them to MEK inhibition’, *Cancer Discovery*, 5(11), pp. 1178–1193. doi: 10.1158/2159-8290.CD-15-0330.
Gellrich, F. F., Beissert, S. and Meier, F. (2018) ‘Immunotherapy for melanoma’, *Der Onkologe*, 24(S2), pp. 99–103. doi: 10.1007/s00761-018-0443-7.
Gershenwald, J. E. *et al.* (2017) ‘Melanoma staging: Evidence-based changes in the American Joint Committee on Cancer eighth edition cancer staging manual’, *CA: A Cancer Journal for Clinicians*, 67(6), pp. 472–492. doi: 10.3322/caac.21409.
Giovannini, M. *et al.* (2000) ‘Conditional biallelic Nf2 mutation in the mouse promotes manifestations of human neurofibromatosis type 2’, *Genes and Development*, 14(13), pp. 1617–1630. doi: 10.1101/gad.14.13.1617.
Green, A. C. *et al.* (2011) ‘Reduced Melanoma After Regular Sunscreen Use: Randomized Trial Follow-Up’, *Journal of Clinical Oncology*, 29(3), pp. 257–263. doi: 10.1200/JCO.2010.28.7078.
Gruenbacher, G. and Thurnher, M. (2017) ‘Mevalonate metabolism governs cancer immune surveillance’, *OncoImmunology*, 6(10), p. e1342917. doi: 10.1080/2162402X.2017.1342917.
Hamilton, G. *et al.* (2009) ‘ATM Regulates a RASSF1A-Dependent DNA Damage Response’, *Current Biology*. Elsevier Ltd, 19(23), pp. 2020–2025. doi: 10.1016/j.cub.2009.10.040.
Hanahan, D. and Weinberg, R. A. (2011) ‘Hallmarks of Cancer: The Next Generation’, *Cell*, 144(5), pp. 646–674. doi: 10.1016/j.cell.2011.02.013.
Harvey, K. F., Pfleger, C. M. and Hariharan, I. K. (2003) ‘The Drosophila Mst ortholog, hippo, restricts growth and cell proliferation and promotes apoptosis’, *Cell*, 114(4), pp. 457–467. doi: 10.1016/S0092-8674(03)00557-9.
Heallen, T. *et al.* (2011) ‘Hippo Pathway Inhibits Wnt Signaling to Restrain Cardiomyocyte Proliferation and Heart Size’, *Science*, 332(6028), pp. 458–461. doi: 10.1126/science.1199010.
Hirate, Y. *et al.* (2013) ‘Polarity-Dependent Distribution of Angiomotin Localizes Hippo Signaling in Preimplantation Embryos’, *Current Biology*. Elsevier Ltd, 23(13), pp. 1181–1194. doi: 10.1016/j.cub.2013.05.014.
Hodi, F. S. *et al.* (2010) ‘Improved Survival with Ipilimumab in Patients with Metastatic Melanoma’, *New England Journal of Medicine*, 363(8), pp. 711–723. doi: 10.1056/NEJMoa1003466.
Hoek, K. S. *et al.* (2006) ‘Metastatic potential of melanomas defined by specific gene expression profiles with no BRAF signature’, *Pigment Cell Research*, 19(4), pp. 290–302. doi: 10.1111/j.1600-0749.2006.00322.x.
Hoek, K. S. and Goding, C. R. (2010) ‘Cancer stem cells versus phenotype-switching in melanoma’, *Pigment Cell & Melanoma Research*, 23(6), pp. 746–759. doi: 10.1111/j.1755-148X.2010.00757.x.

Hong, W. and Guan, K.-L. (2012) 'The YAP and TAZ transcription co-activators: Key downstream effectors of the mammalian Hippo pathway', *Seminars in Cell & Developmental Biology*, 23(7), pp. 785–793. doi: 10.1016/j.semcdb.2012.05.004.
Hou, C.-H. *et al.* (2014) 'Cyr61 promotes epithelial-mesenchymal transition and tumor metastasis of osteosarcoma by Raf-1/MEK/ERK/Elk-1/TWIST-1 signaling pathway', *Molecular Cancer*, 13(1), p. 236. doi: 10.1186/1476-4598-13-236.
Howlader, N. *et al.* (2012) *SEER Cancer Statistics Review, 1975-2009 (Vintage 2009 Populations), National Cancer Institute. Bethesda, MD, based on November 2011 SEER data submission, posted to the SEER web site, April 2012*.
Huang, J. *et al.* (2005) 'The Hippo signaling pathway coordinately regulates cell proliferation and apoptosis by inactivating Yorkie, the Drosophila homolog of YAP', *Cell*, 122(3), pp. 421–434. doi: 10.1016/j.cell.2005.06.007.
Huo, X. *et al.* (2013) 'Overexpression of Yes-associated protein confers doxorubicin resistance in hepatocellullar carcinoma', *Oncology Reports*, 29(2), pp. 840–846. doi: 10.3892/or.2012.2176.
Imajo, M. *et al.* (2012) 'A molecular mechanism that links Hippo signalling to the inhibition of Wnt/β-catenin signalling', *EMBO Journal*. Nature Publishing Group, 31(5), pp. 1109–1122. doi: 10.1038/emboj.2011.487.
Imoto, I. *et al.* (2001) 'Identification of cIAP1 as a candidate target gene within an amplicon at 11q22 in esophageal squamous cell carcinomas.', *Cancer research*, 61(18), pp. 6629–34. Available at: http://www.ncbi.nlm.nih.gov/pubmed/11559525.
Jang, J. W. *et al.* (2017) 'RAC-LATS1/2 signaling regulates YAP activity by switching between the YAP-binding partners TEAD4 and RUNX3', *Oncogene*. Nature Publishing Group, 36(7), pp. 999–1011. doi: 10.1038/onc.2016.266.
Janse van Rensburg, H. J. and Yang, X. (2016) 'The roles of the Hippo pathway in cancer metastasis', *Cellular Signalling*. Elsevier Inc., 28(11), pp. 1761–1772. doi: 10.1016/j.cellsig.2016.08.004.
Jayachandran, A. *et al.* (2014) 'Thrombospondin 1 promotes an aggressive phenotype through epithelial-to-mesenchymal transition in human melanoma', *Oncotarget*, 5(14), pp. 5782–5797. doi: 10.18632/oncotarget.2164.
Jeffs, A. R. *et al.* (2009) 'A Gene Expression Signature of Invasive Potential in Metastatic Melanoma Cells', *PLoS ONE*. Edited by G. Häcker, 4(12), p. e8461. doi: 10.1371/journal.pone.0008461.
Jia, J. (2003) 'The Drosophila Ste20 family kinase dMST functions as a tumor suppressor by restricting cell proliferation and promoting apoptosis', *Genes & Development*, 17(20), pp. 2514–2519. doi: 10.1101/gad.1134003.
Johnson, S., Chen, H. and Lo, P.-K. (2013) 'In vitro Tumorsphere Formation Assays', *BIO-PROTOCOL*, 3(3). doi: 10.21769/BioProtoc.325.
Justice, R. W. *et al.* (1995) 'The Drosophila Tumor-Suppressor Gene Warts Encodes a Homolog of Human Myotonic-Dystrophy Kinase and Is Required for the Control of Cell-Shape and Proliferation', *Genes & Development*, 9(5), pp. 534–546. doi: Doi 10.1101/Gad.9.5.534.
Kakeya, H., Onose, R. and Osada, H. (1999) 'Caspase-mediated Activation of a 36-kDa Myelin Basic Protein Kinase during', *Cancer Research*, 58, pp. 4888–4894.
Kan, Z. *et al.* (2010) 'Diverse somatic mutation patterns and pathway alterations in human cancers', *Nature*, 466(7308), pp. 869–873. doi: 10.1038/nature09208.
Kanai, F. (2000) 'TAZ: a novel transcriptional co-activator regulated by interactions with 14-3-3 and PDZ domain proteins', *The EMBO Journal*, 19(24), pp. 6778–6791. doi: 10.1093/emboj/19.24.6778.

Kango-Singh, M. (2002) 'Shar-pei mediates cell proliferation arrest during imaginal disc growth in Drosophila', *Development*, 129(24), pp. 5719–5730. doi: 10.1242/dev.00168.
Kapoor, A. *et al.* (2014) 'Yap1 activation enables bypass of oncogenic Kras addiction in pancreatic cancer.', *Cell*, 158(1), pp. 185–197. doi: 10.1016/j.cell.2014.06.003.
Kardynal, A. and Olszewska, M. (2014) 'Modern non-invasive diagnostic techniques in the detection of early cutaneous melanoma', *Journal of Dermatological Case Reports*, 8(1), pp. 1–8. doi: 10.3315/jdcr.2014.1161.
Kim, J. *et al.* (2017) 'YAP/TAZ regulates sprouting angiogenesis and vascular barrier maturation', *Journal of Clinical Investigation*, 127(9), pp. 3441–3461. doi: 10.1172/JCI93825.
Kim, M. *et al.* (2006) 'Comparative Oncogenomics Identifies NEDD9 as a Melanoma Metastasis Gene', *Cell*, 125(7), pp. 1269–1281. doi: 10.1016/j.cell.2006.06.008.
Kim, N.-G. *et al.* (2011) 'E-cadherin mediates contact inhibition of proliferation through Hippo signaling-pathway components', *Proceedings of the National Academy of Sciences*, 108(29), pp. 11930–11935. doi: 10.1073/pnas.1103345108.
Kitagawa, M. (2007) 'A Sveinsson's chorioretinal atrophy-associated missense mutation in mouse Tead1 affects its interaction with the co-factors YAP and TAZ', *Biochemical and Biophysical Research Communications*, 361(4), pp. 1022–1026. doi: 10.1016/j.bbrc.2007.07.129.
Lai, Z.-C. *et al.* (2005) 'Control of Cell Proliferation and Apoptosis by Mob as Tumor Suppressor, Mats', *Cell*, 120(5), pp. 675–685. doi: 10.1016/j.cell.2004.12.036.
Lamar, J. M. *et al.* (2012) 'The Hippo pathway target, YAP, promotes metastasis through its TEAD-interaction domain', *Proceedings of the National Academy of Sciences*, 109(37), pp. E2441–E2450. doi: 10.1073/pnas.1212021109.
Lee, J. K. *et al.* (2013) 'MST1 functions as a key modulator of neurodegeneration in a mouse model of ALS', *Proceedings of the National Academy of Sciences*, 110(29), pp. 12066–12071. doi: 10.1073/pnas.1300894110.
Lee, K.-P. *et al.* (2010) 'The Hippo-Salvador pathway restrains hepatic oval cell proliferation, liver size, and liver tumorigenesis', *Proceedings of the National Academy of Sciences*, 107(18), pp. 8248–8253. doi: 10.1073/pnas.0912203107.
Lee, M.-J. *et al.* (2014) 'YAP and TAZ Regulate Skin Wound Healing', *Journal of Investigative Dermatology*. Elsevier Masson SAS, 134(2), pp. 518–525. doi: 10.1038/jid.2013.339.
Lee, S. J. *et al.* (2011) 'Cross-Regulation between Oncogenic BRAFV600E Kinase and the MST1 Pathway in Papillary Thyroid Carcinoma', *PLoS ONE*. Edited by S. B. Lee, 6(1), p. e16180. doi: 10.1371/journal.pone.0016180.
Li, B. *et al.* (2017) 'Significance of PI3K/AKT signaling pathway in metastasis of esophageal squamous cell carcinoma and its potential as a target for anti-metastasis therapy', *Oncotarget*, 8(24). doi: 10.18632/oncotarget.16333.
Lin, L. *et al.* (2015) 'The Hippo effector YAP promotes resistance to RAF- and MEK-targeted cancer therapies', *Nature Genetics*, 47(3), pp. 250–256. doi: 10.1038/ng.3218.
Lin, Z. and Pu, W. T. (2014) 'Harnessing Hippo in the heart: Hippo/Yap signaling and applications to heart regeneration and rejuvenation', *Stem Cell Research*, 13(3), pp. 571–581. doi: 10.1016/j.scr.2014.04.010.
Liu-Chittenden, Y. *et al.* (2012) 'Genetic and pharmacological disruption of the TEAD-YAP complex suppresses the oncogenic activity of YAP', *Genes & Development*, 26(12), pp. 1300–1305. doi: 10.1101/gad.192856.112.
Long, G. V *et al.* (2016) 'Overall Survival and Durable Responses in Patients With BRAF V600-Mutant Metastatic Melanoma Receiving Dabrafenib Combined With Trametinib.', *Journal of clinical oncology :*

official journal of the American Society of Clinical Oncology, 34(8), pp. 871–8. doi: 10.1200/JCO.2015.62.9345.
Lu, L. *et al.* (2010) 'Hippo signaling is a potent in vivo growth and tumor suppressor pathway in the mammalian liver', *Proceedings of the National Academy of Sciences*, 107(4), pp. 1437–1442. doi: 10.1073/pnas.0911427107.
Luo, K. (2017) 'Signaling Cross Talk between TGF-β/Smad and Other Signaling Pathways', *Cold Spring Harbor Perspectives in Biology*, 9(1), p. a022137. doi: 10.1101/cshperspect.a022137.
Manning, S. A. *et al.* (2018) 'Dynamic Fluctuations in Subcellular Localization of the Hippo Pathway Effector Yorkie In Vivo', *Current Biology*. Elsevier Ltd., 28(10), p. 1651–1660.e4. doi: 10.1016/j.cub.2018.04.018.
Mao, B. *et al.* (2014) 'SIRT1 regulates YAP2-mediated cell proliferation and chemoresistance in hepatocellular carcinoma', *Oncogene*, 33(11), pp. 1468–1474. doi: 10.1038/onc.2013.88.
Marti, P. *et al.* (2015) 'YAP promotes proliferation, chemoresistance, and angiogenesis in human cholangiocarcinoma through TEAD transcription factors', *Hepatology*, 62(5), pp. 1497–1510. doi: 10.1002/hep.27992.
Matallanas, D. *et al.* (2007) 'RASSF1A Elicits Apoptosis through an MST2 Pathway Directing Proapoptotic Transcription by the p73 Tumor Suppressor Protein', *Molecular Cell*, 27(6), pp. 962–975. doi: 10.1016/j.molcel.2007.08.008.
McGuire, S. (2016) 'World Cancer Report 2014. Geneva, Switzerland: World Health Organization, International Agency for Research on Cancer, WHO Press, 2015', *Advances in Nutrition*, 7(2), pp. 418–419. doi: 10.3945/an.116.012211.
Meng, Z. *et al.* (2015) 'MAP4K family kinases act in parallel to MST1/2 to activate LATS1/2 in the Hippo pathway', *Nature Communications*. Nature Publishing Group, 6(1), p. 8357. doi: 10.1038/ncomms9357.
Miller, E. *et al.* (2012) 'Identification of Serum-Derived Sphingosine-1-Phosphate as a Small Molecule Regulator of YAP', *Chemistry & Biology*, 19(8), pp. 955–962. doi: 10.1016/j.chembiol.2012.07.005.
Minor, D. R. *et al.* (2015) 'Severe gastrointestinal toxicity with administration of trametinib in combination with dabrafenib and ipilimumab', *Pigment Cell & Melanoma Research*, 28(5), pp. 611–612. doi: 10.1111/pcmr.12383.
Mohseni, M. *et al.* (2014) 'A genetic screen identifies an LKB1–MARK signalling axis controlling the Hippo–YAP pathway', *Nature Cell Biology*. Nature Publishing Group, 16(1), pp. 108–117. doi: 10.1038/ncb2884.
Mouratidis, P. X. E., Colston, K. W. and Dalgleish, A. G. (2007) 'Doxycycline induces caspase-dependent apoptosis in human pancreatic cancer cells', *International Journal of Cancer*, 120(4), pp. 743–752. doi: 10.1002/ijc.22303.
Murakami, M. *et al.* (2005) 'A WW domain protein TAZ is a critical coactivator for TBX5, a transcription factor implicated in Holt-Oram syndrome', *Proceedings of the National Academy of Sciences*, 102(50), pp. 18034–18039. doi: 10.1073/pnas.0509109102.
Murray, L. B., Lau, Y.-K. I. and Yu, Q. (2012) 'Merlin is a negative regulator of human melanoma growth.', *PloS One*, 7(8), p. e43295. doi: 10.1371/journal.pone.0043295.
Nakajima, H. *et al.* (2017) 'Flow-Dependent Endothelial YAP Regulation Contributes to Vessel Maintenance', *Developmental Cell*. Elsevier Inc., 40(6), p. 523–536.e6. doi: 10.1016/j.devcel.2017.02.019.
Nallet-Staub, F. *et al.* (2014) 'Pro-invasive activity of the hippo pathway effectors YAP and TAZ in cutaneous melanoma', *Journal of Investigative Dermatology*, 134(1), pp. 123–132. doi: 10.1038/jid.2013.319.
Nallet-Staub, F. *et al.* (2015) 'Cell Density Sensing Alters TGF-β Signaling in a Cell-Type-Specific Manner, Independent from Hippo Pathway Activation', *Developmental Cell*, 32(5), pp. 640–651. doi: 10.1016/j.devcel.2015.01.011.

Nishioka, N. *et al.* (2009) 'The Hippo Signaling Pathway Components Lats and Yap Pattern Tead4 Activity to Distinguish Mouse Trophectoderm from Inner Cell Mass', *Developmental Cell*. Elsevier Ltd, 16(3), pp. 398–410. doi: 10.1016/j.devcel.2009.02.003.
O'Neill, E. (2004) 'Role of the Kinase MST2 in Suppression of Apoptosis by the Proto-Oncogene Product Raf-1', *Science*, 306(5705), pp. 2267–2270. doi: 10.1126/science.1103233.
O'Neill, E. (2017) 'Ras and the Hippo Pathway in Cancer', in *Conquering RAS*. Elsevier, pp. 25–39. doi: 10.1016/B978-0-12-803505-4.00002-3.
Ogasawara, N. *et al.* (2018) 'Reduction of Membrane Protein CRIM1 Decreases E-Cadherin and Increases Claudin-1 and MMPs, Enhancing the Migration and Invasion of Renal Carcinoma Cells', *Biological and Pharmaceutical Bulletin*, 41(4), pp. 604–611. doi: 10.1248/bpb.b17-00990.
Ogata, M. *et al.* (1999) 'Effects of overexpression of PTP36, a putative protein tyrosine phosphatase, on cell adhesion, cell growth, and cytoskeletons in HeLa cells', *Journal of Biological Chemistry*, 274(18), pp. 12905–12909. doi: 10.1074/jbc.274.18.12905.
Onoda, T. *et al.* (2006) 'Tetracycline analogues (doxycycline and COL-3) induce caspase-dependent and -independent apoptosis in human colon cancer cells', *International Journal of Cancer*, 118(5), pp. 1309–1315. doi: 10.1002/ijc.21447.
Ota, M. and Sasaki, H. (2008) 'Mammalian Tead proteins regulate cell proliferation and contact inhibition as transcriptional mediators of Hippo signaling', *Development*, 135(24), pp. 4059–4069. doi: 10.1242/dev.027151.
Pal, S. K. *et al.* (2016) 'THBS1 is induced by TGFB1 in the cancer stroma and promotes invasion of oral squamous cell carcinoma', *Journal of Oral Pathology & Medicine*, 45(10), pp. 730–739. doi: 10.1111/jop.12430.
Pantalacci, S., Tapon, N. and Léopold, P. (2003) 'The salvador partner Hippo promotes apoptosis and cell-cycle exit in Drosophila', *Nature Cell Biology*, 5(10), pp. 921–927. doi: 10.1038/ncb1051.
Pearlman, R. L. *et al.* (2017) 'Potential therapeutic targets of epithelial–mesenchymal transition in melanoma', *Cancer Letters*, 391, pp. 125–140. doi: 10.1016/j.canlet.2017.01.029.
Pectasides, D. *et al.* (1989) 'Treatment of metastatic malignant melanoma with dacarbazine, vindesine and cisplatin.', *British journal of cancer*, 60(4), pp. 627–9. Available at: http://www.ncbi.nlm.nih.gov/pubmed/2803936.
Pellock, B. J. *et al.* (2007) 'The Drosophila tumor suppressors Expanded and Merlin differentially regulate cell cycle exit, apoptosis, and Wingless signaling', *Developmental Biology*, 304(1), pp. 102–115. doi: 10.1016/j.ydbio.2006.12.021.
Pollock, P. M. *et al.* (2002) 'High frequency of BRAF mutations in nevi', *Nature Genetics*, 33(1), pp. 19–20. doi: 10.1038/ng1054.
Poon, C. L. C. *et al.* (2011) 'The Sterile 20-like Kinase Tao-1 Controls Tissue Growth by Regulating the Salvador-Warts-Hippo Pathway', *Developmental Cell*. Elsevier Inc., 21(5), pp. 896–906. doi: 10.1016/j.devcel.2011.09.012.
Prickett, T. D. *et al.* (2011) 'Exon capture analysis of G protein-coupled receptors identifies activating mutations in GRM3 in melanoma', *Nature Genetics*. Nature Publishing Group, 43(11), pp. 1119–1126. doi: 10.1038/ng.950.
Proskuryakov, S. and Gabai, V. (2010) 'Mechanisms of Tumor Cell Necrosis', *Current Pharmaceutical Design*, 16(1), pp. 56–68. doi: 10.2174/138161210789941793.
Quintana, E. *et al.* (2008) 'Efficient tumour formation by single human melanoma cells', *Nature*, 456(7222), pp. 593–598. doi: 10.1038/nature07567.

Rak, J. *et al.* (2000) 'Oncogenes and tumor angiogenesis: differential modes of vascular endothelial growth factor up-regulation in ras-transformed epithelial cells and fibroblasts.', *Cancer research*, 60(2), pp. 490–8. Available at: http://www.ncbi.nlm.nih.gov/pubmed/10667605.
Rastrelli, M. *et al.* (2014) 'Melanoma: epidemiology, risk factors, pathogenesis, diagnosis and classification', *In vivo*, 28(6), pp. 1005–1011. Available at: http://iv.iiarjournals.org/content/28/6/1005.full.pdf.
Reginensi, A. *et al.* (2013) 'Yap- and Cdc42-Dependent Nephrogenesis and Morphogenesis during Mouse Kidney Development', *PLoS Genetics*. Edited by G. R. Dressler, 9(3), p. e1003380. doi: 10.1371/journal.pgen.1003380.
Ribas, A. *et al.* (2013) 'Hepatotoxicity with Combination of Vemurafenib and Ipilimumab', *New England Journal of Medicine*, 368(14), pp. 1365–1366. doi: 10.1056/NEJMc1302338.
Robert, C. *et al.* (2015) 'Improved Overall Survival in Melanoma with Combined Dabrafenib and Trametinib', *New England Journal of Medicine*, 372(1), pp. 30–39. doi: 10.1056/NEJMoa1412690.
Ruth, M. C. *et al.* (2006) 'RhoC Promotes Human Melanoma Invasion in a PI3K/Akt-Dependent Pathway', *Journal of Investigative Dermatology*, 126(4), pp. 862–868. doi: 10.1038/sj.jid.5700211.
Sabine, A. *et al.* (2015) 'FOXC2 and fluid shear stress stabilize postnatal lymphatic vasculature', *Journal of Clinical Investigation*, 125(10), pp. 3861–3877. doi: 10.1172/JCI80454.
Sahebkar, A. *et al.* (2015) 'Does statin therapy reduce plasma VEGF levels in humans? A systematic review and meta-analysis of randomized controlled trials', *Metabolism*, 64(11), pp. 1466–1476. doi: 10.1016/j.metabol.2015.08.002.
Schlegelmilch, K. *et al.* (2011) 'Yap1 Acts Downstream of α-Catenin to Control Epidermal Proliferation', *Cell*. Elsevier Inc., 144(5), pp. 782–795. doi: 10.1016/j.cell.2011.02.031.
Seidel, C. *et al.* (2007) 'Frequent hypermethylation ofMST1 andMST2 in soft tissue sarcoma', *Molecular Carcinogenesis*, 46(10), pp. 865–871. doi: 10.1002/mc.20317.
Sekido, Y. *et al.* (1995) 'Neurofibromatosis type 2 (NF2) gene is somatically mutated in mesothelioma but not in lung cancer.', *Cancer research*, 55(6), pp. 1227–31. Available at: http://www.ncbi.nlm.nih.gov/pubmed/7882313.
Sensi, M. *et al.* (2011) 'Human Cutaneous Melanomas Lacking MITF and Melanocyte Differentiation Antigens Express a Functional Axl Receptor Kinase', *Journal of Investigative Dermatology*, 131(12), pp. 2448–2457. doi: 10.1038/jid.2011.218.
Shain, A. H. *et al.* (2015) 'The Genetic Evolution of Melanoma from Precursor Lesions', *New England Journal of Medicine*, 373(20), pp. 1926–1936. doi: 10.1056/NEJMoa1502583.
Shieh, J. M. *et al.* (2010) 'Activation of c-Jun N-terminal kinase is essential for mitochondrial membrane potential change and apoptosis induced by doxycycline in melanoma cells', *British Journal of Pharmacology*, 160(5), pp. 1171–1184. doi: 10.1111/j.1476-5381.2010.00746.x.
Shimizu, T., Ho, L.-L. and Lai, Z.-C. (2008) 'The mob as tumor suppressor gene is essential for early development and regulates tissue growth in Drosophila.', *Genetics*, 178(2), pp. 957–965. doi: 10.1534/genetics.107.081570.
Shitara, Y. and Sugiyama, Y. (2006) 'Pharmacokinetic and pharmacodynamic alterations of 3-hydroxy-3-methylglutaryl coenzyme A (HMG-CoA) reductase inhibitors: Drug–drug interactions and interindividual differences in transporter and metabolic enzyme functions', *Pharmacology & Therapeutics*, 112(1), pp. 71–105. doi: 10.1016/j.pharmthera.2006.03.003.
Shultz, L. D. *et al.* (1995) 'Multiple defects in innate and adaptive immunologic function in NOD/LtSz-scid mice.', *Journal of immunology (Baltimore, Md. : 1950)*, 154(1), pp. 180–91. Available at: http://www.ncbi.nlm.nih.gov/pubmed/7995938.

Shultz, L. D. *et al.* (2005) 'Human Lymphoid and Myeloid Cell Development in NOD/LtSz-scid IL2R null Mice Engrafted with Mobilized Human Hemopoietic Stem Cells', *The Journal of Immunology*, 174(10), pp. 6477–6489. doi: 10.4049/jimmunol.174.10.6477.
Shultz, L. D., Ishikawa, F. and Greiner, D. L. (2007) 'Humanized mice in translational biomedical research', *Nature Reviews Immunology*, 7(2), pp. 118–130. doi: 10.1038/nri2017.
Silvis, M. R. *et al.* (2011) 'α-Catenin Is a Tumor Suppressor That Controls Cell Accumulation by Regulating the Localization and Activity of the Transcriptional Coactivator Yap1', *Science Signaling*, 4(174), pp. ra33-ra33. doi: 10.1126/scisignal.2001823.
Solit, D. B. *et al.* (2006) 'BRAF mutation predicts sensitivity to MEK inhibition', *Nature*, 439(7074), pp. 358–362. doi: 10.1038/nature04304.
Song, H. *et al.* (2010) 'Mammalian Mst1 and Mst2 kinases play essential roles in organ size control and tumor suppression', *Proceedings of the National Academy of Sciences*, 107(4), pp. 1431–1436. doi: 10.1073/pnas.0911409107.
Song, X. *et al.* (2015) 'Overall survival in patients with metastatic melanoma', *Current Medical Research and Opinion*, 31(5), pp. 987–991. doi: 10.1185/03007995.2015.1021904.
Sorrentino, G. *et al.* (2014) 'Metabolic control of YAP and TAZ by the mevalonate pathway', *Nature Cell Biology*, 16(4), pp. 357–366. doi: 10.1038/ncb2936.
Spagnolo, F. and Queirolo, P. (2012) 'Upcoming strategies for the treatment of metastatic melanoma', *Archives of Dermatological Research*, 304(3), pp. 177–184. doi: 10.1007/s00403-012-1223-7.
Spugnardi, M. *et al.* (2003) 'Epigenetic Inactivation of RAS Association Domain Family Protein 1 (RASSF1A) in Malignant Cutaneous Melanoma Epigenetic Inactivation of RAS Association Domain Family Protein 1 (RASSF1A) in Malignant Cutaneous Melanoma 1', *Cancer Research*, 1(30), pp. 1639–1643. Available at: http://cancerres.aacrjournals.org/content/63/7/1639.
Stone, N. . *et al.* (2014) '2013 ACC/AHA guideline on the treatment of blood cholesterol to reduce atherosclerotic cardiovascular risk in adults: a report of the American College of Cardiology/American Heart Association Task Force on Practice Guidelines'. Journal of the American College of Cardiology, 63(25 Part, pp. 2889–2934.
Strano, S. *et al.* (2001) 'Physical Interaction with Yes-associated Protein Enhances p73 Transcriptional Activity', *Journal of Biological Chemistry*, 276(18), pp. 15164–15173. doi: 10.1074/jbc.M010484200.
Stryjkowska-Góra, A. *et al.* (2015) 'Statins and cancers', *Współczesna Onkologia*, 3, pp. 167–175. doi: 10.5114/wo.2014.44294.
Tai, K.-Y. *et al.* (2008) 'Axl promotes cell invasion by inducing MMP-9 activity through activation of NF-κB and Brg-1', *Oncogene*, 27(29), pp. 4044–4055. doi: 10.1038/onc.2008.57.
Takahashi, Y. (2005) 'Down-Regulation of LATS1 and LATS2 mRNA Expression by Promoter Hypermethylation and Its Association with Biologically Aggressive Phenotype in Human Breast Cancers', *Clinical Cancer Research*, 11(4), pp. 1380–1385. doi: 10.1158/1078-0432.CCR-04-1773.
Tapon, N. *et al.* (2002) 'salvador Promotes Both Cell Cycle Exit and Apoptosis in Drosophila and Is Mutated in Human Cancer Cell Lines', *Cell*, 110(4), pp. 467–478. doi: 10.1016/S0092-8674(02)00824-3.
Taylor, L. K., Wang, H. C. and Erikson, R. L. (1996) 'Newly identified stress-responsive protein kinases, Krs-1 and Krs-2.', *Proceedings of the National Academy of Sciences of the United States of America*, 93(19), pp. 10099–104. doi: VL - 93.
Tomlinson, V. *et al.* (2010) 'JNK phosphorylates Yes-associated protein (YAP) to regulate apoptosis', *Cell Death & Disease*. Nature Publishing Group, 1(2), pp. e29–e29. doi: 10.1038/cddis.2010.7.

Tsao, H. *et al.* (2012) 'Melanoma: from mutations to medicine', *Genes & Development*, 26(11), pp. 1131–1155. doi: 10.1101/gad.191999.112.
Tsao, H. and Sober, A. J. (1998) 'Ultraviolet radiation and malignant melanoma', *Clinics in Dermatology*. New York, NY: Springer New York, 16(1), pp. 67–73. doi: 10.1016/S0738-081X(97)00191-0.
Udan, R. S. *et al.* (2003) 'Hippo promotes proliferation arrest and apoptosis in the Salvador/Warts pathway', *Nature Cell Biology*, 5(10), pp. 914–920. doi: 10.1038/ncb1050.
Ushio-Fukai, M. *et al.* (2002) 'Novel Role of gp91 phox -Containing NAD(P)H Oxidase in Vascular Endothelial Growth Factor–Induced Signaling and Angiogenesis', *Circulation Research*, 91(12), pp. 1160–1167. doi: 10.1161/01.RES.0000046227.65158.F8.
Vakkila, J. and Lotze, M. T. (2004) 'Opinion: Inflammation and necrosis promote tumour growth', *Nature Reviews Immunology*, 4(8), pp. 641–648. doi: 10.1038/nri1415.
Varelas, X. *et al.* (2008) 'TAZ controls Smad nucleocytoplasmic shuttling and regulates human embryonic stem-cell self-renewal', *Nature Cell Biology*. 1st edn. Elsevier Ltd, 10(7), pp. 837–848. doi: 10.1038/ncb1748.
Varelas, X., Samavarchi-Tehrani, P., *et al.* (2010) 'The Crumbs Complex Couples Cell Density Sensing to Hippo-Dependent Control of the TGF-β-SMAD Pathway', *Developmental Cell*. Elsevier Inc., 19(6), pp. 831–844. doi: 10.1016/j.devcel.2010.11.012.
Varelas, X., Miller, B. W., *et al.* (2010) 'The Hippo Pathway Regulates Wnt/β-Catenin Signaling', *Developmental Cell*. Elsevier Ltd, 18(4), pp. 579–591. doi: 10.1016/j.devcel.2010.03.007.
Vassilev, A. *et al.* (2001) 'TEAD/TEF transcription factors utilize the activation domain of YAP65, a Src/Yes-associated protein localized in the cytoplasm', *Genes & Development*, 15(10), pp. 1229–1241. doi: 10.1101/gad.888601.
Verfaillie, A. *et al.* (2015) 'Decoding the regulatory landscape of melanoma reveals TEADS as regulators of the invasive cell state', *Nature Communications*. Nature Publishing Group, 6, pp. 1–16. doi: 10.1038/ncomms7683.
Walker, T. M. *et al.* (2002) 'Expression of angiogenic factors Cyr61 and tissue factor in uveal melanoma.', *Archives of ophthalmology (Chicago, Ill. : 1960)*, 120(12), pp. 1719–25. Available at: http://www.ncbi.nlm.nih.gov/pubmed/12470148.
Wang, K.-C. *et al.* (2016) 'Flow-dependent YAP/TAZ activities regulate endothelial phenotypes and atherosclerosis', *Proceedings of the National Academy of Sciences*, 113(41), pp. 11525–11530. doi: 10.1073/pnas.1613121113.
Wang, W. *et al.* (2012) 'PTPN14 is required for the density dependent control of YAP1', *Genes Dev*, 26(17), pp. 1959–1971. doi: 10.1101/gad.192955.112.activation.
Wang, W., Huang, J. and Chen, J. (2011) 'Angiomotin-like Proteins Associate with and Negatively Regulate YAP1', *Journal of Biological Chemistry*, 286(6), pp. 4364–4370. doi: 10.1074/jbc.C110.205401.
Wang, X. *et al.* (2017) 'YAP/TAZ Orchestrate VEGF Signaling during Developmental Angiogenesis', *Developmental Cell*, 42(5), p. 462–478.e7. doi: 10.1016/j.devcel.2017.08.002.
Warren, J., Xiao, Y. and Lamar, J. (2018) 'YAP/TAZ Activation as a Target for Treating Metastatic Cancer', *Cancers*, 10(4), p. 115. doi: 10.3390/cancers10040115.
Wei, X., Shimizu, T. and Lai, Z.-C. (2007) 'Mob as tumor suppressor is activated by Hippo kinase for growth inhibition in Drosophila', *The EMBO Journal*, 26(7), pp. 1772–1781. doi: 10.1038/sj.emboj.7601630.
Wennmann, D. O. *et al.* (2014) 'The Hippo pathway is controlled by Angiotensin II signaling and its reactivation induces apoptosis in podocytes', *Cell Death & Disease*, 5(11), pp. e1519–e1519. doi: 10.1038/cddis.2014.476.
Wolchok, J. D. *et al.* (2017) 'Overall Survival with Combined Nivolumab and Ipilimumab in Advanced Melanoma', *New England Journal of Medicine*, 377(14), pp. 1345–1356. doi: 10.1056/NEJMoa1709684.

Wu, S. *et al.* (2003) 'hippo Encodes a Ste-20 Family Protein Kinase that Restricts Cell Proliferation and Promotes Apoptosis in Conjunction with salvador and warts', *Cell*, 114(4), pp. 445–456. doi: 10.1016/S0092-8674(03)00549-X.
Wu, S. *et al.* (2008) 'The TEAD/TEF Family Protein Scalloped Mediates Transcriptional Output of the Hippo Growth-Regulatory Pathway', *Developmental Cell*, 14(3), pp. 388–398. doi: 10.1016/j.devcel.2008.01.007.
Xia, Y. *et al.* (2014) 'YAP/TEAD Co-Activator Regulated Pluripotency and Chemoresistance in Ovarian Cancer Initiated Cells', *PLoS ONE*. Edited by H. Wanjin, 9(11), p. e109575. doi: 10.1371/journal.pone.0109575.
Xiao, G.-H., Chernoff, J. and Testa, J. R. (2003) 'NF2: The wizardry of merlin', *Genes, Chromosomes and Cancer*, 38(4), pp. 389–399. doi: 10.1002/gcc.10282.
Xin, M. *et al.* (2013) 'Hippo pathway effector Yap promotes cardiac regeneration', *Proceedings of the National Academy of Sciences*, 110(34), pp. 13839–13844. doi: 10.1073/pnas.1313192110.
Xiong, H. *et al.* (2017) 'Yes-Associated Protein (YAP) Promotes Tumorigenesis in Melanoma Cells Through Stimulation of Low-Density Lipoprotein Receptor-Related Protein 1 (LRP1)', *Scientific Reports*, 7(1), p. 15528. doi: 10.1038/s41598-017-14764-4.
Xu, P. *et al.* (2013) 'Promotion of Melanoma Cell Invasion and Tumor Metastasis by Microcystin-LR via Phosphatidylinositol 3-Kinase/AKT Pathway', *Environmental Science & Technology*, p. 130712144451004. doi: 10.1021/es4007228.
Xu, T. *et al.* (1995) 'Identifying tumor suppressors in genetic mosaics: the Drosophila lats gene encodes a putative protein kinase.', *Development*, 121(4), pp. 1053–63. doi: 10.1101/gad.3.9.1273.
Yagi, R. *et al.* (1999) 'A WW domain-containing Yes-associated protein (YAP) is a novel transcriptional co-activator', *The EMBO Journal*, 18(9), pp. 2551–2562. doi: 10.1093/emboj/18.9.2551.
Yimlamai, D. *et al.* (2014) 'Hippo Pathway Activity Influences Liver Cell Fate', *Cell*. Elsevier Inc., 157(6), pp. 1324–1338. doi: 10.1016/j.cell.2014.03.060.
Yin, F. *et al.* (2013) 'Spatial Organization of Hippo Signaling at the Plasma Membrane Mediated by the Tumor Suppressor Merlin/NF2', *Cell*, 154(6), pp. 1342–1355. doi: 10.1016/j.cell.2013.08.025.
Yoshikawa, K. *et al.* (2015) 'The Hippo pathway transcriptional co-activator, YAP, confers resistance to cisplatin in human oral squamous cell carcinoma', *International Journal of Oncology*, 46(6), pp. 2364–2370. doi: 10.3892/ijo.2015.2948.
Young, M. R. *et al.* (1999) 'Transgenic mice demonstrate AP-1 (activator protein-1) transactivation is required for tumor promotion', *Proceedings of the National Academy of Sciences*, 96(17), pp. 9827–9832. doi: 10.1073/pnas.96.17.9827.
Yu, F.-X. *et al.* (2012) 'Regulation of the Hippo-YAP Pathway by G-Protein-Coupled Receptor Signaling', *Cell*. Elsevier, 150(4), pp. 780–791. doi: 10.1016/j.cell.2012.06.037.
Yu, F.-X. *et al.* (2014) 'Mutant Gq/11 Promote Uveal Melanoma Tumorigenesis by Activating YAP', *Cancer Cell*. Elsevier Inc., 25(6), pp. 822–830. doi: 10.1016/j.ccr.2014.04.017.
Yu, F.-X., Zhang, K. and Guan, K.-L. (2014) 'YAP as oncotarget in uveal melanoma', *Oncoscience*, 1(7), p. 480. doi: 10.18632/oncoscience.57.
Yu, L. *et al.* (2015) 'Cardiac hypertrophy induced by active Raf depends on Yorkie-mediated transcription', *Science Signaling*, 8(362), pp. ra13-ra13. doi: 10.1126/scisignal.2005719.
Yuan, H. *et al.* (2015) 'Genetic variants in Hippo pathway genes YAP 1, TEAD 1 and TEAD 4 are associated with melanoma-specific survival', *International Journal of Cancer*, 137(3), pp. 638–645. doi: 10.1002/ijc.29429.

Zanconato, F. *et al.* (2015) 'Genome-wide association between YAP/TAZ/TEAD and AP-1 at enhancers drives oncogenic growth', *Nature Cell Biology*, 17(9), pp. 1218–1227. doi: 10.1038/ncb3216.
Zanconato, F., Cordenonsi, M. and Piccolo, S. (2016) 'YAP/TAZ at the Roots of Cancer', *Cancer Cell*, 29(6), pp. 783–803. doi: 10.1016/j.ccell.2016.05.005.
Zender, L. *et al.* (2006) 'Identification and Validation of Oncogenes in Liver Cancer Using an Integrative Oncogenomic Approach', *Cell*, 125(7), pp. 1253–1267. doi: 10.1016/j.cell.2006.05.030.
Zeng, H. *et al.* (2015) 'CRIM1, a newfound cancer-related player, regulates the adhesion and migration of lung cancer cells', *Growth Factors*, 33(5–6), pp. 384–392. doi: 10.3109/08977194.2015.1119132.
Zhang, H. *et al.* (2009) 'TEAD Transcription Factors Mediate the Function of TAZ in Cell Growth and Epithelial-Mesenchymal Transition', *Journal of Biological Chemistry*, 284(20), pp. 13355–13362. doi: 10.1074/jbc.M900843200.
Zhang, L. *et al.* (2008) 'The TEAD/TEF Family of Transcription Factor Scalloped Mediates Hippo Signaling in Organ Size Control', *Developmental Cell*, 14(3), pp. 377–387. doi: 10.1016/j.devcel.2008.01.006.
Zhang, L. *et al.* (2015) 'NDR Functions as a Physiological YAP1 Kinase in the Intestinal Epithelium', *Current Biology*, 25(3), pp. 296–305. doi: 10.1016/j.cub.2014.11.054.
Zhang, N. *et al.* (2010) 'The Merlin/NF2 Tumor Suppressor Functions through the YAP Oncoprotein to Regulate Tissue Homeostasis in Mammals', *Developmental Cell*, 19(1), pp. 27–38. doi: 10.1016/j.devcel.2010.06.015.
Zhao, B. *et al.* (2007) 'Inactivation of YAP oncoprotein by the Hippo pathway is involved in cell contact inhibition and tissue growth control', *Genes & Development*, 21(21), pp. 2747–2761. doi: 10.1101/gad.1602907.
Zhao, B. *et al.* (2008) 'TEAD mediates YAP-dependent gene induction and growth control', *Genes & Development*, 22(14), pp. 1962–1971. doi: 10.1101/gad.1664408.
Zhao, B. *et al.* (2009) 'Both TEAD-Binding and WW Domains Are Required for the Growth Stimulation and Oncogenic Transformation Activity of Yes-Associated Protein', *Cancer Research*, 69(3), pp. 1089–1098. doi: 10.1158/0008-5472.CAN-08-2997.
Zhao, B. *et al.* (2010) 'The Hippo-YAP pathway in organ size control and tumorigenesis: an updated version', *Genes & Development*, 24(9), pp. 862–874. doi: 10.1101/gad.1909210.
Zhao, B. *et al.* (2011) 'Angiomotin is a novel Hippo pathway component that inhibits YAP oncoprotein', *Genes & Development*, 25(1), pp. 51–63. doi: 10.1101/gad.2000111.
Zheng, Y. *et al.* (2015) 'Identification of Happyhour/MAP4K as Alternative Hpo/Mst-like Kinases in the Hippo Kinase Cascade', *Developmental Cell*, 34(6), pp. 642–655. doi: 10.1016/j.devcel.2015.08.014.
Zhou, D. *et al.* (2009) 'Mst1 and Mst2 Maintain Hepatocyte Quiescence and Suppress Hepatocellular Carcinoma Development through Inactivation of the Yap1 Oncogene', *Cancer Cell*. Elsevier Ltd, 16(5), pp. 425–438. doi: 10.1016/j.ccr.2009.09.026.
Zhou, X. *et al.* (2015) 'Estrogen regulates Hippo signaling via GPER in breast cancer', *Journal of Clinical Investigation*, 125(5), pp. 2123–2135. doi: 10.1172/JCI79573.
Zhu, H. *et al.* (2015) 'Proton-sensing GPCR-YAP signalling promotes cell proliferation and survival', *International Journal of Biological Sciences*, 11(10), pp. 1181–1189. doi: 10.7150/ijbs.12500.

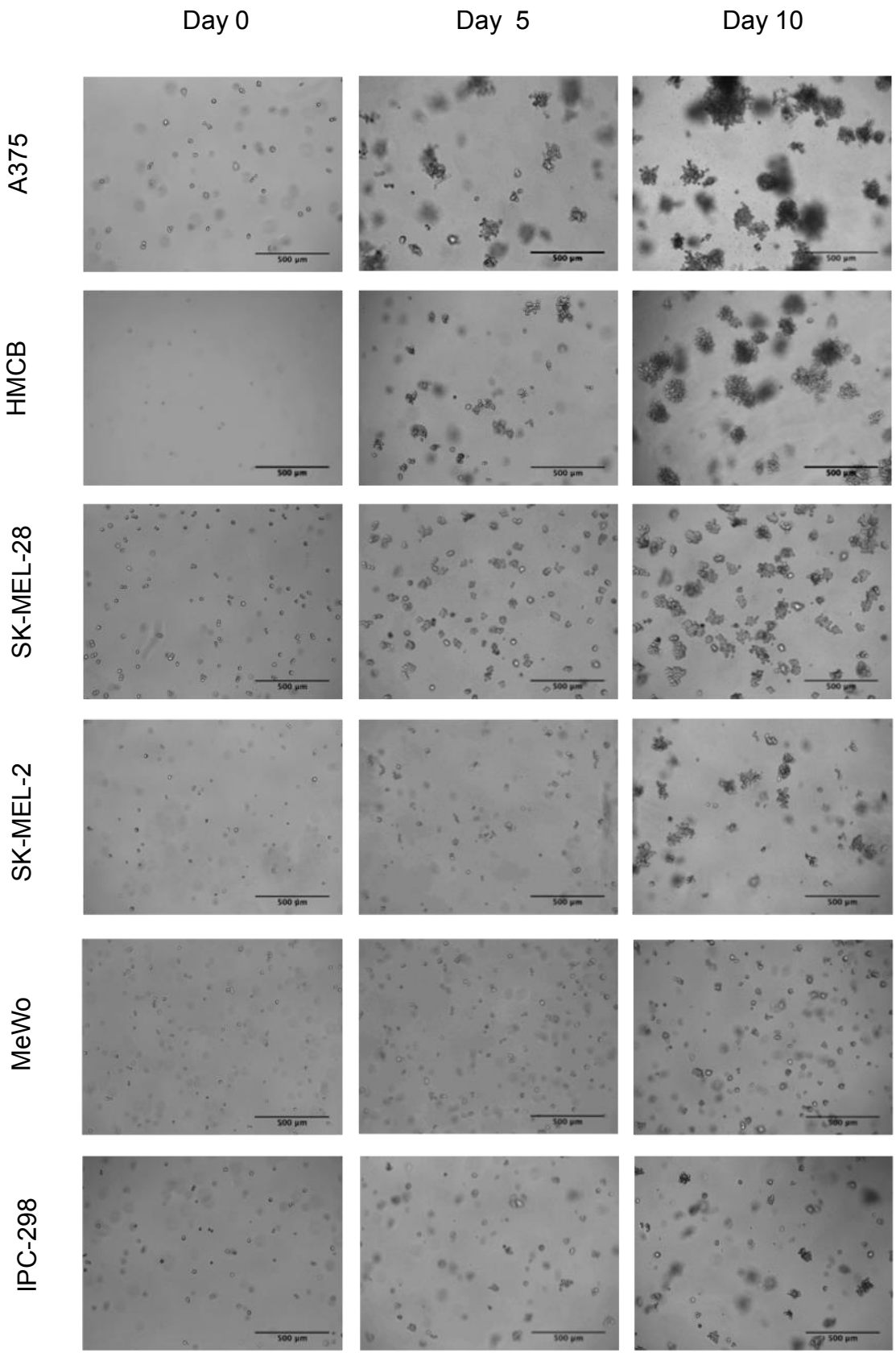

Figure 1

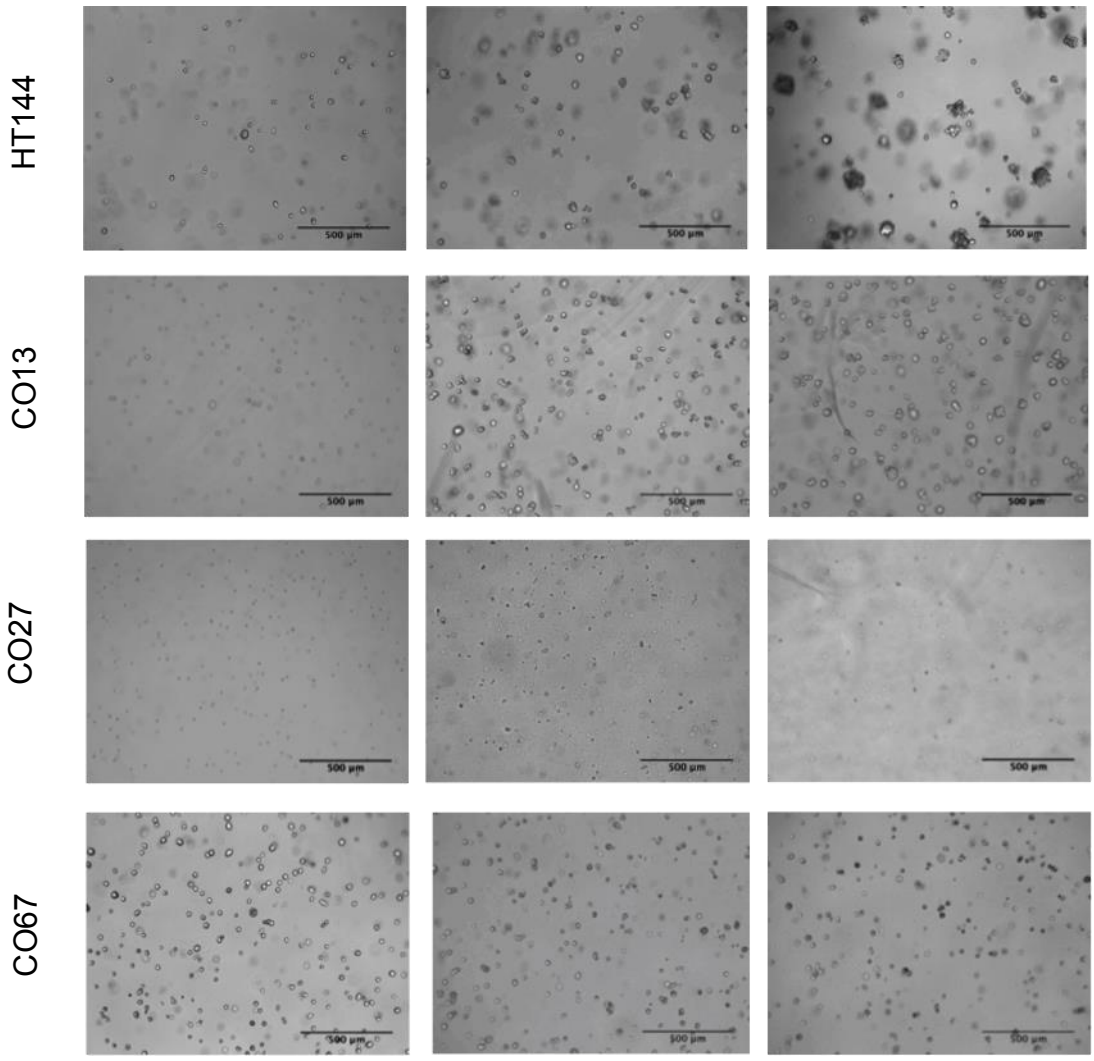

Figure 1. Growth of ten melanoma cell lines in soft agar

A panel of ten melanoma cell lines were grown in soft agar in 96-well plates for two weeks. Images were taken on day 0, day 5, and day 10, using a Zeiss Axiovert microscope, showing the growth of the cell colonies. Scale bar, 500 μm. The experiments were performed in triplicate.

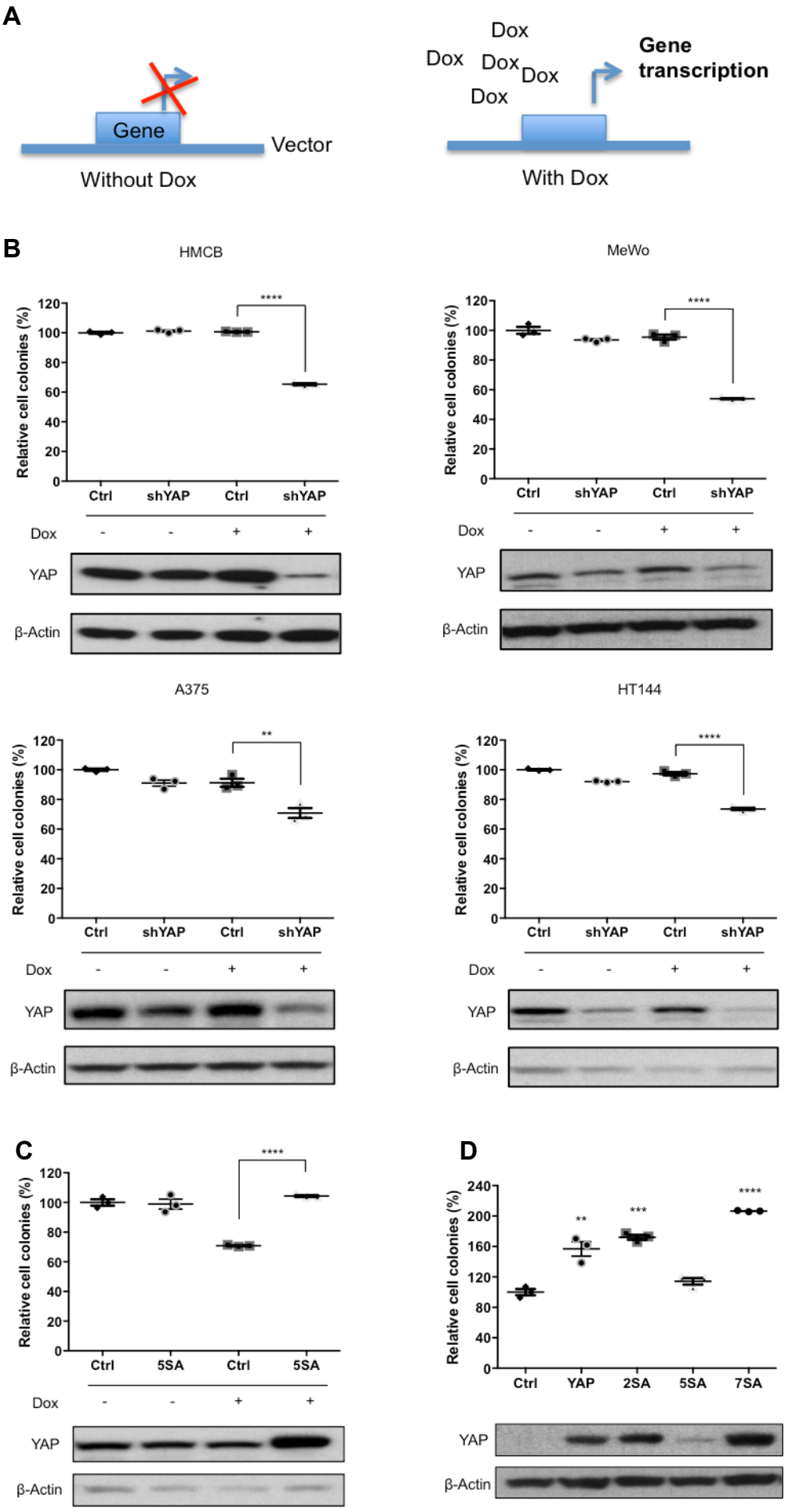
A
Gene
Vector
Without Dox
Dox
Dox
Dox
Dox
Gene transcription
With Dox
B
HMCB
MeWo
A375
HT144
Relative cell colonies (%)
Ctrl
shYAP
Dox
YAP
β-Actin
C
5SA
D
YAP
2SA
5SA
7SA

Figure 2

Figure 2. YAP influences the ability of the colony formation of melanoma cells

(A) Schematic representation of the tet-on system. Left, The encoded gene by a vector is not able to express without Dox. Right, The gene encoded by the vector is able to express when Dox is applied.

(B) Knockdown of YAP by shRNA decreased colonies of HMCB, MeWo, HT144, and A375 cells in soft agar assays. Values were normalised to that of vector control without Dox. Western blot analysis confirmed the knockdown of YAP.

(C) Expression of YAP-5SA increased colonies of MeWo cells grown in soft agar. Values were normalised to that of vector control without Dox. Western blot analysis confirmed the expression of YAP-5SA using a total YAP antibody.

(D) MeWo cells overexpressing wt-YAP, and expressing YAP-2SA, YAP-5SA, or YAP-7SA generated more colonies in soft agar. Values were normalised to that of vector control. Expressions of YAP were detected using western blot analysis.

The experiments were performed in triplicate. Data are presented as mean ± standard deviation. **P<0.01. ***P<0.001. ****P<0.0001. Dox, doxycycline. Ctrl, control. YAP, wt-YAP. 2SA, YAP-2SA. 5SA, YAP-5SA. 7SA, YAP-7SA.

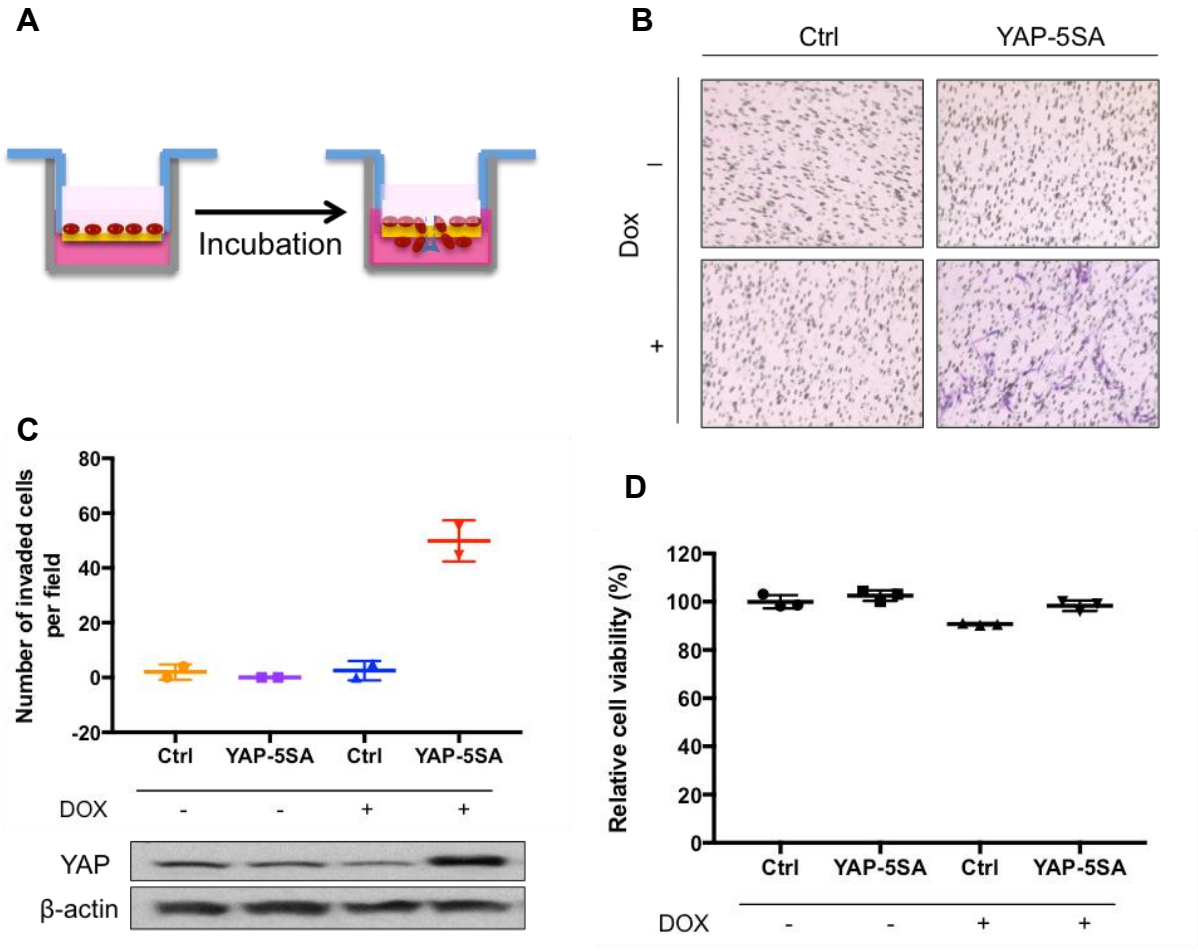

Figure 3. YAP promotes invasion of **melanoma cells**

(A) Schematic diagram of the invasion assay using transwell inserts. A permeable transwell insert (blue) separated the 24-well chamber into upper and lower layers. Matrigel (yellow) was added onto the upper layer. Cells (red) were seeded with P/S-free RPMI (light pink) into the upper layer and attracted by the RPMI supplemented with 10% FBS (deep pink) placed in the lower chamber. After 48 hrs of incubation, invasive cells moved down to the lower side of the insert via pores on the insert membrane.

(B) Representative microscopic fields of invaded cells in transwell invasion assays. MeWo-Ctrl and MeWo-YAP-5SA cells were seeded as described in (A). Dox was applied on cells 24 hrs before cell seeding. Images were taken using a Zeiss Axiovert microscope. Magnification, x100.

(C) Number of invaded cells per field. Five fields were randomly selected from each sample. Data represent the mean number of invaded cells per field. Western blot analysis confirmed the expression of YAP-5SA. Experiments were performed in duplicate, so statistical analysis was not applicable.

(D) Viability of MeWo-Ctrl and YAP-5SA cells that were seeded simultaneously with the invasion assay. Values were normalised to Ctrl-Dox cells. Data are presented as mean ± standard deviation. Ctrl, control. Dox, doxycycline.

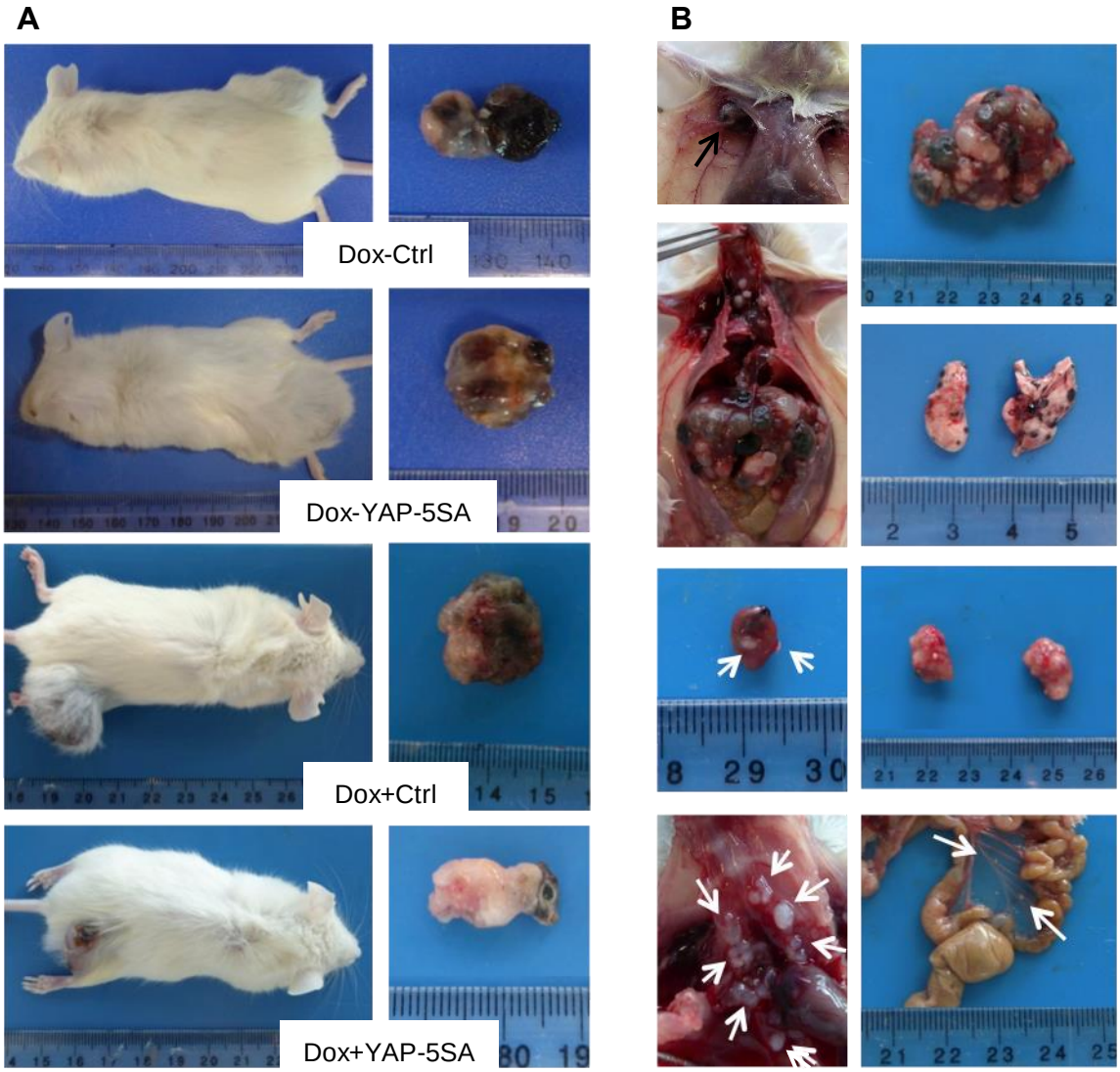

Figure 4. Establishment of a spontaneous murine metastasis xenograft model

(A) Representative images of xenograft mice and primary tumours. Mice were subcutaneously injected with MeWo Ctrl or YAP-5SA cells. Mice were randomly chosen to be treated with (+) or without (-) Dox when primary tumours were 5 mm. Primary tumours were harvested by autopsy when the longest diameters of tumours were 20 mm. n=8.

(B) Representative images of metastases in different organs. Left panel, top to bottom: lymph node, thoracic and abdominal cavity, heart, and pleura. Right panel, top to bottom: liver, lung, kidney, and mesentery. Arrows indicate metastatic nodules.

Ctrl, control. Dox, doxycycline.

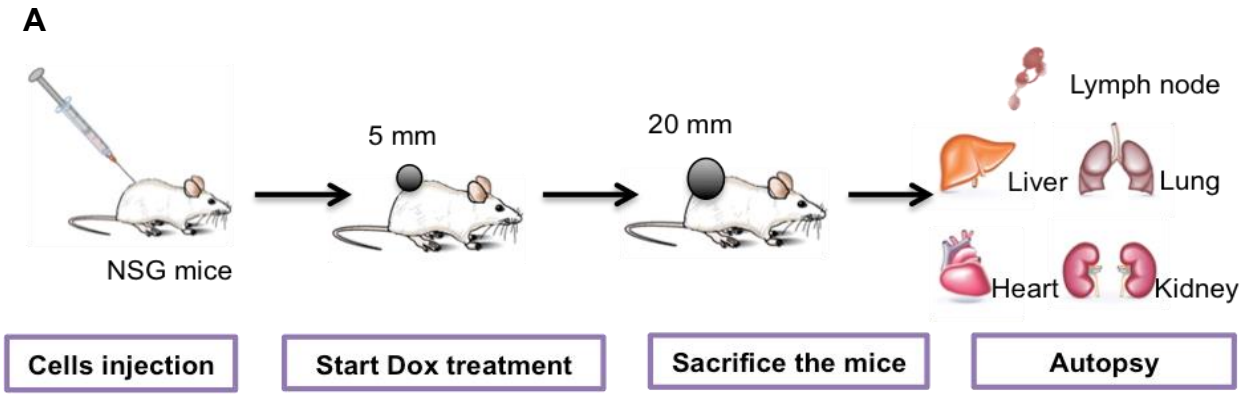
A
NSG mice
5 mm
20 mm
Lymph node
Liver
Lung
Heart
Kidney
Cells injection
Start Dox treatment
Sacrifice the mice
Autopsy

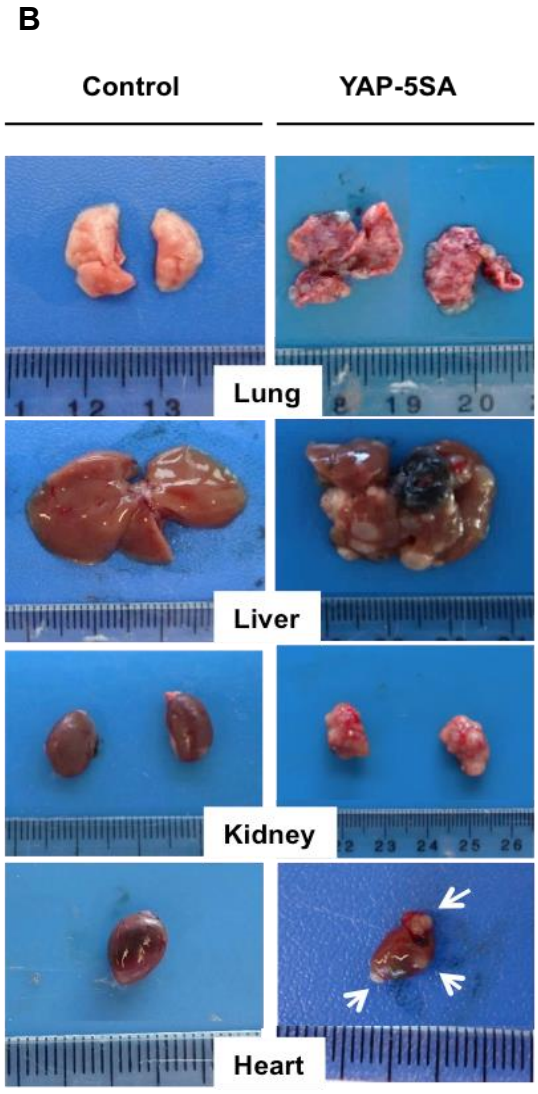
B
Control
YAP-5SA
Lung
Liver
Kidney
Heart

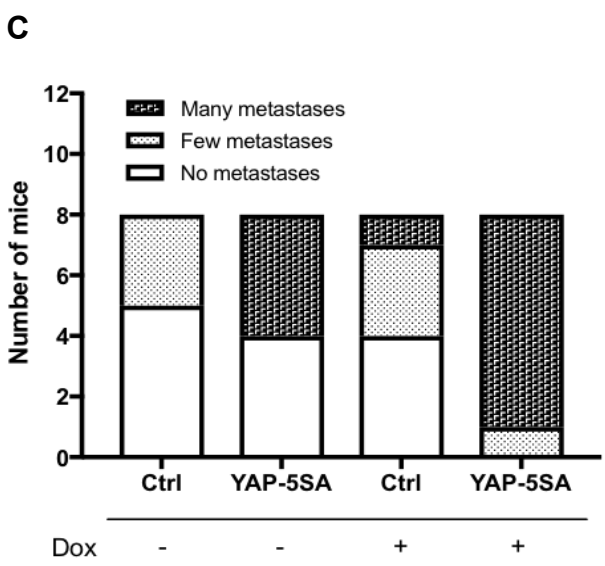
C
Many metastases
Few metastases
No metastases
Number of mice
Ctrl
YAP-5SA
Ctrl
YAP-5SA
Dox
-
-
+
+

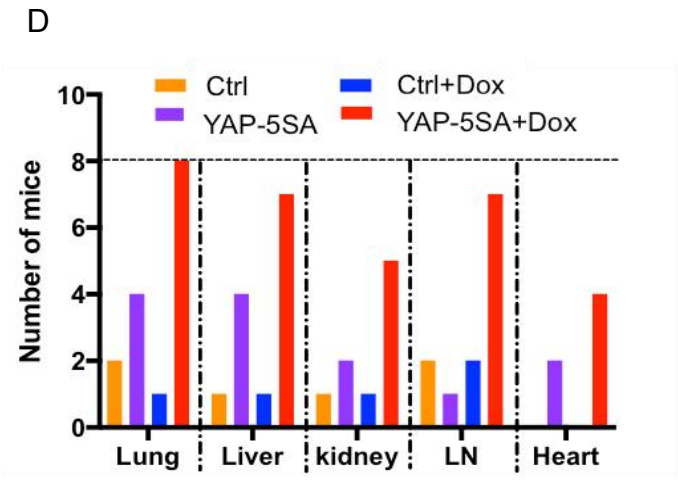
D
Ctrl
YAP-5SA
Ctrl+Dox
YAP-5SA+Dox
Number of mice
Lung
Liver
kidney
LN
Heart

Figure 5-1

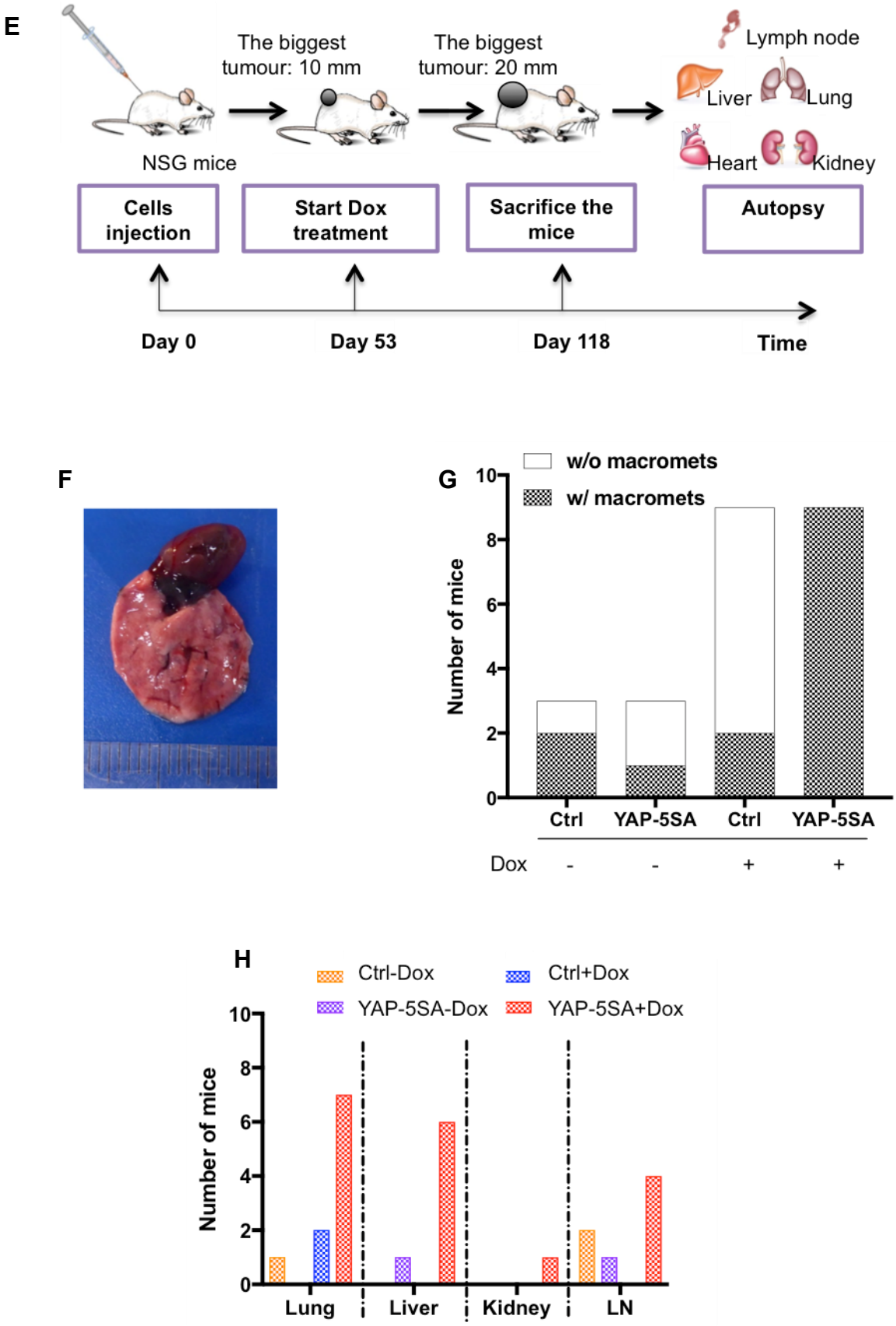
E
The biggest tumour: 10 mm
The biggest tumour: 20 mm
Lymph node
Liver
Lung
Heart
Kidney
NSG mice
Cells injection
Start Dox treatment
Sacrifice the mice
Autopsy
Day 0
Day 53
Day 118
Time
F
G
w/o macromets
w/ macromets
Number of mice
Ctrl
YAP-5SA
Ctrl
YAP-5SA
Dox
H
Ctrl-Dox
Ctrl+Dox
YAP-5SA-Dox
YAP-5SA+Dox
Number of mice
Lung
Liver
Kidney
LN

Figure 5-2

Figure 5. YAP promotes melanoma macrometastasis

(A) Schematic workflow of the first round of the *in vivo* experiment. Mice were subcutaneously injected into the right flanks with MeWo Ctrl or YAP-5SA cells. Dox treatment started when the tumours reached 5 mm, and mice were sacrificed when primary tumours reached 20 mm. Organs shown were collected by autopsy, and metastases in organs were examined with naked eyes.

(B) Representative images of different organs in YAP-5SA expressing mice and control mice. Arrows indicate metastatic nodules.

(C) Number of mice with macrometastases in each group of mice. Macrometastases in organs were examined with naked eyes. (Many metastases, Number of metastatic nodules >10; Few, <10; No, =0)

(D) Number of mice with macrometastases in individual organs. LN, lymph node.

(E) Schematic of the second round of the *in vivo* experiment. Mice were subcutaneously injected into the right flanks with MeWo Ctrl or YAP-5SA cells. For mice that were chosen to receive Dox, the Dox treatment started at the same time when the biggest tumour reached 10 mm. All mice were sacrificed at the same time when the biggest tumour reached 20 mm. Organs shown were collected by autopsy, and macrometastases in organs were examined with naked eyes.

(F) A representative image of metastatic lung whose metastatic nodules were hard to distinguish with naked eyes.

(G) Number of mice with macrometastases in each group. Macrometastases in organs were examined with naked eyes. w/o, without. w/, with.

(H) Number of mice with macrometastases in individual organs. LN, lymph node.

In (B), (C), and (D), mice were treated as described in (A). n = 8.

In (F), (G), and (H), mice were treated as described in (E). Ctrl-Dox and YAP-5SA-Dox: n = 3. Ctrl+Dox and YAP-5SA+Dox: n=9.

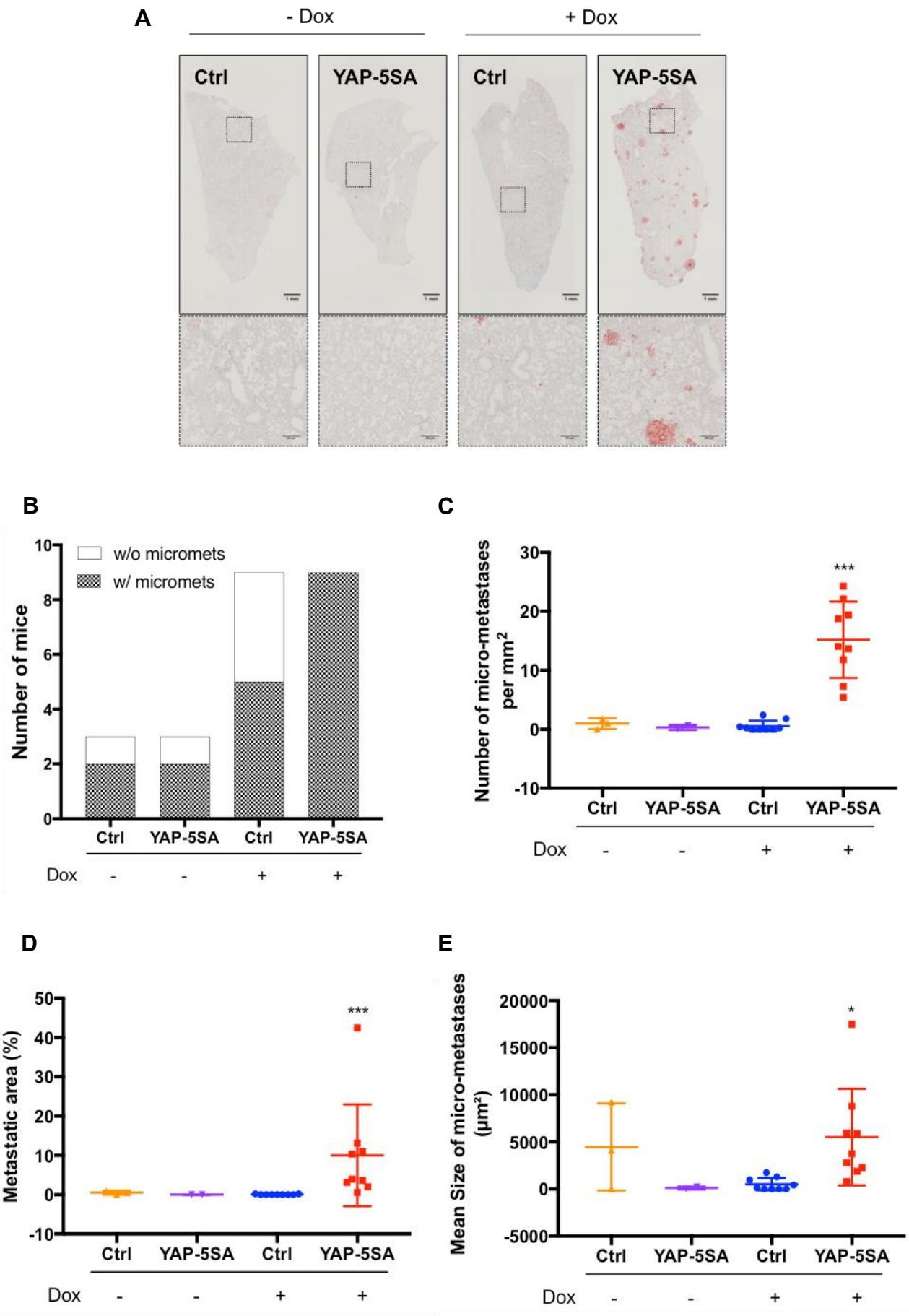
A
- Dox
+ Dox
Ctrl
YAP-5SA
Ctrl
YAP-5SA
B
w/o micromets
w/ micromets
Number of mice
Ctrl
YAP-5SA
Ctrl
YAP-5SA
Dox - - + +
C
Number of micro-metastases per mm²
***
Ctrl
YAP-5SA
Ctrl
YAP-5SA
Dox - - + +
D
Metastatic area (%)
***
Ctrl
YAP-5SA
Ctrl
YAP-5SA
Dox - - + +
E
Mean Size of micro-metastases (µm²)
*
Ctrl
YAP-5SA
Ctrl
YAP-5SA
Dox - - + +

Figure 6

Figure 6. YAP promotes melanoma micrometastasis

(A) Representative images of stained lung tissues from FFPE blocks. Lung tissues were harvested from mice sacrificed in the second round of the *in vivo* experiment. One paraffin section was used from each sample. The lung tissues were stained with a human mitochondria antibody. The red colour indicates anti-human mitochondria positive area. Scale bar, top, 1 mm; bottom, 200 μm.

(B) Number of mice with micrometastases in each group of mice. One anti-mitochondria antibody-stained section was chosen from each sample of lung tissues. w/o, without. w/, with.

(C) Number of micrometastases per mm^2 lung tissues.

(D) The percentage of micrometastatic area in total area.

(E) The mean size of micrometastases in lungs.

In (B), (C), (D), and (E), samples were generated as described in (A). For each sample, one anti-mitochondria antibody-stained section was used. Ten fields were randomly chosen and analysed from each section. Each dot represents an individual mouse. Ctrl-Dox and YAP-5SA-Dox: n = 3. Ctrl+Dox and YAP-5SA+Dox: n=9. Data are presented as mean ± standard deviation. *P<0.05. ***P<0.001. Ctrl, control. Dox, doxycycline.

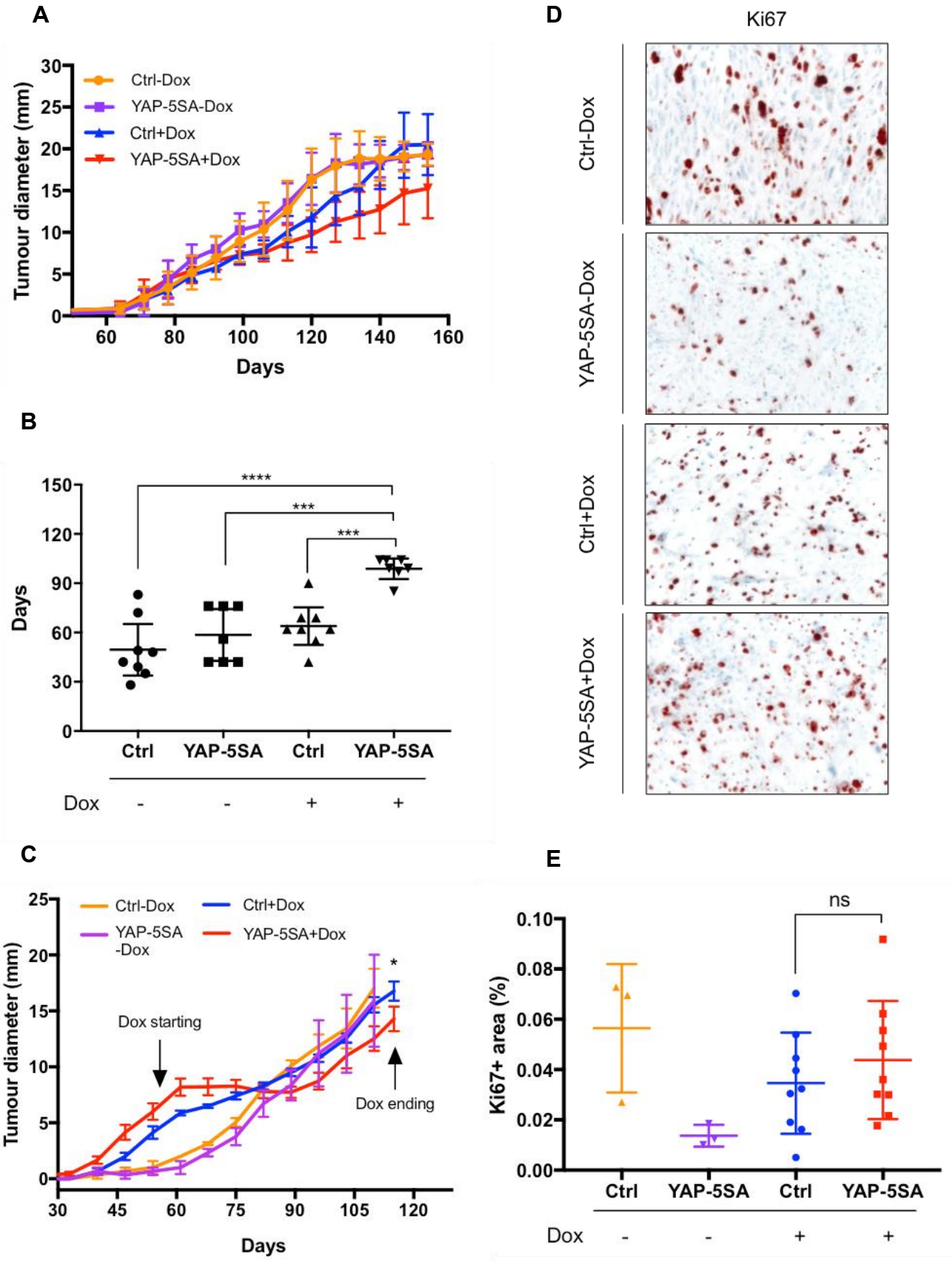
A
Tumour diameter (mm)
Days
Ctrl-Dox
YAP-5SA-Dox
Ctrl+Dox
YAP-5SA+Dox
B
Days
****
***
***
Ctrl
YAP-5SA
Ctrl
YAP-5SA
Dox
C
Tumour diameter (mm)
Days
Ctrl-Dox
YAP-5SA -Dox
Ctrl+Dox
YAP-5SA+Dox
Dox starting
Dox ending
*
D
Ki67
Ctrl-Dox
YAP-5SA-Dox
Ctrl+Dox
YAP-5SA+Dox
E
Ki67+ area (%)
ns
Ctrl
YAP-5SA
Ctrl
YAP-5SA
Dox

Figure 7

Figure 7. YAP causes primary melanoma xenograft tumours to grow slower

(A) Tumour growth chart of the first *in vivo* experiment. Tumour diameters were subsequently monitored during development from the day of injection (day 0) until the day of sacrifice.

(B) Time period between tumour diameters from 5 mm to 20 mm. Data were generated from the first *in vivo* experiment.

(C) Tumour growth chart of the second *in vivo* experiment. Tumour diameters were subsequently monitored during development from the day of injection (day 0) until the day of sacrifice. Arrow heads indicate Dox starting and ending time points.

(D) Representative images of Ki67-stained primary tumour tissues. The Ki67 staining was performed with tumour tissues collected from the second in vivo experiment. Images were taken by the Olympus BX51 microscope. Magnification, x400.

(E) Percentage of Ki67 positive (Ki67+) area in total area. One field full with viable cells was randomly chosen and analysed from each section.

In (D) and (E), samples were generated from the second *in vivo* experiment. Each dot represents an individual mouse. Data are presented as mean ± standard deviation. ns, $P>0.05$. ***$P<0.001$. Ctrl, control. Dox, doxycycline.

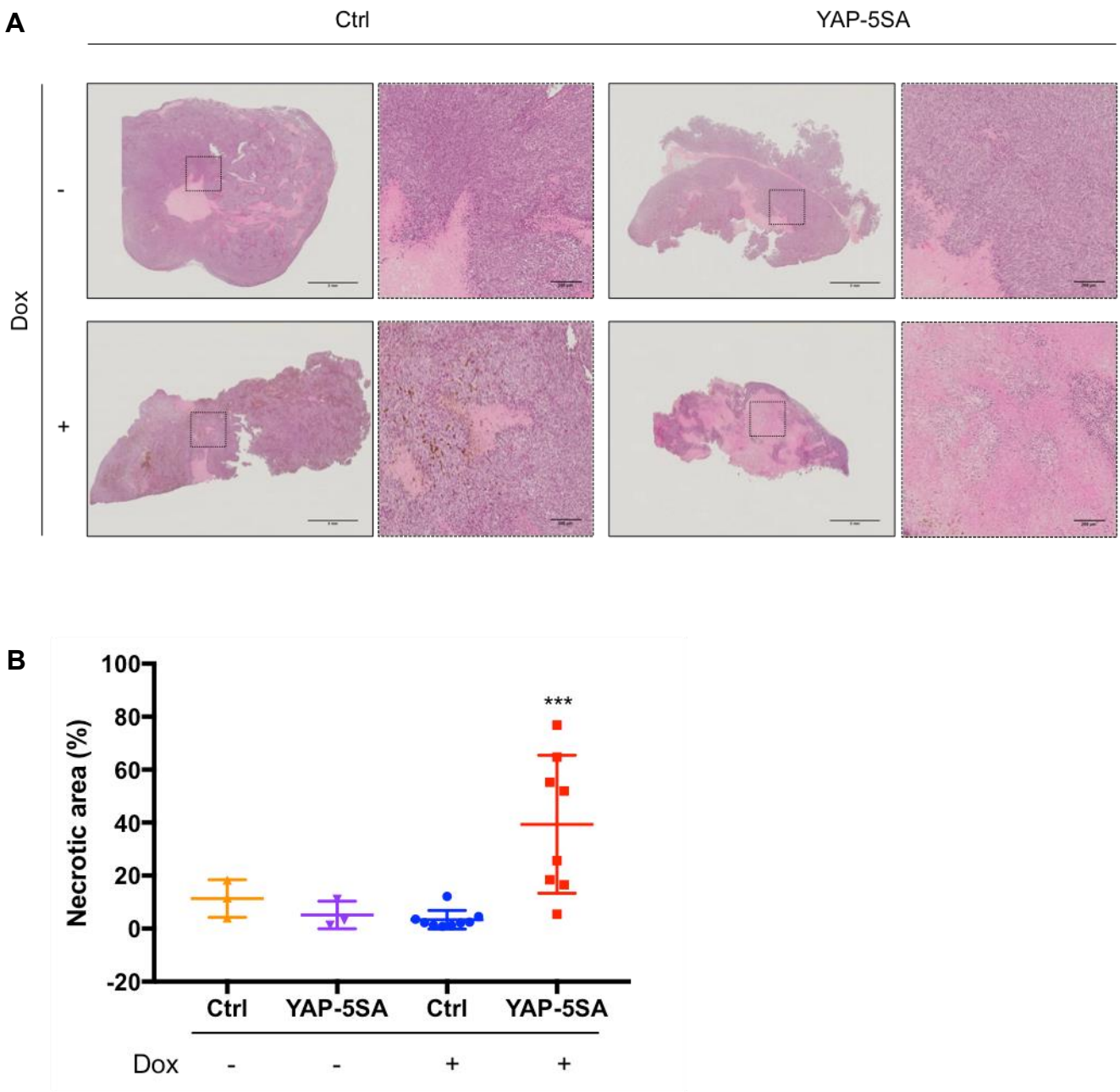

Figure 8. YAP promotes necrosis of primary melanoma

(A) Representative images of primary tumour tissues stained with H&E from FFPE blocks. The primary tumour tissues were collected from the second *in vivo* experiment. One H&E-stained section was performed from each sample. Whole sections were scanned by the Olympus VS120 Virtual Slide Microscope. Scale bar, left, 2 mm; right, 200 μm.

(B) Percentage of necrotic area in total area of tumour tissues. Analysis was performed with whole section-scanned images. Each dot represents an individual mouse. Ctrl-Dox and YAP-5SA-Dox: n = 3. Ctrl+Dox and YAP-5SA+Dox: n=9. Data are presented as mean ± standard deviation. ***P<0.001. Ctrl, control. Dox, doxycycline.

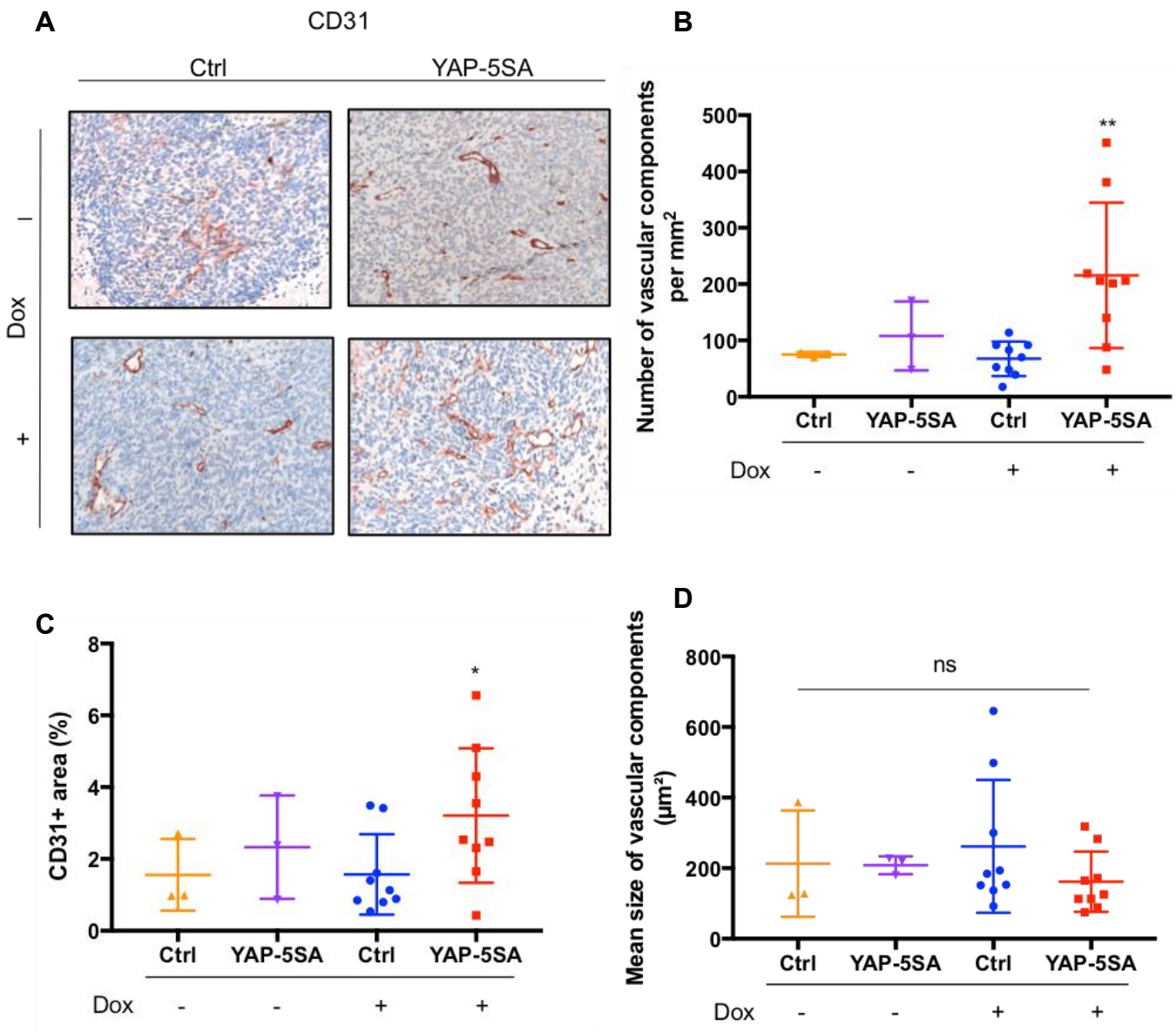

Figure 9. YAP promotes vascularization of primary melanoma

(A) Representative images of primary tumour tissues stained with the CD31 antibody. Primary tumour tissues were collected from the second *in vivo* experiment. One CD31-stained section was performed from each sample. Red indicates CD31 positive (CD31+) area/vascular components. Images were taken using the Olympus BX51 microscope. Magnification, x200.

(B) Number of vascular components per mm^2 tumour tissues.

(C) The percentage of CD31+ area in total area.

(D) The mean size of vascular components in primary tumours.

In (B), (C), and (D), analyses were performed with CD31-stained samples prepared as described in (A). Each dot represents an individual mouse. Ctrl-Dox and YAP-5SA-Dox: n = 3. Ctrl+Dox and YAP-5SA+Dox: n=9. Data are presented as mean ± standard deviation. ns, P>0.05. *P<0.05. **P<0.01. Ctrl, control. Dox, doxycycline.

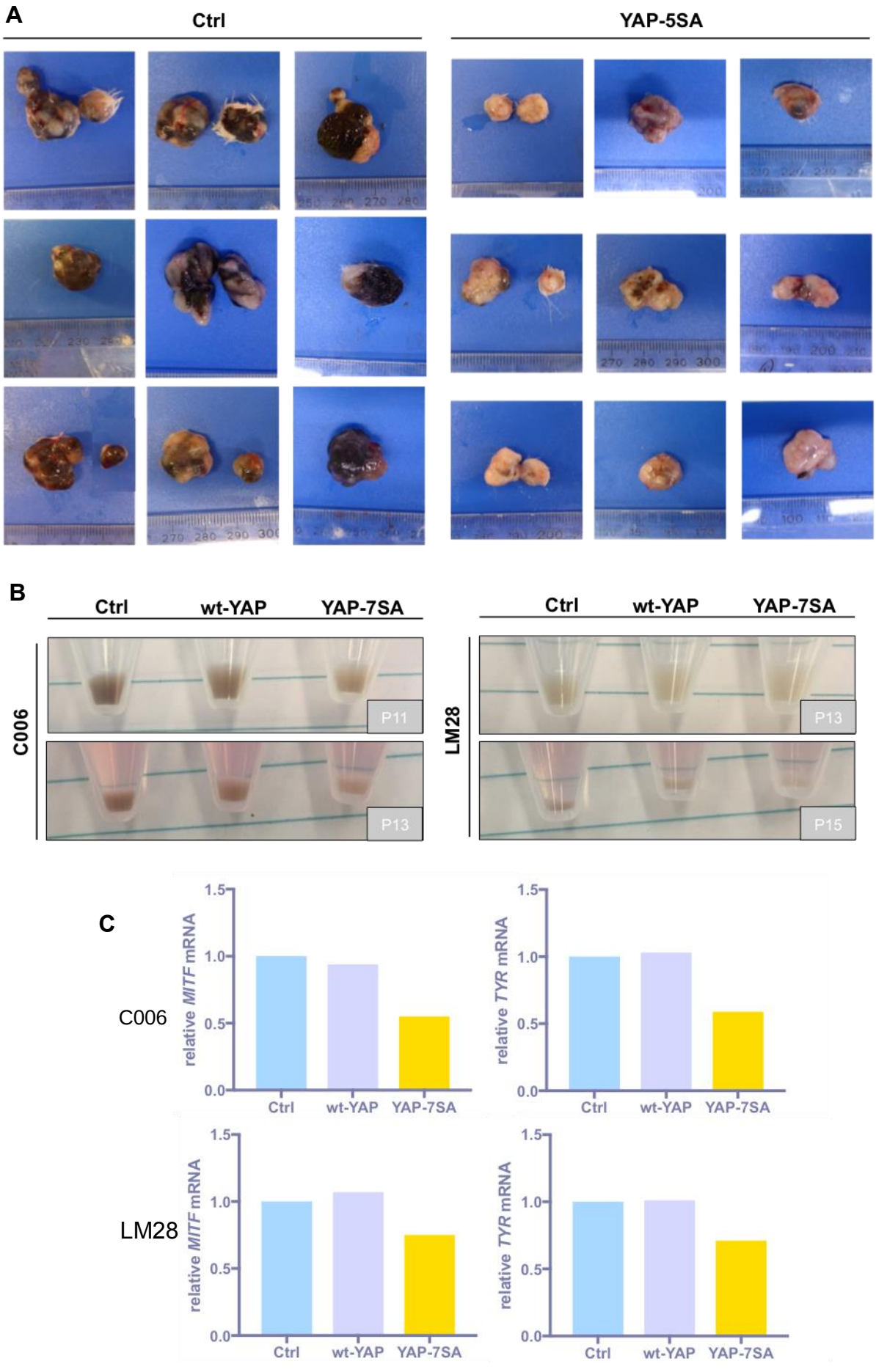
A
Ctrl
YAP-5SA
B
Ctrl
wt-YAP
YAP-7SA
C006
P11
P13
Ctrl
wt-YAP
YAP-7SA
LM28
P13
P15
C
C006
LM28
relative MITF mRNA
relative TYR mRNA
1.5
1.0
0.5
0.0
Ctrl
wt-YAP
YAP-7SA

Figure 10

Figure 10. YAP causes depigmentation of melanoma

(A) Images of primary tumours that expressed YAP-5SA or not (Ctrl). Tumours were generated from the second *in vivo* experiment. n=9.

(B) Representative images of cell pellets of transfected C006 and LM28 cells. Cells were transfected with empty vectors or vectors expressing either wt-YAP or YAP-7SA. P, passage number.

(C) mRNA levels of *MITF* and *TYR* in transfected cells. Upper panel, C006 cells. Lower panel, LM28 cells. Experiments were performed in duplicate, so statistical analysis was not applicable.

Ctrl, control.

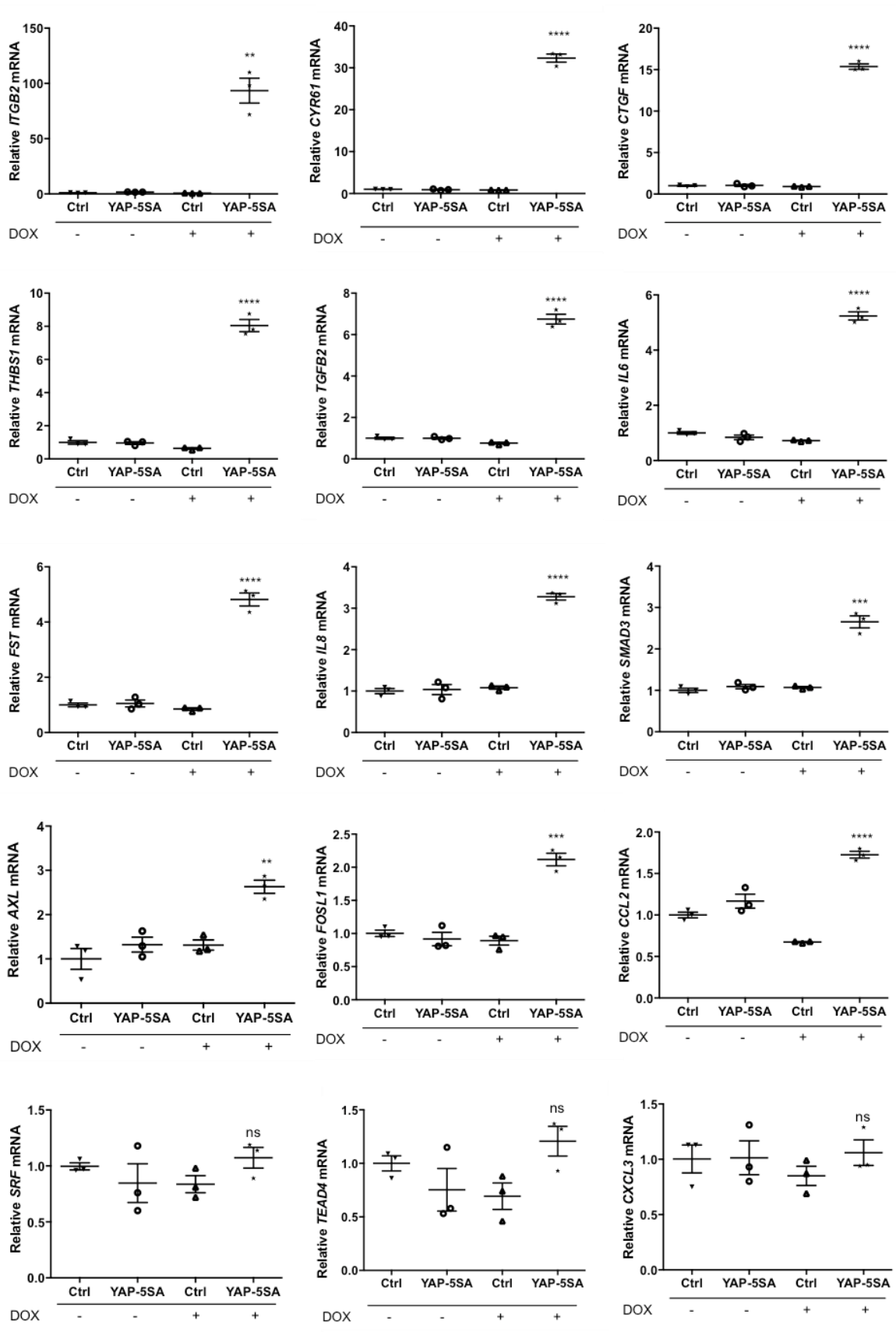
Relative ITGB2 mRNA
Relative CYR61 mRNA
Relative CTGF mRNA
Relative THBS1 mRNA
Relative TGFB2 mRNA
Relative IL6 mRNA
Relative FST mRNA
Relative IL8 mRNA
Relative SMAD3 mRNA
Relative AXL mRNA
Relative FOSL1 mRNA
Relative CCL2 mRNA
Relative SRF mRNA
Relative TEAD4 mRNA
Relative CXCL3 mRNA
Ctrl
YAP-5SA
DOX
ns

Figure 11

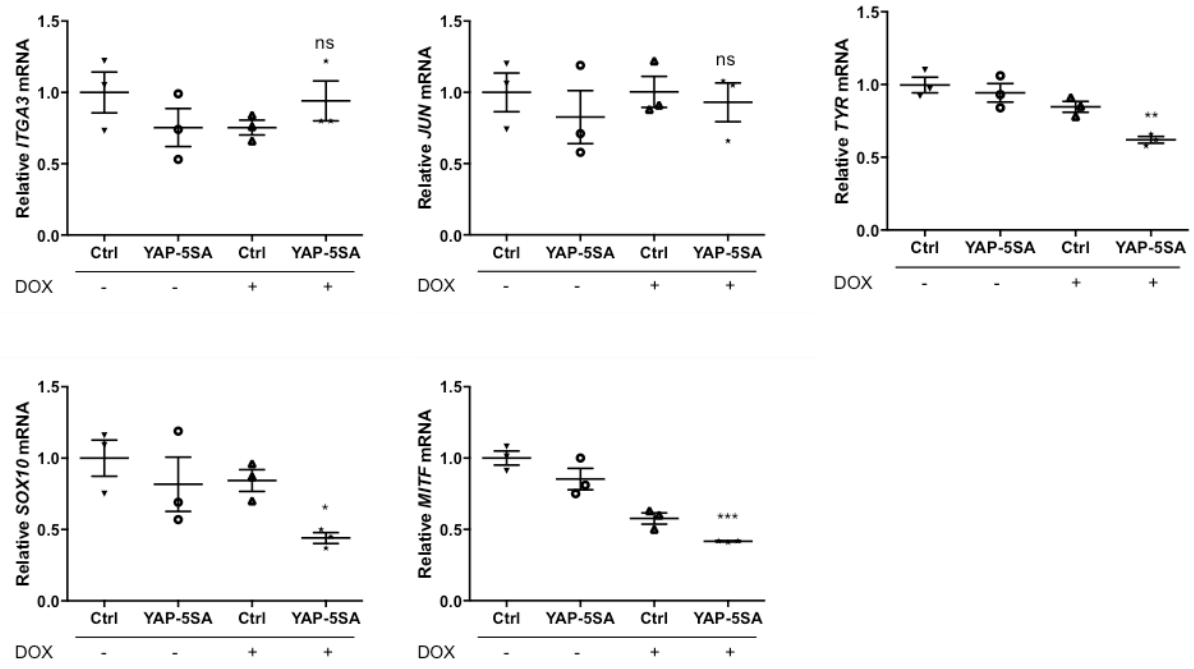

Figure 11. Validation of RNAseq data by qPCR

mRNA levels of 20 genes measured by qPCR. Experiments were performed in triplicate. Measurements were normalised to MeWo-Ctrl cells without Dox treatment. Data are presented as mean ± standard deviation. ns, P>0.05. *P<0.05. **P<0.01. ***P<0.001. ****P<0.0001. Ctrl, control. Dox, doxycycline.

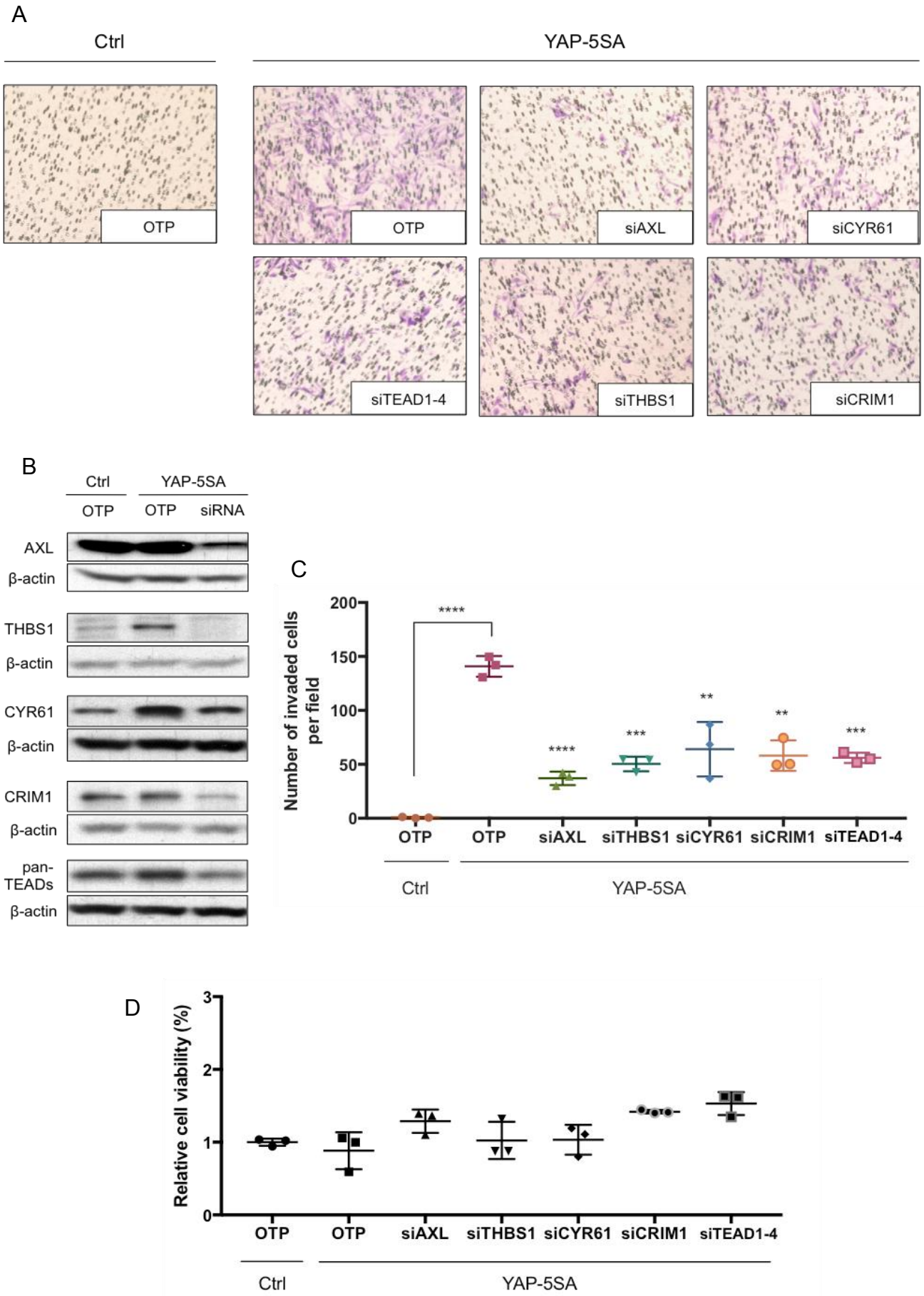
A
Ctrl
YAP-5SA
OTP
OTP
siAXL
siCYR61
siTEAD1-4
siTHBS1
siCRIM1
B
Ctrl
YAP-5SA
OTP
OTP
siRNA
AXL
β-actin
THBS1
β-actin
CYR61
β-actin
CRIM1
β-actin
pan-TEADs
β-actin
C
Number of invaded cells per field
200
150
100
50
0
****
****
***
**
**
***
OTP
OTP
siAXL
siTHBS1
siCYR61
siCRIM1
siTEAD1-4
Ctrl
YAP-5SA
D
Relative cell viability (%)
3
2
1
0
OTP
OTP
siAXL
siTHBS1
siCYR61
siCRIM1
siTEAD1-4
Ctrl
YAP-5SA

Figure 12

Figure 12. Identification of YAP target genes that mediate invasion of melanoma cells

(A) Representative microscopy of invaded MeWo cells that expressing YAP-5SA or not (Ctrl) using transwell invasion assays. Cells were transfected with OTP or siRNAs that target *AXL, THBS1, CYR61, CRIM1*, or *TEAD1-4*. Magnification, x100.

(B) Western blot analysis confirmed efficient knockdown of target genes in YAP-5SA expressing MeWo cells.

(C) Quantification of invaded cells. Five fields were randomly selected in each sample. Each spot represents one sample.

(D) Viability of MeWo Ctrl and YAP-5SA cells that were seeded simultaneously with the invasion assay. Values were normalised to Ctrl-Dox cells.

Experiments were performed in triplicate. Data are presented as mean ± standard deviation. **P<0.01. ***P<0.001. ****P<0.0001. Ctrl, control.

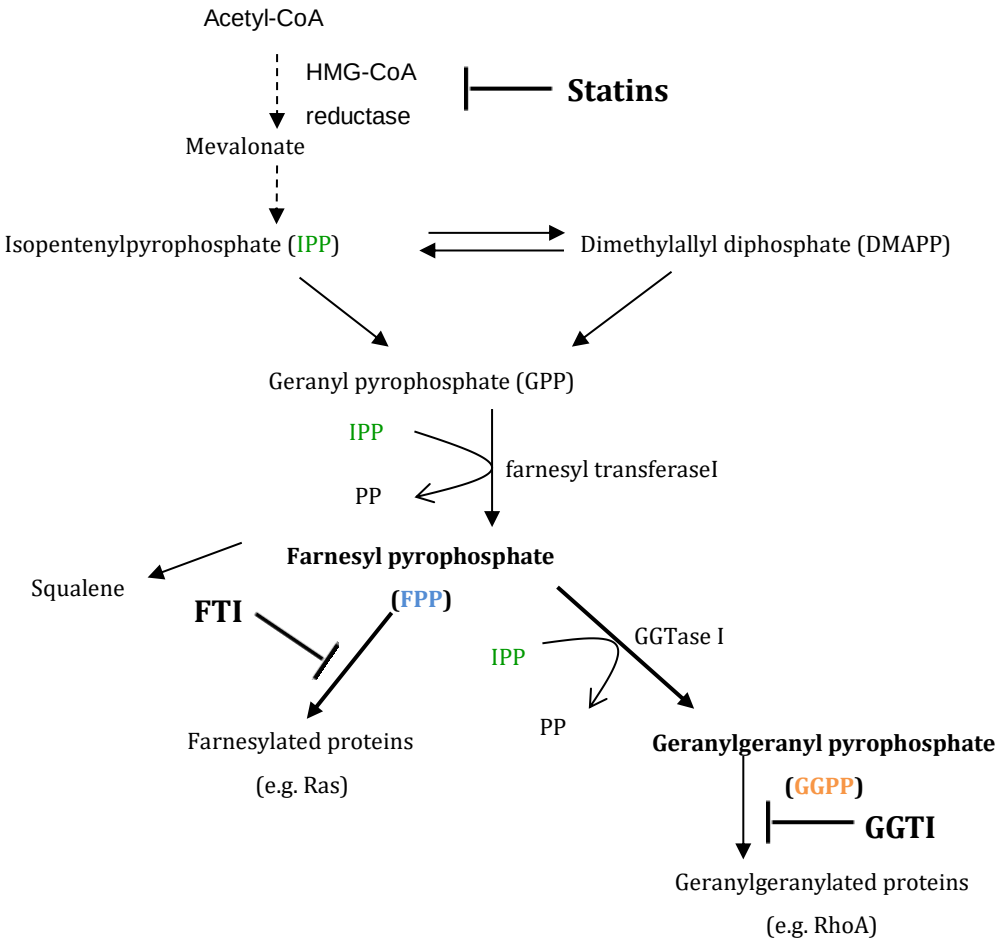

Figure 13. Statins block the mevalonate pathway

Schematic diagram of the mevalonate pathway which synthesises lipids and cholesterol. Statins inhibit the pathway from an early stage, limiting all downstream products. FPP and GGPP are two intermediates of the pathway, finally attached to farnesylated proteins and geranylgeranylated proteins respectively. FTI and GGTI can inhibit the syntheses of the two types of proteins respectively. Graph adapted from (Sorrentino et al., 2014.; Gruenbacher and Thurnher, 2017.).

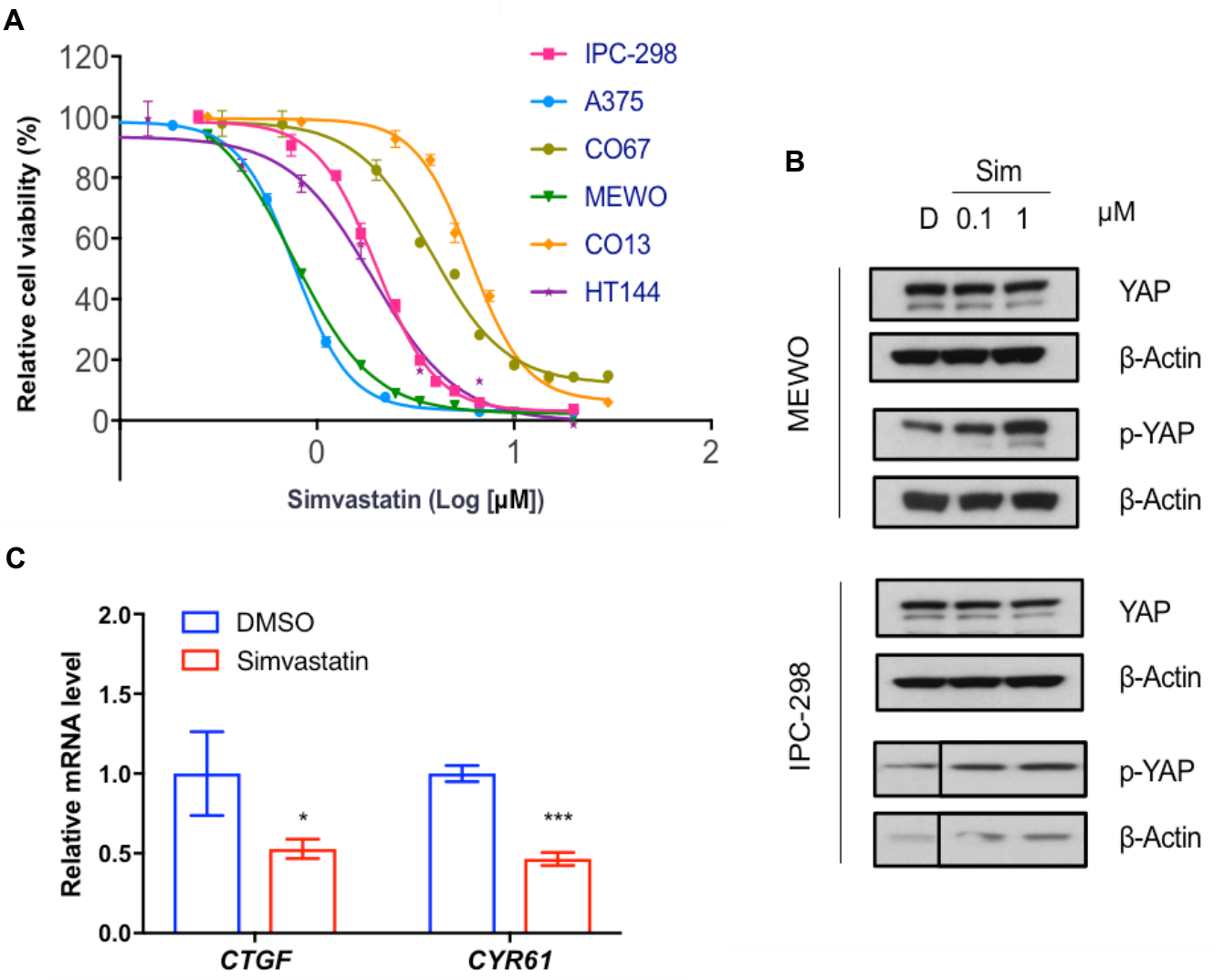

Figure 14. Simvastatin inhibits melanoma cell viability and inactivates YAP

(A) Dose-response curves of melanoma cell lines. Cells were treated with gradient concentrations of simvastatin for 3 days.

(B) Western blot analysis of total YAP and phosphorylated YAP (p-YAP) level with MeWo and IPC-298 cell lines. Cells were treated with DMSO (D), 0.1 μM or 1 μM of simvastatin (Sim) for 6 hrs.

(C) mRNAs levels of *CYR61* and *CTGF* in MeWo cells treated with 1 μM of simvastatin for 6 hrs. Measurements were normalised to cells treated with DMSO.

Experiments were performed in triplicate. Data are presented as mean ± standard deviation. *P<0.05. ***P<0.001.

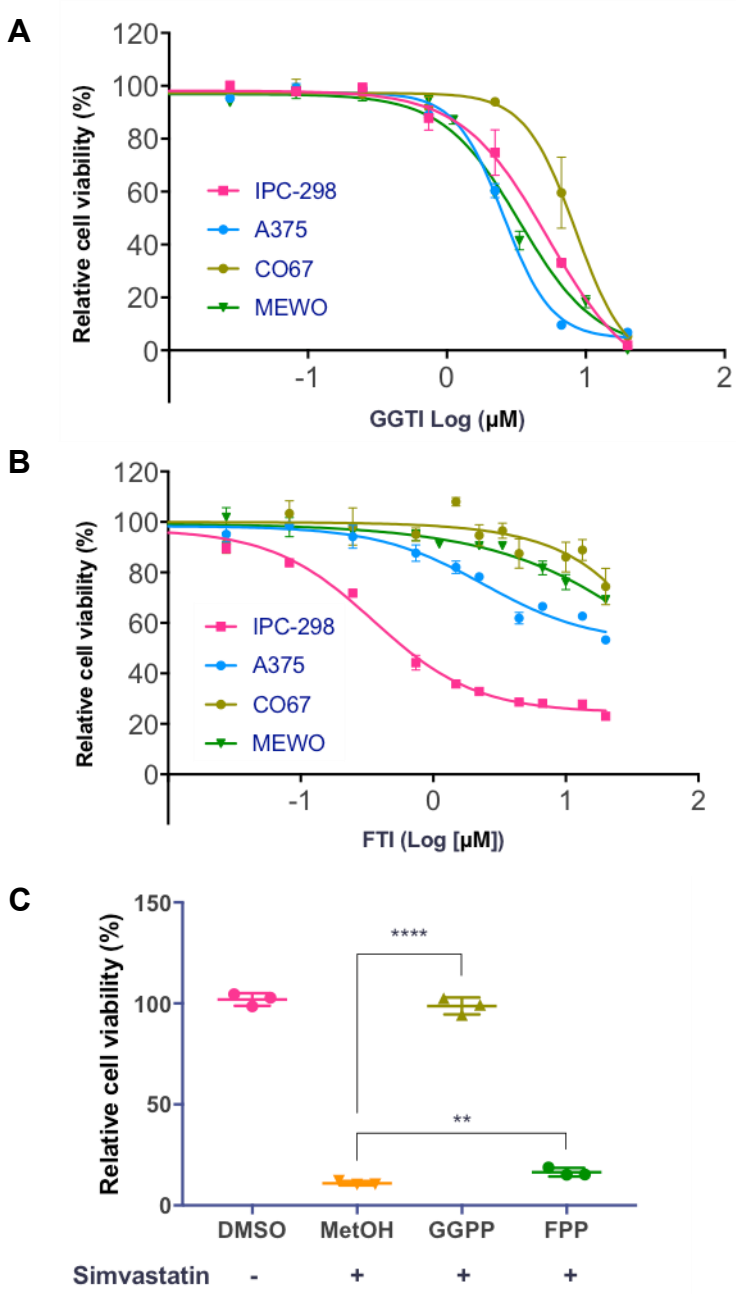

Figure 15. Simvastatin inhibits melanoma cell viability through suppression of GGPP

(A) Dose-response curves of melanoma cell lines. Cells were treated with gradient concentrations of GGTI for 3 days.

(B) Dose-response curves of melanoma cell lines. Cells were treated with gradient concentrations of FTI for 3 days.

(C) Viability of MeWo cells. Cells were firstly treated with 5 μM of simvastatin amd methanol (MetOH), 7 μM of GGPP, or FPP for 3 days. Measurements were normalised to DMSO control cells.

Experiments were performed in triplicate. Data are presented as mean ± standard deviation. **P<0.01. ****P<0.0001. MetOH, methanol.

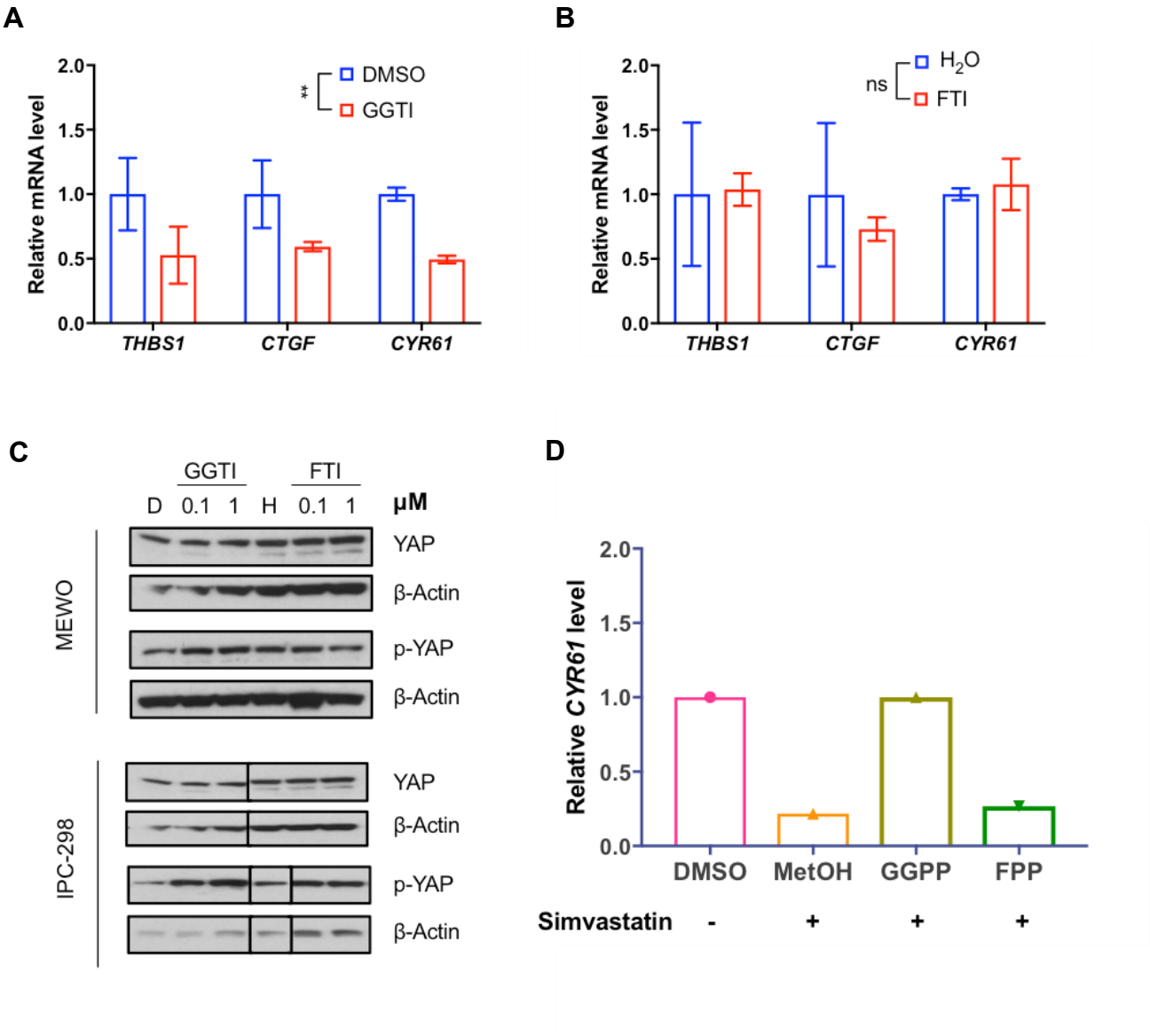

Figure 16. Simvastatin inhibits YAP activity through suppression of GGPP

(A) mRNAs levels of *THBS1*, *CYR61* and *CTGF* in MeWo cells treated with DMSO or 1 μM of GGTI for 6 hrs. Measurements were normalised to cells treated with DMSO, solvent of GGTI.

(B) mRNAs levels of *THBS1*, *CYR61* and *CTGF* in MeWo cells treated with H_2O or 1 μM of FTI for 6 hrs. Measurements were normalised to cells treated with H_2O, solvent of FTI.

(C) Western blot analysis of total YAP and phosphorylated YAP (p-YAP) level with MeWo and IPC-298 cell lines. Cells were treated with DMSO (D), 0.1 μM and 1 μM of GGTI, H_2O (H), and 0.1 μM and 1 μM of FTI for 6 hrs.

(D) mRNAs levels of *CYR61* in MeWo cells. Cell were treated with 0.1 μM of simvastatin plus methanol (MetOH), GGPP, or FPP for 6 hrs. Data were normalised to DMSO control cells. The experiment was performed once.

Experiments were performed in triplicate unless noted. Data are presented as mean ± standard deviation. ns, $P>0.05$. **$P<0.01$.

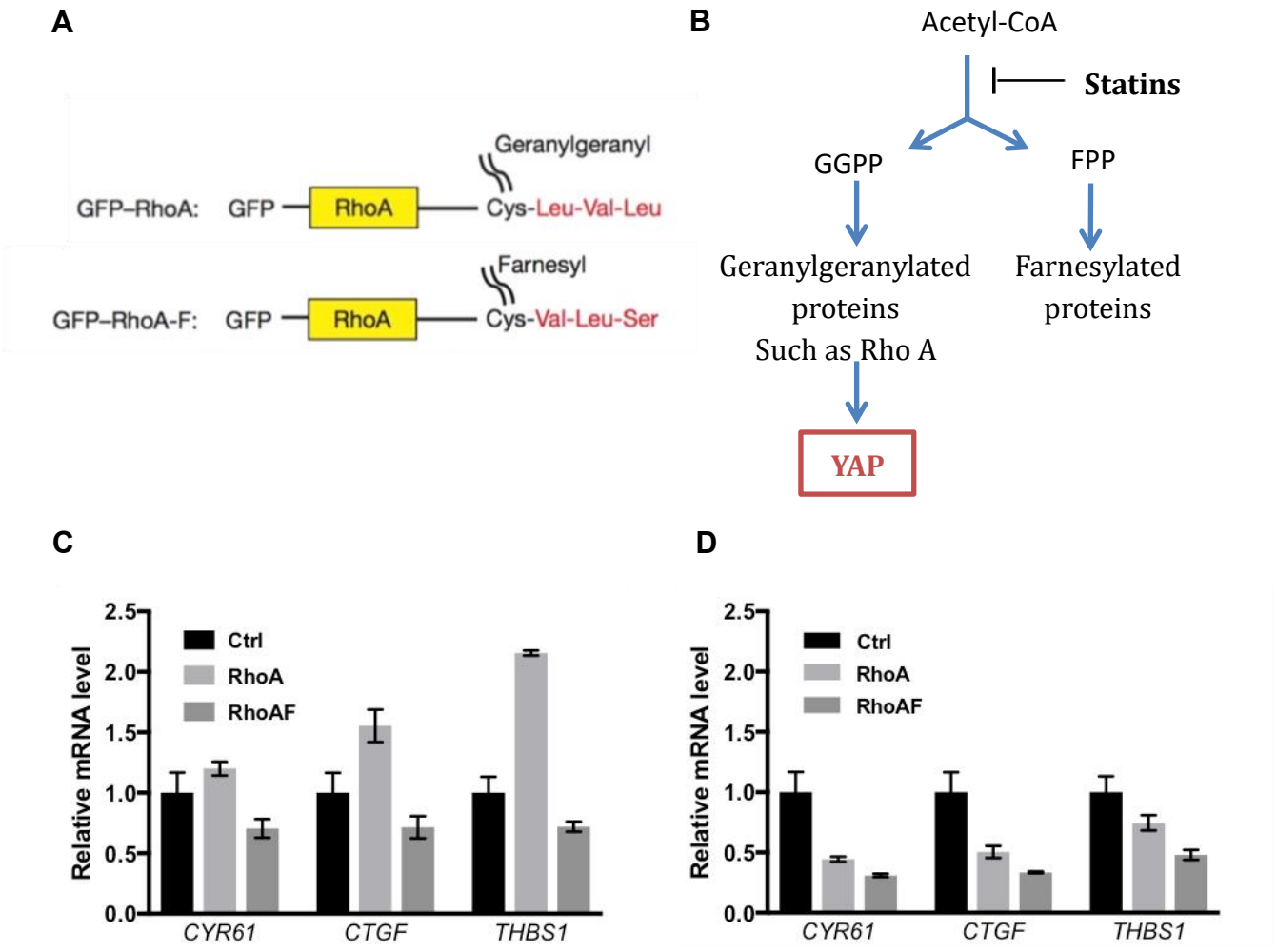

Figure 17. Investigation of RhoA in inactivation of YAP

(A) Schematic diagram of RhoA with a consensus geranylgeranylation-specific sequence (Cys-Leu-Val-Leu) and the mutant RhoA-F with a consensus farnesylation-specific sequence (Cys-Val-Leu-Ser). Graph adapted from Sorrentino, G. et al., 2014.

(B) Schematic hypothesis of the potential mechanism in which statins inhibit YAP activity.

(C) mRNAs levels of *CYR61, CTGF,* and *THBS1* in MeWo RhoA and RhoA-F cells that were treated with 1 μM of FTI for 6 hrs. Measurements were normalised to RhoA or RhoA-F cells that were not treated with FTI.

(D) mRNAs levels of *CYR61, CTGF,* and *THBS1* in MeWo RhoA and RhoA-F cells that were treated with 1 μM of GGTI for 6 hrs. Measurements were normalised to RhoA and RhoA-F cells that were not treated with GGTI.

Experiments were performed in duplicate, so statistical analysis was not applicable.

Table 1. Optimised cell densities for melanoma cell lines in soft agar assay

Cell line	Seeding density for soft agar assay (cells/well)
A375	500 or 1,000
HMCB	1,200 or 2,400
TH144	2,200 or 4,400
IPC-298	1,500 or 3,000
MeWo	3,000 or 6,000
SK-MEL-28	2,000 or 4,000
SK-MEL-2	1,250 or 2,500
C013	2,700 or 5,400
C027	10,000 or 20,000
C067	3,000 or 6,000

Table 2. Relative mRNA levels measured by RNAseq and qPCR

Gene	Relative mRNA level measured by RNAseq	Relative mRNA level measured by qPCR
ITGB2	4.29	93.46
CYR61	4.43	38.15
CTGF	2.69	15.37
THBS1	3.17	8.04
TGFB2	2.76	6.75
IL6	2.70	5.24
FST	2.44	4.82
IL8	1.50	3.28
SMAD3	1.22	2.65
AXL	0.84	2.63
FOSL1	1.20	2.11
CCL2	1.14	1.73
SRF	0.35	1.29
TEAD4	1.46	1.24
CXCL3	0.63	1.06
ITGA3	0.59	0.94
JUN	-0.67	0.93
TYR	-0.49	0.62
SOX10	-0.49	0.44
MITF	-0.35	0.42

Appendix 1. Melanoma cell lines used in this project

Cell line	Genotype	Source
A375	*BRAF*	ATCC
HMCB	*wt*	ATCC
TH144	*BRAF*	ATCC
IPC-298	*NRAS*	DSMZ
MeWo	*wt*	ATCC
SK-MEL-28	*BRAF*	NCI panel
SK-MEL-2	*NRAS*	NCI panel
C013	*NRAS*	QIMR
C027	*NRAS*	QIMR
C067	*wt*	QIMR

* QIMR, QIMR Berghofer medical research institute; *wt*, wild-type for *BRAF* and *NRAS* mutations.

Appendix 2. Reagents, buffers and media

Name	Brand/Catalgue number
0.5% Trypsin-EDTA (10x)	Gibco, #15400-054
10% Neutral-Buffered Formalin	Australian Biostain, #ANBFP
AEC+ substrate-chromogen	Dako, #K3461
Ajax Finechem D.P.X. neutral mounting medium	Thermo Fisher, #AJA3197
Bolt™ MES SDS Running Buffer	Invitrogen, #B0002
Bovine Serum Albumin (BSA)	Roche, #10735078001
Certified™ PCR Low-Melt Agarose	Bio-Rad, #1613113
Collagenase IV	Worthington, #4189
cOmplete™ Protease Inhibitor Cocktail	Roche, #11697498001
DAPI	Roche, #10236276001
DMEM:F12+15mM HEPS 450ml	Gibco, #11965-092
DNase I	Sigma, #D4527
ECL™ Prime Western Blotting Detection Reagent Kit	GE Healthcare, #RPN2232
Eosin	Sigma, #E4382
Fast SYBR® Green Master Mix	Applied Biosystems, #4385612
Fetal Bovine Serum (FBS)	Gibco, #10437028
FPP	Sigma, #F6892
FTI-277	Sigma, #F9803
FuGENE® HD Transfection Reagent	Promega, E2311
GGPP	Sigma, #G6025
GGTI-298	Sigma, #G5169
Haemotoxylin (Mayer's Haematoxylin)	Amber Scientific
HBSS-/-	Gibco, #14185052
Histolene	Trajan, # 11031
Lipofectamine RNAiMAX transfection reagent	Invitrogen, #13778075
Matrigel® Growth Factor Reduced (GFR) Basement Membrane Matrix	Corning, #354230
Nuclease-free water	Promega, #P119C
Oligo(dT)15 Primer	Promega, #C1101
Opti-MEM Reduced Serum Media	Gibco, #31985088
OptiPrep™ Density Gradient Medium	Sigma, #D1556
Penicilin Streptomycin (P/S)	Gibco, #15140-122
PhosSTOP™ phosphatase inhibitor	Roche, #4906845001
Polybrene Infection Transfection Reagent	Merck, #TR-1003-G
ProLong Gold Antifade Mountant	Invitrogen, #P36930
RNaseOUT Recombinant RNase Inhibitor	Invitrogen, #10777019
RPMI 1640 + 20mM HEPES (RPMI)	Gibco, #31800089
Set of dATP, dCTP, dGTP, dTTP	Promega, #U1330

Simvastatin	Sigma, #S6196
SuperScript™ III Reverse Transcriptase	Invitrogen, #18080093
Target retrieval solution (pH 9)	Dako, #S2367
TRIzol Reagent	Invitrogen, #15596026
TSA® biotin detection kit	PerkinElmer, #NEL700A001KT

Name	Composition
Alamar blue reagent	Unit: % (w/v) 1.5×10^2 Resazurin 2.5×10^3 Methylene Blue 3.25×10^2 Potassium hexacyanoferrate (III) 4.22×10^2 Potassium hexacyanoferrate (III) trihydrate
Antigen retrieval solution used for CD31 staining	390 mg $CaCl_2$ 75 mg Trypsin 15 ml Tris buffer 285 ml dH2O
Crystal Violet	1 g Crystal Violet 500 ml methanol 500 ml dH2O
Digest media used for tumour dissociation	9 ml HBSS-/- (warmed) 1 ml Collagenase IV (2000 u/ml, final 200 u/ml) 50 µl CaCl2 (1M, final 5 mM) 50 µl DNase (10,000 u/ml, final 50 u/ml)
PBS (Dulbecco's)	2.7 mM KCl 1.5 mM KH_2PO_4 136.9 mM NaCl 8.9 mM Na_2HPO_4•7H2O
RIPA buffer	150 mM NaCl 0.5% sodium deoxycholate 1% Triton X-100 0.1% SDS 50 mM Tris-HCl, pH 7.5
Scott's tap water	2 g $NaHCO_3$ 20 g $MgSO_4$ 1 L dH_2O
Staining media	568 mg BSA 57 ml dH2O 5.7 ml 1M Hepes pH 7.4 (Sigma) 5.7 ml 100x PenStrep (Invitrogen) 500 ml Leibovitz's L15 media (Invitrogen)
TBS (10x)	24 g Tris 88 g NaCl

	900 ml dH2O pH to 7.6 with 12 N HCl Add dH_2O to a final volume of 1 L
Transfer buffer (10x)	60.5 g Tris 20 g SDS 288.25 g Glycine dH2O up to 2 L
Trypsin-EGTA (TEG) (10x)	40 mg EGTA (Merck, # 324626.25) 10 mg PVA (Sigma, # P8136-250G) 90 ml PBS 10 ml 2.5% trypsin (Sigma, # T4549-100ML)
TEG (1x)	Dilute TEG (10x) in HBSS-/-

Appendix 3. Antibodies

Name	Application	Dilution	Reactivity	Host	Source
Primary antibodies					
YAP Antibody	WB	1:1000	Human	Rabbit	CST, #4912S
Phospho-YAP (Ser127) Antibody	WB	1:1000	Human	Rabbit	CST, #4911S
Axl (C89E7) mAb	WB	1:1000	Human	Rabbit	CST, #8661S
Thrombospondin-1 Antibody (A6.1)	WB	1:1000	Human	Mouse	Novus Biologicals, #NB100-2059
CYR61 (D4H5D) XP® Rabbit mAb	WB	1:1000	Human	Rabbit	CST, #14479S
CRIM1 Antibody	WB	1:1000	Human	Rabbit	Sigma, #SAB3500847
Pan-TEAD (D3F7L) Antibody	WB	1:1000	Human	Rabbit	CST, #13295
β-Actin Antibody	WB	1:2000	Human	Rabbit	CST, #4967S
Human mitochondria antibody	IHC	1:1000	Human	Mouse	Merck, #MAB1273
Ki67 Antibody	IHC	1:150	Human	Mouse	Dako, #M7240
CD31 Antibody	IHC	1:100	Mouse	Rat	BD Biosciences, #550274
Secondary antibodies					
Peroxidase AffiniPure Goat Anti-Rabbit IgG	WB	1:5000	Rabbit	Goat	Jackson ImmunoResearch, #111-035-003
Peroxidase AffiniPure Goat Anti-Mouse IgG	WB	1:5000	Mouse	Goat	Jackson ImmunoResearch, #115-035-003
ImmPRESS™ HRP Anti-Rat IgG	IHC	N/A	Rat	Goat	Vector, #LS-J1062
ImmPRESS™ HRP Anti-Mouse IgG	IHC	N/A	Mouse	Horse	Vector, #MP-7402
Biotinylated rabbit anti-rat IgG antibody	IHC	1:200	Rat	Rabbit	Vector, #BA-4000

*CST, Cell Signalling Technology

Antibodies used in FACS

Name	Dilution	Clone	Conjugate	Reactivity	Source
HLA-ABC	1:5	G46-2.6-PE	PE	Human	BD Pharmingen, #555553
CD45	1:200	30-F11	APC	Mouse	BD Pharmingen, #559864
Ter119	1:100	TER-119	APC	Mouse	BD Pharmingen, #561033
CD31	1:100	390	APC	Mouse	eBioscience, #17-0311-82

Appendix 4. Sequences of siRNAs

Gene	Sequences
YAP1	GGUCAGAGAUACUUCUUAA
	CCACCAAGCUAGAUAAAGA
	GAACAUAGAAGGAGAGGAG
	GCACCUAUCACUCUCGAGA
AXL	GAAAGAAGGAGACCCGUUA
	CCAAGAAGAUCUACAAUGG
	GGAACUGCAUGCUGAAUGA
	GAAGGAGACCCGUUAUGGA
CYR61	GGGCAGACCCUGUGAAUAU
	GGCCAGAAAUGUAUUGUUC
	GGUCAAAGUUACCGGGCAG
	GCAGCAAGACCAAGAAAUC
THBS1	GGACUGCGUUGGUGAUGUA
	GUACAGAAACGUAGUCGUC
	UCAUUAGAGUGGUGAUGUA
	GUACAGAAAUAACGAGGAA
CRIM1	GGAGAAACGUGGAACAUUG
	GAACUGGACUGAUGACCAA
	GGGAAGGACUGCAUUAAUG
	CCAGAGCUCUCAUGCAGUA
TEAD1	CACAAGACGUCAAGCCUUU
	GAAAGGUGGCUUAAAGGAA
	CGAUUUGUAUACCGAAUAA
	CCCAAUGUGUGAAUAUAUG
TEAD2	CGAAGGAAAUCAAGGGAAA
	GCAGUUGAUUCUUACCAGA
	GGAAUGAACUGAUCGCCCG
	GGAAGACCCGAACUCGAAA
TEAD3	GGACAAAGCCCUUCAGAGC
	UCUACAAGCUCGUCAAAGA
	GAUUGAAGGAGCUCUAUGA
	UUGAUUGCACGCUAUAUUA
TEAD4	GACAGAGUAUGCUCGCUAU
	UCAAGCACCUCCCUGAGAA
	GGACACUACUCUUACCGCA
	GUGCAUUGCCUAUGUCUUU

*siRNAs were ordered from Dharmacon using siGENOME SMARTpool.

Appendix 5. Sequences of primers

Gene	Forward primers	Revers primers
ITGB2	GGTCATCTGGAAGGCTCTGA	CACCAAGTGCTCCTAACTCTCA
CYR61	GGTCAAAGTTACCGGGCAGT	GGAGGCATCGAATCCCAGC
CTGF	CCAATGACAACGCCTCCTG	TGGTGCAGCCAGAAAGCTC
THBS1	AGCATGGTCCTGGAACTCAG	CAGCTCATTGGCCAACTCTT
TGFB2	CTTTGGATGCGGCCTATTGC	TCCAGCACAGAAGTTGGCAT
IL6	GACAGCCACTCACCTCTTCA	AGTGCCTCTTTGCTGCTTTC
FST	AGTCCAGTACCAAGGCAGATGT	GGTCACACAGTAGGCATTATTGG
IL8	CTGCGCCAACACAGAAATTA	ATTGCATCTGGCAACCCTAC
SMAD3	GCAGAACGTCAACACCAAGTGCAT	ATTCACGCAGACCTCGTCCTTCTT
AXL	CACCTCCCTGCAGCTTTC	CTCAGGTTGAAGGGGGTG
FOSL1	TGCCACCCTAGCCAATGTCT	TGGAGTTGGATGTGGGATACTG
CCL2	GATCTCAGTGCAGAGGCTCG	TGCTTGTCCAGGTGGTCCAT
SRF	AGAAGGCCTATGAGCTGTCC	TTGCCGGTCTCACTGGTGAT
TEAD4	AACAGCGTGCTGGAGAACTT	CTCACTGGCTGACACCTCAA
CXCL3	CGCCCAAACCGAAGTCAT	GTGCTCCCCTTGTTCAGTATCT
ITGA3	CTTCAAACGGAACCAGAGGA	ATGCCAGACTCACCCATCAC
JUN	TTCTATGACGATGCCCTCAACGC	GCTCTGTTTCAGGATCTTGGGGTTAC
TYR	ACTTACTGGGATAGCGGATGCCTCT	TGCATTGGCTTCTGGATAAACTTCTT
SOX10	AAGCCTCACATCGACTTCGG	TCCATGTTGGACATTACCTCGT
MITF	AAACCCCACCAAGTACCACA	ACATGGCAAGCTCAGGAC